Africa Center of Excellence for Water Management

Addis Ababa University

Hydraulic analysis of water systems to reduce the adverse effects of transient pressures (The case of Ras Hailu dual-purpose reservoir site and its respective distribution zones)

by

Bezawit Limenih

A thesis submitted to the Africa center of Excellence for Water Management at Addis Ababa University in partial fulfillment of the requirements for the Master of Science in Water Management Degree (water supply and sanitation)

Under the Supervision of Dr. Shimelis Kebede

Assistant professor of Chemical Engineering (Process and Environmental)

Addis Ababa Institute of Technology, Addis Ababa University

December, 2021

Addis Ababa, Ethiopia

APPROVAL AND ACCEPTANCE

This paper has been reviewed and approved by the student advisor, by the examiners, and by the Director of graduate studies: We would like to certify with our signature that this thesis entitled, **"Hydraulic analysis of water systems to reduce the adverse effects of transient pressures (The case of Ras Hailu dual-purpose reservoir site and its respective distribution zones)"** is the original work of the student that it contains all the required contents.

APPROVED BY

DR. SHIMELIS KEBEDE ________________
Advisor Signature

DR. TAMRU TESSEME ________________
Internal Examiner Signature

DR. MEBRUK MOHAMMED ________________
External Examiner Signature

DR. ________________
Director of Graduate Studies Signature

DECLARATION

I, MS. Bezawit Limenih, declare that this thesis is my own independent work and efforts. All external sources have been properly acknowledged implying that any information I used for my research has been properly credited and referenced in accordance with academic principles and ethics.

08/10/21

SIGNATURE DATE

CERTIFICATION

I, the undersigned, Dr. Shimelis Kebede, Assistant professor of Chemical Engineering (Process and Environmental) Addis Ababa Institute of Technology, Addis Ababa University: certify that Ms. Bezawit Limenih conducted her Master's Thesis under my supervision.

08/10/21

SIGNATURE DATE

ABSTRACT

Hydraulic transient occurrences occur because of planned or unexpected operating changes, such as pump shutdowns and quick valve closures. They induce an abrupt change in the equilibrium state of a pressurized water distribution system that can result in failure of pumps, system fatigue, pipe ruptures or bursts, and even unclean/dirty water ingress. Until recently, most water systems were planned and operated without taking into account the possible impact of hydraulic transients. However, as computer software technology has advanced, user-friendly transient flow analysis software is increasingly being utilized to model transient behavior in pipe networks and design preventative measures to appropriately protect the system from such threats. In this study, a transient analysis was performed on three distribution network zones that are found in the Rufael and St. Paul sub-branches that fed from the Gefersa water treatment plant transmission network branch via the Ras Hailu reservoir & pumping station site using the transient modeling software HAMMER. To determine system's real transient behavior, a hydraulic model database depicting the real system dynamics was created & simulated using WaterGEMS software. It was then imported to HAMMER software and computational simulations for transient state were conducted for the worst-case pump trip/shutdown scenario considering that three pumps that were pumping water to their respective distribution zones through the three pumping pipelines were simultaneously shutoff due to a sudden power outage. The findings demonstrated that the rising portion of all the three pumping pipelines have been experiencing negative pressure waves which travel along the system, causing the pressure in the pipelines to fall rapidly, and creating low or negative pressures to the pumping pipelines as well as to their respective distribution zones. Similarly, at a certain time, the negative pressures at some pumping pipeline segments have been reduced to vapor pressure of the liquid, during which the water vaporizes and forms a vapor pocket that may cause cavitation and water column separation, which can cause catastrophic pipeline failures due to significant pressure surges caused by the vapor cavities collapsing. Therefore, to effectively protect the pumping pipelines, appropriate surge protection devices (double acting air valves and hydropneumatic tanks) were proposed, and initially, transient analysis was performed by installing air/vacuum valve in highly elevated areas where low and/or negative pressures were predicted and at some parts of the pumping pipelines where vapor cavities were found. The results showed that the presence of air/vacuum valves in these locations has successfully helped to reduce the cavities, but there were still negative pressures in the system. So the author decided to install hydropneumatic tanks/air chambers just downstream of the pump stations and found that the installation of a hydropneumatic tank was the best option to uplift the minimum pressure transient and reduce the maximum pressure transient in the system within acceptable limits. Even more so when the hydropneumatic tank is used in combination with air valves, it provides an adequate protection to the pumping system and reduce the potential damage to the pipeline.

Keywords: hydraulic transients, transient analysis, power outage, pump shutdown, pumping pipeline, surge protection devices

ACKNOWLEDGEMENTS

I respectfully write this note of gratitude to God who has helped me in all my endeavors, who has done more than I could ever have imagined who has given me the strength and will to complete my thesis successfully. In the midst of all this, it is impossible not to thank her, Mother of God, the Blessed Virgin Mary! Her intercession, prayers, sympathies, and blessings were and still are so special and inexhaustible to me. Let me always be grateful to you, Holy Mother, for there are many reasons to thank you.

While I believe that words alone cannot express the extent of gratitude, I am grateful that I have been fortunate enough to have an advisor like Dr. Shimelis Kebede after so many ups and downs. I am truly grateful for his sincerity, support, constructive suggestions and encouragement, which has always been my stronghold and pillar of strength.

I also wish to acknowledge the members of the Addis Ababa Water and Sewerage Authority who provided me with the necessary data and material required to perform this research. In this regard, my special thanks go to all the staff of AAWSA, Addis Ketema Branch Office.

I would like to express my gratitude to the African Center of Excellence for Water Management (ACEWM) for providing me with this opportunity, as I consider this opportunity to be a milestone in my academic growth and for the financial support provided to assist this thesis. The support is greatly acknowledged.

I would like to specifically thank my father and mother for all the sacrifices they have made so far to bring me to this point and to their unwavering support and encouragement. More especially my sincere gratitude goes to my mother, who is not only my mother but also my friend, my mentor, my strength. Without her, this thesis would be a never-ending story.

Finally, thank you to all who have contributed, directly or indirectly, to the success of this thesis. May God reward you all! `

TABLE OF CONTENTS

LIST OF TABLES

LIST OF FIGURES

LIST OF ABBREVIATION

AAWSA	Addis Ababa Water and Sewerage Authority
ACEWM	Africa Centre of Excellence for Water Management
AWWA	America Water Works Association
CIS	Customer Information System
DTM	Digital Terrain Model
EPS	Extended period simulation
GIS	Geographic Information System
GWTP	Gefersa Water Treatment Plant
HDPE	High-density polyethylene pipes
HGL	Hydraulic Grade Line
MoWR	Minister of Water Resource
MOC	Method of characteristic
PVC	Polyvinyl chloride pipes
SCADA	Supervisory Control and Data Acquisition
RHPS1-P1	Ras Hailu Pump Station One – Pump One
RHPS1-P2	Ras Hailu Pump Station One – Pump Two
RHPS2-P1	Ras Hailu Pump Station Two – Pump One
RHPS2-P2	Ras Hailu Pump Station Two – Pump Two
RHPS3-P1	Ras Hailu Pump Station Three – Pump One
RHPS3-P2	Ras Hailu Pump Station Three – Pump Two
RHPS3-P3	Ras Hailu Pump Station Three – Pump Three
UFW	Unaccounted for Water
WCM	Wave characteristic method
WDN	Water Distribution Network
WDS	Water Distribution System

1 INTRODUCTION

1.1 Background

It is assumed that water supply systems operate under steady-state hydraulic conditions. However, this assumption is frequently violated due to the intrinsically non-deterministic behavior of consumers, planned or accidental operational changes, pressure management, and failures. The problem is becoming more acute as water utilities are adopting aggressive pump optimization and adaptive pressure control. The nature of stochastic operational changes (such as: pump shutdown due to unexpected power outage, pump startup/shutoff, & rapid valve closing/opening) may generate a variety of pressure transients, hydraulic instabilities, and dynamic variations. This paper focuses primarily on analyzing hydraulic transients or pressure surges in the system caused by sudden power outage and provide design recommendations for control of adverse pressure surges.

Pressure transients are a hydraulic phenomenon that can be introduced in pipe networks when flow is affected by some disturbance that it alters the flow velocity, such as the valve opening or closure, the pump start-up or shutdown, sudden change in demand such as firefighting, and during main break. Transients consist of pressure waves that propagate throughout the distribution network causing significant pressures in certain locations (Rathnayaka et al., 2013; Duan et al., 2014).

The relevance of understanding transient behavior stems from the potential for damage to our crucial water distribution infrastructure. There are two possible categories of damage that can occur because of pressure transient events. The first is catastrophic failure, which is produced by high magnitude force caused by quick pressure transient waves. These occurrences were more common in large pumping mains and resulted in water network equipment damage. Smaller magnitude and repeated pressure transient events, on the other hand, may cause excessive burden on a pipe, gradually weakening it and could hasten its failure (Starczewska, 2015). Besides major and minor structural failures, transients have the potential to cause water quality failures through facilitating the intrusion of contaminants from the surrounding groundwater and through apertures in pipe wall (Hampson, 2014).

Because hydraulic transients can have such devastating consequences, their analysis is critical for determining the values of transient pressures that can result from flow control operations and establishing design criteria for system equipment and devices to provide an acceptable level of protection against system failure due pipe collapse or bursting. Thankfully, in light of the overall technological advancement, hydraulic transient simulation models are now widely used. These models are used to analyze 'what if' scenarios related with decisions about safe system operation, as well as to evaluate potentially objectionable pressure transients that could lead to unacceptable operating circumstances arising in the system and jeopardizing its integrity (Jung et al., 2009).

Currently, most water utilities are becoming more and more accustomed to use technologies such hydraulic simulation models to evaluate the overall operational and technical performance of their water distribution network. However, when it comes to the Addis Ababa Water and Sewerage Authority, which manage and monitor the overall Addis Ababa water supply system, much remains to be done in terms of using various technologies to identify and address problems that disrupt water distribution system performance like pressure transients. To cite just one example, water mains be at risk in different places. In this case, one of the tasks that can be done by the Authority is to send technicians to the place where the pipe is said to be broken and repair it as usual not where the exact location and reason for the failure was predicted. Managing the system in such a way makes the impact of pressure transients, which are considered to be the main reason for the loss in hydraulic integrity, less noticeable.

As a result, using a hydraulic modeling software HAMMER, this research attempts to examine the prospective impact of transient events that may occur accidental but with serious harm to both system components and users in order to reduce the adverse effects of the resultant transient high and low pressures. On the basis of this, as the transient model expands and is adopted by AAWSA, it will be easier to estimate the severity of transient pressures allowing damaged water pipelines to be replaced and other mitigation measures to be developed ahead of time.

1.2 Problem Statement

Transient conditions in the hydraulic system are usually caused by system flow control operations that are performed as part of the routine operation of a water distribution system, such as opening and closing valves & starting and stopping pumps, as well as some unintentional events such as sudden power outage and pipeline breakage.

In context of Addis Ababa, the existing water sources are finding it difficult to meet consumer's water demand in light of the rapidly growing population in the city. As a result, a water-shifting schedule is implemented by AAWSA in most of the Addis Ababa distribution network zones. It is therefore a common practice in such piping systems that valves are closed and opened frequently in order to shift water between different parts of the network at different times. In addition to valve operations, pumps are stopped and started too often by operators in order to carry out their daily activities. In case of such daily operations, the fact that no transient protection devices are installed can initiate abrupt unsteady condition in pressure-flow state that gives rise to hydraulic transients in the system on a regular basis.

Another basic problem in almost all areas of Addis Ababa is power outage (sudden interruption of energy supply). This makes the issue even more serious, especially when it happens in the vicinity of pump stations. Moreover, such an unexpected event causes the pumps to suddenly shut-off. The pumps become shutdown, which means that the pressure at the discharge of the pumps rapidly decreases and negative pressure wave starts to propagate down the pipeline causing low pressures elsewhere in the system (Wood et al., 2005).

The potential damage that the hydraulic transients may cause to the system depends on the existing situation of the pipe network and surge protection devices. In the selected region, more than half of the pipelines are over 40 years old and as a result, they are likely to be weakened by corrosion or other external factors and may lost their integrity. Such a situation would be conducive to transient conditions for rupturing a pipe directly through excessive pressure or exploiting an existing weakness to damage a pipe indirectly (Karney et al., 1990). In addition, although it was advisable to install transient protection devices to protect systems from such unintentional transients, the fact that the network does not currently have any technically sound surge protection devices and that the whole system is manually operated and the performance is completely dependent on the operator's skill and experience, the damage that hydraulic transients may cause will be significant.

1.3 Research Objective

1.3.1 General Objective

The main objective of this research is to analyze the selected water transmission and distribution system response to the most common transient phenomenon i.e. sudden pump shutdown due to power outage using HAMMER transient simulation software.

1.3.2 Specific Objectives

Taking the main objective as mentioned above, the following specific objectives are expected to be achieved.

- To develop a hydraulic Extended Period Simulation model that is supposed to represent the actual system in order to provide the initial and boundary conditions for the subsequent transient analysis using a hydraulic modeling software WaterGEMS.
- To perform a transient analysis associated with the simultaneous shutdown of three pumps in the pump stations due to electric power cut using HAMMER software.
- To identify system areas that are most prone to transients and suggest preventive measures that mitigate the impact of such transient events to a desirable extent.
- To develop recommendations to support the utility in making practical decisions regarding transients based on the results obtained from the transient simulation

1.4 Research Questions

Research questions that will be raised in this thesis are the following:

- How should the system operate over transient events?
- What is the contribution of pressure transients to prevent the system from functioning properly?
- Which areas are more susceptible to pressure transients?

1.5 Significance of the study

A typical source of disturbance that is commonly neglected in WDS analysis is due to water hammer or transient conditions. Although it is well known that the pressure generated during transient conditions should be an important consideration when a system is being designed, there is a widespread belief that transient conditions are intrinsically less severe in network applications and as a result, they have not received as much attention as they should. Accordingly, the main benefit of this study is to give an insight into the most common cause of hydraulic transients and transient modeling considerations to all stakeholders in the sector. In connection to this, the study suggests how water utilities can use the hydraulic surge models to develop operational alternatives and to prepare contingency plans for the identified deficiencies associated with transients during hydraulic transient analysis. Hopefully, all the insights raised in this study are expected to be used as a baseline in solving other similar existing water supply problems of other distribution zones in the city.

1.6 Scope, Limitation and Delimitation

Scope: - Successful hydraulic and transient modeling for the selected water distribution system involved several major tasks that comprised the overall scope of the research. These are;

- *Data Collection*: - all the available information including AutoCAD files showing all pipes, storage facilities, and valves in the system, Contour map along with corresponding digital terrain model (DTM), Customer consumption billing data, Specifications for the storage tanks and pumps were collected from the Addis Ababa Water and Sewerage Authority for developing a hydraulic model.
- *Computer Model Development*: - Both a hydraulic and transient simulation models were generated for the existing water system using WaterGEMS and HAMMER. Descriptive parameters that are known for each component were entered appropriately.
- *Field Testing*: - Performing a field test for calibration purpose. In this particular fieldwork, pressure measurements were collected from the selected sample locations using high-speed pressure data loggers. Measurement data were copied to a personal computer and analyzed using a software developed for this measuring instrument.
- *Model Calibration*: - Results from field-testing were compared to model behavior, and data in the model were adjusted until it reasonably agreed with measured system performance.

Delimitation: - Although this study attempts to meet almost all of the goals set, it is clear that there are some delimitations. Of these:

- Based on transient simulation model results (as predicted by the model), it was necessary to install pressure monitoring devices in most susceptible areas to verify whether the output of the model is compatible with ground. In order to achieve this, a field-monitoring program needs to be conducted over a long period of time. However, it could not be included in this study because of the difficulty to obtain permission from the utility to use such devices for a long period of time, the limited knowledge available to use the devices for this purpose, site accessibility (security issues), and financial issues.
- Although, the outputs from the transient model allow us to identify pipes that are prone to failure and need repair, it would be good for the research completeness if risk analysis was done in advance in order to determine the pipes probability and impact of failure. However, long-term pipe breakage data on the order of years should be acquired from the utility. In fact, in the context of our country, the probability of systematically recording information is low and could not be included in this study.

Limitations: - the following are some of the limitations that were outside the scope of the author's consent that prevent the entire study from being complete.

- Availability of reliable data
- Lack of previous research studies on the topic
- Time constraints

1.7 Structure of the thesis

This thesis is a collection of relevant topics that comprises of the following chapters:

Chapter 1: - is an introduction part that corresponds to all the topics that have been described so far.

Chapter 2: - explores literatures that have been written at various times in related to the present study and provides a background required to understand the fundamentals of hydraulic transients and hydraulic modelling & simulation theories, water distribution system analysis, and transient analysis.

Chapter 3: - provides general information about the study area water supply system and describes all activities that were done in order to attain the objectives of the research. The approach that was taken and the methodology used are fully described.

Chapter 4: - presents a comprehensive overview of the findings of the key simulations (hydraulic and transient) performed for the selected system and discusses them extensively.

Chapter 5: - provides concluding remarks based on the extent to which the study has achieved its objectives and the major findings of the study. It also provides recommendation for the work to be done in the future in this regard.

Under Appendices, collection of major tabular data for the relevant parameters attributed to the study are included.

2. LITERATURE REVIEW

2.1 Hydraulic Transients

The flow and pressure condition/situation that occurs in a hydraulic system between an initial steady-state condition and a final steady-state condition" is known as a hydraulic transient (Walski et al. 2003). These conditions are often referred to as "events" due to the relatively short time frame over which transients are analyzed. Transient events are initiated by changes in hydraulic devices (i.e., pumps or valves) or boundary conditions (i.e., tanks, reservoirs, or demands). These events can create serious consequences for water utilities if not considered in design and operation (Wood, 2005).

2.1.1 Fundamentals of pressure transients

The definition of hydraulic transients implies that there is a change in the system as it goes from one steady-state to another. The flow during this transition period is called unsteady flow (which varies with time at a given location (Wood et al., 2005). Extreme changes in flow conditions in a network have the ability to create considerable high and low dynamic pressures in pipe systems, proportional to the change in velocity if sufficiently rapid. The fluctuating oscillations can frequently exceed steady-state operating pressures in magnitude, with the lowest pressures being negative (Gullick et al., 2004). And along with rapid changes in flow, hydraulic transients are responsible for inducing pressure waves. These pressure waves travel at acoustic or sonic velocity; however, they are also dependent on the elasticity of the pipe walls (Wood et al., 2005). These pressure waves can bring dramatic increases or decreases in pressure depending on the initiation of the transient. Friction losses in the pipe cause energy losses which reduce the wave's amplitude over time and eventually bring the system to a new steady-state.

2.1.1.1 Governing Equations

The fundamental equations that describe hydraulic transients are developed from the basic conservation relationships of physics or fluid mechanics. They can be fully described by Newton's second law (equation of motion) and conservation of mass (kinematic relation). These equations can incorporate typical hydraulic devices and their interactions with the wave conditions in the pipes. Applying these basic laws to an elementary control volume, a set of nonlinear hyperbolic partial differential equations can be derived. If x is the distance along the pipe centerline, t is time, and partial derivatives are represented as subscripts, the governing equations for transient flow can be written as:

Continuity equation: -

$$H_t + \frac{\mathbf{c^2}}{\mathbf{gA}}\mathbf{Qx} \quad = 0 \ldots\ldots\ldots\ldots\ldots\ldots\ldots\ldots\ldots\ldots\ldots \text{(1)}$$

Momentum (dynamic): -

$$H_x + 1/Ga\ (Q_t - f(Q)) = 0 \ldots\ldots\ldots\ldots\ldots\ldots\ldots\ldots\ldots \text{(2)}$$

Where, H is the pressure head (pressure/density), Q is the volumetric flow rate, c is the sonic wave speed in the pipe (c is the pipe's sonic wave speed), A is the cross-sectional area, g is the gravitational acceleration, and f(Q) is a pipe-resistance (nonlinear) term that is a function of flow rate.

These two governing relations, in conjunction with the boundary equation for specific devices, accurately describe the wave propagation phenomenon that occurs in a distribution system during a transient event. However, no analytical solution exists for these equations except for simple applications that neglect or greatly simplify the boundary conditions and the pipe-resistance term (Boulos et al, 1990). When pipe junctions, pumps, surge tanks, air vessels, and other hydraulic components are included, the basic equations are further complicated. As a result, numerical methods are used to integrate or solve the transient-flow equations.

2.1.1.2 Characteristic time

It is a pipeline characteristic time which helps in determining which equation to use to evaluate transients. The pressure wave generated by a flow control operation propagates with speed a and reaches the other end of the pipeline in a time interval equal to L/a seconds. The same time interval is necessary for the reflected wave to travel back to its origin, for a total of 2L/a seconds. The quantity of 2L/a is termed the characteristic time for the pipeline. It is used to classify the relative speed of a maneuver that causes a hydraulic transient (Walski et. al., 2003).

If flow control operation produces a velocity change ΔV in a time interval (T_M) less than or equal to a pipeline's characteristic time, the operation is considered "rapid". Flow control operations that occur over an interval longer than the characteristic time are designed "gradual" or "slow". The classifications are summarized in Table 2.1 below.

Table 2.1 Flow control operations classification based on system characteristic time

Operation Time	**Operation classification**
$T_M = 0$	Instantaneous
$T_M < 2L/a$	Rapid
$T_M > 2L/a$	Gradual
$T_M >> 2L/a$	Slow

Source: (Walski et. al., 2003)

2.1.1.3 Magnitude and speed of transients

Fluid properties, along with the structural characteristics of the pipe, govern the behavior of transients in WDS. Exact equations simulating the maximum pressure change and wave velocity are in the form of complex coupled hyperbolic differential equations (M. H. Chaudhry, 1987).

The widely accepted Joukowsky equation gives the change in transient pressure head caused by the instantaneous change in velocity. The Joukowsky equation provides an estimate of the maximum change in head (ΔH) created when water with velocity V is brought to a sudden stop:

$$\mathbf{\Delta H = \pm \frac{a}{g} \Delta V} \quad \text{……………………………………………(3)}$$

Where; a is the acoustic wave speed and g is acceleration due to gravity. The negative sign represents a propagation traveling upstream and the positive sign represents a propagation traveling downstream.

Wave Celerity / Speed: - Korteweg developed an equation in 1878 that allowed wave celerity to be calculated as a function of pipeline elasticity and liquid compressibility. A general expression for the wave speed is:

$$a = \sqrt{\frac{\frac{E_V}{\rho}}{1+\frac{DE_V}{eE}\Psi}} \quad \text{…………………………………………....(4)}$$

Where; a is the characteristic wave speed (m/s); Ev is the bulk modulus of elasticity for the liquid (Pa); ρ is liquid density (kg/m3); D is the pipe diameter (mm); e is the pipe wall thickness (mm); E is the Young's Modulus for pipe material; and Ψ is the pipeline support factor.

2.1.2 Causes of transients

The intermediate-stage flow, when the conditions are changing from one steady state to another, is termed transient-state flow. In other words, the transient conditions are initiated whenever the steady state conditions are disrupted. Such a disturbance may be caused by changes, planned or accidental, in the setting of the control equipment of a man-made system and by changes in the inflow or outflow of a natural system (M. H. Chaudhry, 1987). These disturbances have the potential to propagate pressure waves that travel at the speed of sound in the fluid medium. The speed of sound depends on the compressibility of water and the elastic properties of the pipe.

The following typical events that require transient considerations have been mentioned by many researchers

- Pump start up or shut down (during flow control operation or incidental)
- Valve closing and opening
- Rapid changes in demand conditions
- Changes in transmission conditions
- Some surge protection devices malfunctioning
- Break in a pipeline

Among all currently known causes, changes in pump operation are believed to account for the majority of transient related problems in WDS. (D. Starczewska, 2016).

2.1.3 Potential impacts

A transient pressure waves can distribute throughout the system creating high and low pressure, and these pressures can have adverse effects on the hydraulic system including structural and water quality failures. (Boulos et. al., 2005), have summarized the common consequences of transients in this way.

Maximum pressure in the system: - During transient events, the maximum pressures can cause damage in pipelines, tunnels, valves, or other equipment. Sometimes, the damage can result in the loss of human life. On the other hand, high pressures may not necessarily destroy pipelines or other devices, but can cause cracks in internal linings, damage connections between pipes or cause deformations in equipment. This equipment could be valves, air valves, or even hydraulic transient protection devices. Moreover, high pressures may result in leakages in hydraulic systems even though no visible damage can be noticed.

Vacuum conditions and cavitation: - Occurrence of local vacuum conditions at specific locations that may result in cavitation either within specific devices such as pumps or within a pipe. Vacuum conditions (i.e., low pressures in the system that are close to the vapor pressure of the fluid) should be avoided because they can cause high stresses and strains in the system. This is due to the fact that, as pressure drops in a system and approaches the vapor pressure of the fluid, the fluids begin to boil, resulting in the formation of air bubbles. When these tiny air bubbles are transported to a high-pressure region by advection, they implode, and cause excessive stresses on the pipe walls.

Hydraulic vibrations: - Strong hydraulic vibrations may damage pipeline, internal lining, or system equipment. Such long-term moderate surges may gradually lead to fatigue failure. Oscillations of water masses through a pipeline may also cause vibrations and suction of air into the pipeline. Therefore, neglecting such influences during the design phase may lead to system damage.

Water quality and health implications: - Hydraulic transients may result in objectionable effects on water quality and have serious health implications. High intensities of fluid shear stresses from hydraulic transients may cause erosion and resuspension of settled particles as well as biofilm detachment. Moreover, low-pressure transients can cause the intrusion of contaminated ground water into a pipe at a leaky joint and/or through cracks in a pipe. Depending on the size of the leaks, the volume of intrusion might range from a few liters to hundreds of liters, depending on the size of the leaks.

2.1.4 Factors affecting hydraulic transients

According to (Chowdhury et al. 2011) the magnitude of the transient pressure peaks depends on many factors, and some of these factors are:

a. *Pipeline length:* - the longer the pipeline the stronger the hydraulic transients. Branched pipeline configuration is better in handling transients
b. *Pipeline profile:* - Pipe profile has a direct effect on minimum transient pressure if water column separation takes place, because profile is associated with initial hydraulic energy. On the other hand, Pipe length influences on the reflection time and the inertia of water inside the pipe. The longer the pipe is, longer the time it takes for the wave to reflect at the

outlet and return to the starting point. In addition, longer pipes convey larger mass of water which affects the moment of inertia of the water column.

c. *Dead end pipes:* - In most distribution systems, loops are formed to ensure system reliability and flexibility. In the areas which have branch system, significant numbers of dead-end pipes are common. Dead end pipes are more sensitive in the event of water column separation or of negative transient pressure. The intensity of negative surge at the dead ends is higher than any other location. Therefore, resultant surge behavior is very much affected by the quantity and the layout pattern of dead ends.
d. *Pipe cover setting:* - Due to the pressure changes created by disturbance, there will be oscillations of the pipe in the ground. Therefore, the filling around the pipe will have a great effect on the wear of the pipe. Sharp stones, for example, can tear the pipe exterior. For submerged pipes, consideration must also be given to the depth of the pipe because the pipe wall is subject to the difference in pressure between the pressure inside the pipe and the external pressure from the surrounding water. If the pressure from the surrounding water is greater than the pressure inside the pipe, there is a risk of collapse or buckling.
e. *Rate of change of the flow:* - the more rapidly the flow changes, the higher are the generated hydraulic transients. Flow change depends on the valve operation, pump characteristics.

2.1.5 Hydraulic Transient analysis

The understanding of the severity of transient events resulted in consideration of pressure transient analysis in engineering applications. A comprehensive investigation of transient algorithms was not possible until recently when the advances in computational technology enabled a numerical analysis of the phenomenon. Researchers started to develop computational solutions to fluid flows in pipes. In this period the most famous model was developed (Streeter and Wylie, 1967) in which a transient solution was undertaken using Eulerian based Method of Characteristic (MOC) and Lagrangian based Wave Characteristic Method (WCM), which was initially termed as the Wave Plan Method (Wood et al., 1966).

Numerical Models: - Using mathematical models to analyze flow in water distribution system networks has been in existence for more than 60 years.

a. Method of Characteristics (MOC)

The Method of Characteristics (MOC) is a Eulerian approach to solving transient problems. In a Eulerian approach, fluid motion is given by completely defining properties (i.e., pressure, density, velocity, etc.) as functions of space and time. Information about the flow is obtained at fixed points in space as the fluid flows through those points. Munson et al. (2009, cited in Hoagland, 2016)

The MOC tracks a disturbance in time-space grid using a numerical model based on characteristics (Jung et al., 2009)

Although it is the most precise of the Eulerian approaches in terms of representing the governing equations, solving a typical transient pipe flow problem needs multiple calculations. Specially, if the pipe system becomes more complex, the number of required calculations increases, and a computer program is required for practical applications (Wood et al., 2005). The MOC expresses partial differential equations of motion and continuity as four total differential equations in finite difference form Wylie and Streeter (1978, cited in Hoagland, 2016). The two partial differential equations of motion (momentum) and continuity are shown in Equations 19 and 20, respectively.

$$\frac{\partial H}{\partial t} + gA\frac{\partial H}{\partial x} + \frac{fQ/Q/}{2DA} = 0 \text{.............................(5)}$$

$$\frac{\partial H}{\partial t} + \frac{a^2}{gA}\frac{\partial Q}{\partial x} = 0 \text{......................................(6)}$$

These equations are one-dimensional unsteady flow equations which are simplified and broken down into the four total differential equations;

$$\frac{g}{a}\frac{dH}{dt} + \frac{dV}{dt} + \frac{fV/V/}{2D} = 0 \text{.............................. (7)}$$

$$\frac{dx}{dt} = +a \text{.. (8)}$$

$$-\frac{g}{A}\frac{dH}{dt} + \frac{dV}{dt} + \frac{fV/V/}{2D} = 0 \text{............................ (9)}$$

$$\frac{dx}{dt} = -a \text{.. .(10)}$$

These equations are solved simultaneously in order to obtain a solution for each predefined spatial increment over a specific time period. There are often many spatial increments per pipe when analyzing water distribution system transients using the MOC. The solution methodology is quite stable; however, it requires a very large number of calculations for networks with many pipes.

b. Wave Characteristic Method (WCM)

The Lagrangian approach follows changes in pressure waves (both positive and negative amplitude) as they move through the pipe network, updating the network's state only when a change happens, such as when a pressure wave hits the pipe's end node (Wood et al., 2005).
The Wave Characteristic Method (WCM) follows a Lagrangian approach to analyze transient events. The Lagrangian approach involves following individual fluid particles as they move and determining how the fluid particle's properties change as a function of time. Munson et al. (2009, cited in Hoagland, 2016).
For complex water distribution systems, the WCM typically requires orders of magnitude fewer calculations which allows for a much faster simulation time" (Wood et al., 2005). The WCM incorporates the same partial differential equations as the MOC into the solution methodology. However, the WCM does not require calculations for a fixed spatial grid for each time interval. Rather, the WCM only makes calculations when change is occurring in the system (Hoagland, 2016). Generally, for many researchers to date, the MOC or the WCM are the most commonly used numerical solution for modelling pressure transients. In addition, the most of the available on the market software incorporate one of these methods.

Computational hydraulic transient analyses are mainly undertaken in the design stage of pipe systems and focus particularly on the protection of pumping stations. Researchers, who were aware of the impacts of the transient, exhorted to carry out water hammer analysis also for every major system design or operation change (Kroon et al., 1984). A pressure transient analysis carried out in the operational stage is essential for diagnosis of system component malfunctions or for understanding the causes of a pipe burst.

Modern computers models can greatly simplify the highly time-consuming methods for hydraulic transient analysis. Nowadays, several commercial software packages for performing transient analysis in a complex pumping systems and piping networks are available. Among them Bentley HAMMER, KYPIPE (Pipe Surge) and Info Surge are the most widely used computer models. But the technical capabilities, user interface, solution methods, graphical display, and technical support and training vary considerably among the packages. The features of commonly available computer packages to analyze pressure transients using the WCM and MOC are given in Table 2.2 highlighting their advantages and disadvantages.

Table 2.2 Summary of available computer packages for pressure transient analysis

Method of calculation	Name of the computer package	Advantages	Disadvantages
Wave Characteristic method	Surge 2000	➢ Computational efficiency and stability of calculations (suitable for very large networks). ➢ Suitable for pressure sensitive demand calculation. ➢ Dynamic friction option. ➢ Fully integrated with GIS software and steady state modelling software package, PIPE2000. ➢ Intrusion calculation.	➢ Single step friction calculation per pipe leads to the limitationson length of single pipe section.
	H20Surge/ InfoSurge	➢ Computational efficiency and stability of calculations (suitable for very large networks). ➢ Fully integrated with GIS and CAD software. ➢ User driven real time functionality that allows running EPS simulations and surging run for desired critical time with automatic calculation of boundary conditions. ➢ Intrusion calculation.	➢ Single step friction calculation per pipe leads to the limitationson length of single pipe section.
Method of Characteristics	Hammer	➢ Distributed pipe friction can be included. ➢ HAMMER can run on any of four supported platforms - GIS, CAD, MicroStation, and stand-alone offering true interoperability.	➢ Computationally inefficient and instability, depending on the selection of computational time.

Source: (Rathnayaka et al. 2013)

2.1.6 Transient controls

Ideally a hydraulic system design process will include an adequate investigation and specification of equipment and operational procedures to avoid undesirable transients. However, in reality, transients will still occur despite the design parameters; hence, remedial measures are required to keep transient conditions from seriously disturbing the proper functioning of an existing system. Accordingly, two possible strategies for controlling transient pressures are presented by (Walski et. al., 2003). These are:

1. Focus on minimizing the possibility of transient conditions during project design by specifying appropriate system flow control operations and avoiding the occurrence of emergency and unusual system operations.
2. Pay special attention in reducing the risk of transient conditions during project design by specifying appropriate system flow control activities and avoiding the occurrence of emergency and atypical system operations.
3. To install transient protection devices to control potential transients that may occur due to uncontrollable events such as power failures and other equipment failure.
4. Install transient protection devices to prevent potential transients caused by unpredictable occurrences like power outage and other equipment failures.

2.1.7 Protection devices

The engineer would like to design flow control equipment in such a way that major transients are avoided as much as feasible. The engineer can use a transient model to test different valve working speeds, pipe sizes, and pump settings to see if the transient effects can be kept to acceptable levels. If transients cannot be prevented, special transient control devices may be required (Walski et. al., 2003). Some methods of transient prevention include:

- *Slow opening and closing of valves*: Longer pipeline systems typically necessitate slower valve operation times. To avoid creating transients, operators should be taught on correct valve operation.
- *Proper hydrant operation*: Transients in smaller distribution pipework are most commonly caused by closing fire hydrants too quickly. Personnel from the fire and water departments should be instructed on how to use hydrants properly.
- *Proper pump controls*: Pump flow can be slowly controlled using numerous means, except in the event of a power failure. Transients can be reduced by ramping pump speeds up and down using soft starts or variable-speed drives, but a similar effect can be achieved at a lesser cost by slowly opening and closing pump control valves downstream of the pumps. The control valve should be slowly opened once the pump is started and slowly closed before the pump is shut down.

- *Lower pipeline velocity*: Allowing higher velocities can reduce pipeline size and consequently cost. However, when pipe size decreases, the risk of significant transient's increases. Although it is usually not cost-effective to raise pipe size sufficiently to reduce transients, the impact of transients on pipe sizing should not be overlooked throughout the design phase.

In connection with this, the protective equipment listed below are required to control the maximum and minimum pressures already occurring in the system.

Pump inertia: - is the pump's resistance to acceleration or deceleration. For a given pump and motor combination, pump inertia is constant. The higher a pump inertia, the longer it takes for it to cease spinning after being turned off, and vice versa. Because they have more rotational mass, larger pumps have higher inertia. Pumps with larger inertias can help manage transients by moving water through the pump for a longer duration as they decelerate slowly. A flywheel can be used to improve the inertia of a pump. Due to the mechanical issues connected with starting high inertia pumps, the magnitude of pump inertia required to properly regulate transient pressures renders this control impracticable for lengthy systems. As a result, boosting pump inertia as a means of managing transient pressures in lengthy piping systems is not suggested.

Air Chambers / hydropneumatic tanks and Surge Tanks: - during high pressure transients, air chambers and surge tanks allow water out of the system while adding water during low pressure transients. they should be near to the point where the initial flow change occurs. A pressure vessel containing water and a volume of air that is maintained by an air compressor is known as an air chamber. The pressure and flow in the system reduces when the pump is turned off, and as a result, the air in the air chamber expands, forcing water into the system. A surge tank is a relatively modest open tank connected to the hydraulic system. it is situated so that the normal water level and the hydraulic grade line are at the same elevation. when the pump fails, the surge tank takes over and feeds the system with water by gravity. This regulates the amplitude of the low-pressure transient caused by the pump stopping.

Air-release/vacuum valves: - are installed at high points in a pipeline to prevent low pressure (cavitation) by emitting air into the pipe when the line pressure drops below atmospheric conditions. The air is then expelled (ideally at a lower rate) when the line pressure exceeds atmospheric pressure. Two-stage air valves release the air through a smaller orifice to prevent the "air slam" that occurs when all of the air is released and the water column rejoins. A three-stage air valve is designed to release the air through a second (smaller) orifice to further reduce the air slam (Wood et al., 2005).

Pressure-relief valve: - ejects water out of a side orifice to prevent excessive high-pressure surges. The valve is activated when the line pressure at a specified location (not necessarily at the valve) reaches a preset value. Relief valves are used to regulate fluid flow, and prevent pressure from surpassing a certain level.

Anticipator relief valve: - to control high pressure transient peaks, it might be used instead of a pressure relief valve. It is critical for safeguarding pumps, pumping equipment and all applicable pipelines from harmful pressure surges induced by fast changes in flow velocity within a pipeline as a result of an abrupt pump stop due to power outage. When a pump losses power, there is normally a down surge in pressure followed by an up surge in pressure. on the initial low-pressure wave, the surge control valve opens, deflecting the returning high pressure wave from the system. in effect, the valve has anticipated the return of a high-pressure wave and is open to absorb the surge that caused the damage. After that, the valve will slowly close without causing any additional pressure surges (M. Elbashir and S. Amoah, 2007

Check Valve: - allows flow only in one direction and closes when flow reversal is impending. For transient control, check valves are usually installed with other devices such as a pump-bypass line. Pumps are also often equipped with a check valve to prevent flow reversal. Because check valves do not close instantaneously, it is possible that before closure a substantial backflow may occur that can produce additional and sometimes large surges in the system. One of the great advantages of a check valve is that it can prevent pipes from draining. Not only does this save product, but also pipe filling is often problematic from a transient-control perspective. Thus, keeping the pipe full of water tends to reduce startup transients (Wood et al., 2005).

Pump-by pass line: - In low-head pumping systems that have a positive suction head, a bypass line around the pumps can be installed to allow water to be drawn into the discharge line following a power failure and a downsurge. Bypass lines are usually short pipe segments equipped with a check valve preventing backflow (from the pump discharge to the suction side) and installed parallel to the pump in the normal flow direction. They are activated when the pump suction head exceeds the discharge head and are useful for two reasons: to prevent high-pressure buildup on the pump-suction side, and to prevent cavitation on the pump-discharge side (Wood et al., 2005).

2.2 Water Distribution Modelling

Present day modeling consists of using a software program to run numerical simulations. These simulations replicate the dynamics of a real or proposed system mathematically and can be used to predict the system's response to various boundary conditions without disturbing the real infrastructure (Walski et al. 2003). The fundamental equations and specific simulation types as applied to water distribution systems are:

2.2.1 Conservation principles

Water distribution networks can be analyzed and solved using the three conservation laws: mass, energy, and momentum. Steady-state and extended-period simulations can be solved using mass and energy conservation laws, while transient analysis also requires the conservation of momentum principle.

Conservation of Mass: - The conservation of mass principle states that the quantity of mass in a closed system must remain constant over time. Unless mass is added or removed from the closed system, the quantity of mass must remain the same. As water distribution systems convey water, a constant fluid density is assumed. Therefore, the mass flow rate into the system must equal the mass flow rate out of the system (assuming no internal storage). The principle of conservation of mass based on volumetric flowrate can be summarized by Equation 11, which is a simplified form of the continuity equation.

$$\sum Qin = \sum Qout \ (2) \ \ldots\ldots\ldots\ldots\ldots\ldots\ldots\ldots\ldots\ldots\ldots\ldots(11)$$

In Equation 10, $\sum Qin$ is the volumetric flow rate entering the system and $\sum Qout$ is the volumetric flow rate exiting the system. The volumetric flow rate is equal to the average velocity of the fluid entering a pipe multiplied by the cross-sectional area of the pipe. This is summarized by Equation 12.

$$Q = VA \ldots\ldots\ldots\ldots\ldots\ldots\ldots\ldots\ldots\ldots\ldots\ldots\ldots\ldots\ldots\ldots(12)$$

Where Q represents the volumetric flow rate, V represents the cross-sectional averaged velocity, and A represents the cross-sectional area of the pipe (assuming the pipe flows full). Therefore, by multiplying the velocity of a fluid traveling through a pipe by the cross-sectional area of the inside of the pipe (assuming closed conduit flow), the flow rate of the fluid can be calculated.

Conservation of Energy: - The conservation of energy principle states that the total energy at a specified point in a system equals the energy at a downstream point, plus the energy losses (e.g. friction, minor) or gains (e.g. head gain from pump). This principle is derived from the first law of thermodynamics. Reworded, the conservation of energy principle states that energy can neither be created nor destroyed, but that it transfers from one form to another. In water distribution systems, the conservation of energy between two points can be written using a modified Bernoulli's equation.

$$\frac{\mathbf{P_1}}{\boldsymbol{\gamma}} + \mathbf{z_1} + \frac{\mathbf{V_1}^2}{\mathbf{2g}} + \mathbf{H_G} = \frac{\mathbf{P_2}}{\boldsymbol{\gamma}} + \mathbf{Z_2} + \frac{\mathbf{V_2}^2}{\mathbf{2g}} + \mathbf{H_L} \ldots\ldots\ldots\ldots\ldots (13)$$

Where; $\frac{p}{\gamma}$ is equal to the pressure head, z is equal to the elevation head, $\frac{V^2}{2g}$ is equal to the velocity head, H_G is equal to head gains from pumps, and H_L is equal to head losses. Specifically, P is pressure, γ is the specific weight of the fluid, V is the velocity of the fluid, and g is acceleration due to gravity. Note that all of the units are in length terms (i.e., feet or meters), and the subscripts 1 and 2 denote position 1 and 2, respectively. Terms without a subscript (i.e., HG and HL) refer to gains and losses between position 1 and 2.

In water distribution systems, there are several simplifying assumptions that are made pertaining to the energy equation at specific points in a network that help in the analysis. For example, water is exposed to atmospheric pressure (i.e., zero-gauge pressure) at storage tanks. Additionally, the velocity at the surface of storage tanks and reservoirs is assumed to be zero due to the relatively large cross-sectional area. The terms in the modified Bernoulli Equation are grouped to make up the energy grade line (EGL) and the hydraulic grade line (HGL), of which the formulas are shown in Equations 14 and 15, respectively

$$EGL = \frac{p}{\gamma} + z + \frac{V^2}{2g} \qquad (14)$$

$$HGL = \frac{p}{\gamma} + z \qquad (15)$$

Energy gains in the system are represented by head gains from pumps. Head gains from pumps are a function of the flow rate through the device. This relationship is best presented in the form of a head discharge curve, also called a pump head characteristic curve.

Energy losses in the system are represented as head losses. Head losses are comprised of two components: 1) frictional head loss and 2) minor head loss. Frictional losses are created due to the fluid's contact with the pipe wall, while minor losses are created due to turbulent flow through various network components such as valves, bends, and fittings.

Conservation of Momentum: - Newton's second law of motion for a system states that the time rate of change of the linear momentum of the system is equal to the sum of external forces acting on the system. To simplify this statement, the resultant force acting on a fluid element is equal to the rate of change in momentum. A simplified version of the momentum equation for one dimensional pipe flow is shown in Equation 16

$$\frac{\partial H}{\partial x} = -\frac{1}{gAL} * \frac{\partial Q}{\partial t} + f(Q) \qquad (16)$$

Where H is the pressure head, Q is the volumetric flow rate, g is the gravitational acceleration, A_L is the pipe cross sectional area, and (Q) is a pipe resistance term. Flow conditions are expressed relative to spatial (∂x) and time (∂t) variations.

2.2.2 Fundamental equations

There are a number of fundamental equations used in water distribution system modeling that are used almost universally to quantify energy losses within a system. Two widely accepted equations for quantifying frictional head loss are the Darcy-Weisbach equation and the Hazen Williams equation. Each of these equations will be discussed, as well as the method for quantifying minor losses.

Darcy-Weisbach Equation: - The famously known Darcy-Weisbach equation is used to predict frictional head loss (h_{Lf}) based on conduit length (L) and diameter (D), gravitational acceleration (g), the velocity of the fluid (V), and a roughness factor (f) which is called the Darcy-Weisbach friction factor.

$$\mathbf{h_{Lf}} = \mathbf{f}\frac{\mathbf{LV^2}}{\mathbf{D2g}} = \frac{\mathbf{8fLQ^2}}{\mathbf{gD^5\pi^2}} \quad (17)$$

Hazen-Williams Equation: - One of the most widely used equations for predicting frictional head loss in pipe flow is the Hazen-Williams equation, shown in Equation 18, where Cf is a unit conversion factor, and C is the empirically derived Hazen-Williams "C-factor" which represents the internal roughness of the pipe.

$$\mathbf{h_{Lf}} = \frac{\mathbf{C_f L}}{\mathbf{C^{1.852} D^{4.87}}}\mathbf{Q^{1.852}} \quad (18)$$

Where; Cf is a unit conversion factor, C is the empirically derived Hazen-Williams "C-factor, D is pipe diameter, L is length of pipe and Q is pipe flow rate.

Minor Losses: - The Head losses that occur at various system components such as valves, intersections, and bends are called minor losses, due to the relatively small amount of energy that is lost compared to frictional losses. These minor losses are due to turbulent eddies that are developed as the flow moves through the various appurtenances and bends. The minor loss equation is

$$\mathbf{h_{LM}} = \mathbf{K_l}\frac{\mathbf{V^2}}{\mathbf{2g}} \quad (19)$$

Where; the minor loss coefficient, K_L, is experimentally determined for each of the various appurtenances (i.e., valves, bends, etc.). However, due to the often-insignificant proportion of energy loss, minor losses are typically ignored in water distribution system models. Minor losses may play a more significant role in other portion of the system such as pump stations, where there are more fittings and higher velocities (Walski et al. 2003).

General Form Head Loss Equation: - Note that both frictional and minor losses are dependent on the velocity of the fluid in the pipe. The equation for total head is

$$h_{LT} = h_{Lf} + h_{LM} = K_P Q^s + K_M Q^2 \quad (20)$$

Where the frictional head loss term is represented by $K_P Q^s$, where K_P is the pipe resistance coefficient, and s is the exponent for the flow rate which varies depending on the loss equation that is used; the minor loss term is represented by $K_M Q^2$, where K_M is the minor loss resistance coefficient. The head loss prediction equations are embedded in the K_P term for frictional head loss. The various K_P terms with their respective prediction equations are given by;

Darcy-Weisbach K_P Term: -

$$\mathbf{K_p = f\frac{L}{2gDA^s}} \quad (21)$$

Hazen-Williams K_P Term: -

$$\mathbf{K_p = \frac{C_f L}{C^s D^{4.87}}} \quad (22)$$

The minor loss resistance coefficient, K_M, is calculated by summing the individual minor loss coefficients (K_L) and dividing by the gravitational acceleration term (g) and the area of the conduit (A) squared as shown in Equation 23

$$\mathbf{K_M = \frac{\sum K_L}{2gA^2}} \quad (23)$$

Energy Gains: - Pumps represent energy gains in water distribution system analysis. The energy-gain from a constant power pump (E_P) can be calculated by Equation 24

$$\mathbf{E_p = \frac{550 * HP}{62.4 * Q}} \quad (24)$$

Where, (HP) is the pump's horsepower, and (Q) is the flowrate.

2.2.3 Steady-State Modelling

The purpose of steady-state modeling is to calculate pressure and flow rates throughout a distribution system at a specific instant in time. With respect to transient analysis, steady-state analysis must be performed prior to analyzing the effects of a transient event. For steady-state analysis, boundary conditions (i.e., tank and reservoir levels) are set and remain constant as the simulation solves for pressure and flow. Real water distribution systems cannot be described by a single set of equations but rather a continuity equation for each node in the system and an energy equation for each loop or path (Walski et al., 2003).

2.2.4 Extended-Period Simulations

Although not required for transient analysis, extended-period simulations can offer further insight into the hydraulic dynamics of a particular system. The purpose of an extended-period simulation is to analyze a system's response (i.e., pressure and flow changes) to external demands over a predefined period of time. Throughout the simulation, various boundary conditions may change such as nodal demands and tank levels. Operational conditions may also change as pumps are switched off and on and valves are opened or closed. Simulations are often used to observe tank level fluctuations over a 24-hour period, and also in water quality simulations to keep track of water age or chlorine residual.

The analysis of an extended-period simulation is consisting of running multiple steady-state simulations at specified moments in the simulation time which are called computational intervals. A computational interval is typically on the order of minutes or hours, and is dependent upon what time scale the user wishes to observe the system's response. For each computational interval, a single steady state simulation is performed. However, the volume of water that enters or exits the closed system is calculated based on the equation 25.

$$V_w = Q \times t_c \ldots\ldots\ldots\ldots\ldots\ldots\ldots\ldots\ldots\ldots\ldots\ldots\ldots (25)$$

Where; V_w is the volume of water, Q is volumetric flow rate and t_c is the computational time interval.

Demand nodes are considered as volume sinks while reservoirs and tanks are considered as volume sources. Thus, the amount of water entering and exiting tanks is closely monitored and the resulting tank levels are calculated based on tank geometry. Note that reservoirs are modeled as infinite sources of water which remain at a constant elevation.

2.3 Overview of Previous studies

At different times, different studies have tried to assess the structural and water quality failure that pressure transients cause on water distribution systems.

According to (EPA, 2003) transient events can accelerate water quality problems by surging high pressures within the system. They may spread settled particles through the pipes. On the other side, the low-pressure transient may cause the intrusion of contamination into the pipes at leaky joints or pipe breaks. Common reasons for pressure drop in WDS include pump operation, flushing and hydrant operations, changes in demand, main breaks, valve operation and power failures.

(Gullick et al., 2005) also reinforced this idea with the results of their study. They noted that most surge events resulted in a negative pressure are caused by the sudden shutdown of pumps at a pump station because of either unintentional (e.g., power outages) or intentional (e.g. pump stoppage or startup tests) circumstances.

The study by (LeChevallier et al., 2004) examines the potential public health risks associated with the intrusion of contamination into WDS resulting from transient low or negative pressures and discovered that pipeline leaks represent a possible doorway for groundwater entry into treated drinking water during negative pressure events, and the fecal markers and culturable human viruses are prevalent in the soil and water outside of the distribution system.

In the same manner (Friedman et al., 2004) suggests that negative pressure transients can occur, and that the intruded water can travel downstream from the site of entry. And concluded that Locations with the highest potential for intrusion are sites experiencing leaks and breaks, areas of high-water table, and flooded air-vacuum valve vaults.

By reinforcing the above statement (Fleming et al. 2005) tried to analyze the Characteristics of the distribution system that increase distribution system susceptibility to low or negative pressures and their results indicate that Locations close to a pump station, Locations greater than one mile away from elevated storage, High elevated areas, Areas near dead ends, Areas located near a hydrant on a major main and Areas with low static pressures are more susceptible to low or negative pressures.

In April 2002, a Giardia outbreak occurred at a trailer park in New York State causing six residents to become seriously ill. Contamination was attributed to a power outage, which created a negative pressure transient in the distribution system. This allowed water to enter the system through either a cross-connection inside a mobile home or through a leaking underground pipe that was near sewer crossings. Blackburn et al. (2004 cited in Fleming et al. 2005)

According to (Rathnayaka et al., 2013) severe corrosion coupling with a lower pressure can trigger the pipe to failure rather than higher pressure acting on less corroded pipe. Therefore, it is highly significant to obtain the accurate corrosion details of the pipe along with the precise transient pressures to determine the failure condition of water pipelines.

Similarly, a study by (Kodikara et al., 2015) states that the failure mode of many failed pipes is longitudinal fracture that indicates pressure driven failure (with the presence of corrosion). The pipe failures that occurred due to pressure indicted that a moderate magnitude of pressure transients is capable of failing deteriorated pipes.

(El-Turki., 2013) in his thesis investigate the possibility of the failure as a result of extreme pressure build up in the pipeline from transients and confirmed that the maximum pressure in the system easily exceeded the bar rating (mechanical strength) of the pipeline. This means that the burst will be occurred due to this excessive pressure build up in the system.

(Fecser et al. 2019) tried to analyze a transient phenomenon on the curved pipe sections and results revealed that the water hammer structurally affects curved pipe sections. The risk of pipe bursts is the highest at the curved section.

(Hoagland, 2016) identified strong relationships between both transient pressure fluctuations and pipe failures, and daily pressure fluctuations from standard system operations and pipe breaks.

- Most of the studies cited here, indicate that pressure transients have a significant contribution to potential WDS damage. Furthermore, some also have tried to devise ways to reduce their impact like:

(Jung and Karney, 2006) investigated the influences of transient events by modeling pressure fluctuations due to system failures or an operational rapid change in valves. They observed that if there is no transient protection device in the system, after exerting a sudden surge, the pipe experiences considerable pressure surge with high frequency until it returns to its normal pressure condition.

(Carmona-Paredes et al., 2019) similarly pointed out their mitigation mechanism and suggest that air pockets in combination with existing devices like Air vacuum valves can protect the system adequately from transients and avoiding potential damage to the pipeline.

3. RESEARCH METHODOLOGY

In this chapter, an inline of all the activities that were carried out to achieve the objectives of the research are presented in detail.

3.1 Description of the study area

This study was conducted in Addis Ababa city. The emergence of Addis Ababa, which means 'new flower' in Amharic, can be traced back to 1886 (Elias et al., 2018) and was named by Empress Taitu after the flower of mimosa trees she found around Filwoha springs, where the earliest settlement of the city was started (Erena et.al., 2017). Addis Ababa is geographically located at the heart of the nation, 9º05´'N latitude and 38º45'E longitude. Its average altitude is 2,400 meter above sea level, with the highest elevations at Entoto Hill to the north reaching 3,200 meters (Erena et.al., 2017). Its physical landscape is a mixture of undulating and rugged topography in the northern and central parts of the city, while relatively gentle morphology and flat areas characterize the city's southern reaches Mahiteme (2008, cited in Getinet, 2019).

The total population of Addis Ababa is 3,273, 000 based on (CSA, 2015) projection with an annual rate of population growth 2.1%. However, with the current population growth rate, some recent reports estimate that Addis Ababa's population could reach 5 million after 10 years. It is expected that the influx of people from different parts of Ethiopia (because of economic reason, as the city enjoys a relatively higher concentration of facilities, infrastructure and industries compared with other parts of the country) will increase the population even further.

Addis Ababa has sub-tropical highland climate with a constant moderate temperature of roughly 23 °C average high and 11°C average low throughout the year. The main rainy season, Kiremt, is from June to early October, and between early March and mid-April, there is short period of rainfall called Belg. The average annual rainfall is about 1,200 mm, out of which close to 80% falls during the main rainy season NMA (2017, cited in Erena D. et.al., 2017).

Addis Ababa is at present supplied mainly with surface water from the Legedadi water treatment plant which is situated in the Eastern Part of the City and the Gefersa water treatment plant in the western part of the city. The Gefersa water treatment plant is supplied from the Gefersa dam and reservoir with an average daily production of 31,000m^3/day, while the Legedadi water treatment plant is supplied from the Dire and Legedadi dams and reservoirs with an average daily production of 192,000m^3/day. Additional supplies are provided from groundwater sources, including Akaki wellfield to the south of Addis Ababa and other wells and springs operating at various locations in the city with a daily yield of 257,500 m^3/day (TROPICS,2019). Thus, the total presently available supply from these sources is 479,500 m^3/day.

According to the information obtained from AAWSA, the distribution network of Addis Ababa is currently divided into 70 distribution zones based on the transmission network branch from which they are supplied. 53 of the zones are supplied from the transmission network service reservoirs or through direct connections to the transmission network pipes. The rest are borehole zones, supplied from local boreholes only without any connection to the transmission network.

To illustrate a bit, the transmission network comprises of water source collection works, network pumping stations & service reservoirs, and interconnecting pipelines. The transmission network supplies the distribution network pipes, typically via service reservoirs. The distribution network pipes extend as far as the individual consumers and include the consumer supply connections. Accordingly, this study focuses on the Gefersa WTP transmission network branch which consists of DN700/DN500 gravity transmission main, conveying the treatment plant production directly to the Core-Kolfie sub-system together with the Ras Hailu dual purpose reservoir site, from which water is pumped to Rufael and St. Paul sub-systems.

The Rufael sub-system follows the alignment of Ambo Road. The reservoir, which supplies the distribution system by gravity, is fed by pumped supply from Ras Hailu (RH) reservoir. The main consumers are domestic, with some institutional use and small-scale industries, while the St. Paul sub-system covers a relatively small area west of the Belay Zeleke road and straddles Arbaynoch Street. Water for gravity distribution comes from the St. Paul reservoir, which is fed by pumped supply from Ras Hailu (RH) reservoir. The distribution systems also get water directly from Ras Hailu reservoir by pumping. The main consumers are domestic. In order to further illustrate the Gefersa WTP transmission network branch, a summary is provided in Table 3.1.

Table 3.1 Summary of the Gefersa WTP Transmission Network Branch Distribution Zones

Supply Transmission Network Branch	Supply Transmission Network Sub-branch	Distribution Network Zones	Supply Source
Gefersa Water Treatment Plant	Core-Kolfe	*CRK-RH-G (Core Kolfe - Ras Hailu - Gravity)*	By gravity from the Ras Hailu service reservoir and directly from Gefersa main
		CRK-WB-G (Core Kolfe - Weybila Maryam - Gravity)	Pocket borehole zone
	Rufael	*RU-ASK-G (Rufael – Asko - Gravity)*	By gravity from the Asko Gabriel reservoir and from borehole sources
		RU-IYM-P (Rufael - Iyasu Minch - Pump)	By pumping from Iyassu Minch Old pumping station
		RU-KA-OLD-G (Rufael – Kale Old – Gravity)	From boreholes through Kale Old reservoir and from Iyassu Minch New pumping station
		RU-KA-NEW-G (Rufael – Kale New – Gravity)	By gravity from Kale New reservoir and borehole sources
		RU-RU-G (Rufael – Rufael – Gravity)	By gravity from Rufael New and Old reservoirs via a DN350 pump main from Ras Hailu service reservoir
		RU-KM-G (Rufael – Kidanemihret – Gravity)	Pocket borehole zone
	St Paul	*ST-RH-P (St. Paul – Ras Hailu – Pump)*	By pumping from the Ras Hailu reservoir
		ST-ST-G (St. Paul – St. Paul – Gravity)	By gravity from the St Paul reservoir

Source: (TROPICS, 2019)

The three distribution network zones supplied from the Gefersa WTP transmission network branch via the Ras Hailu service reservoir and the pump mains namely *RU-RU-G, ST-ST-G, &ST-RH-P* were selected for this study and considered jointly for hydraulic modelling. Figure 3.1 shows the location of the study area with respect to the map of Ethiopia and Addis Ababa while Figure 3.2 depicts the location of the selected distribution zones in the Gefersa WTP transmission network branch.

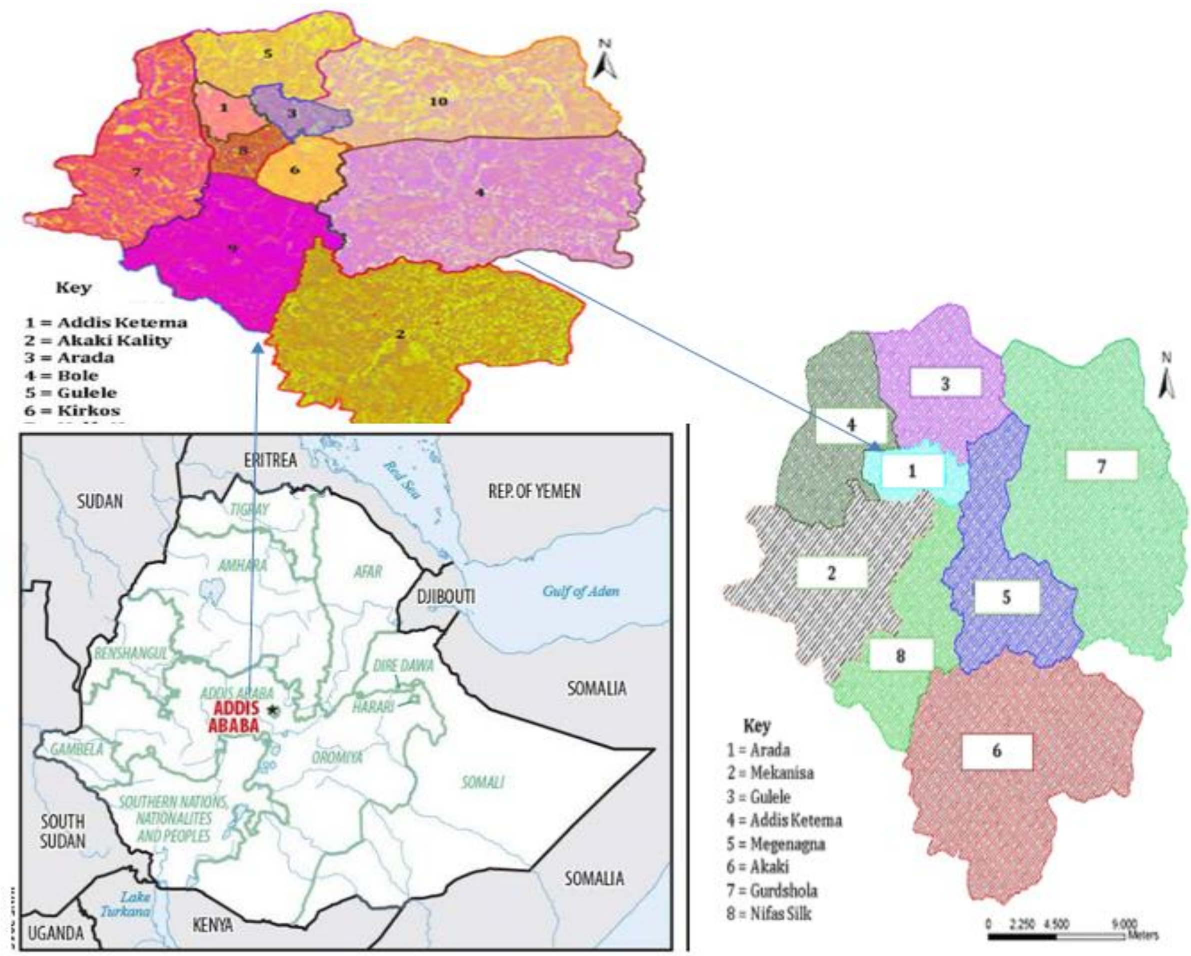

Figure 3.1 Location of the study area with respect to map of Ethiopia and Addis Ababa

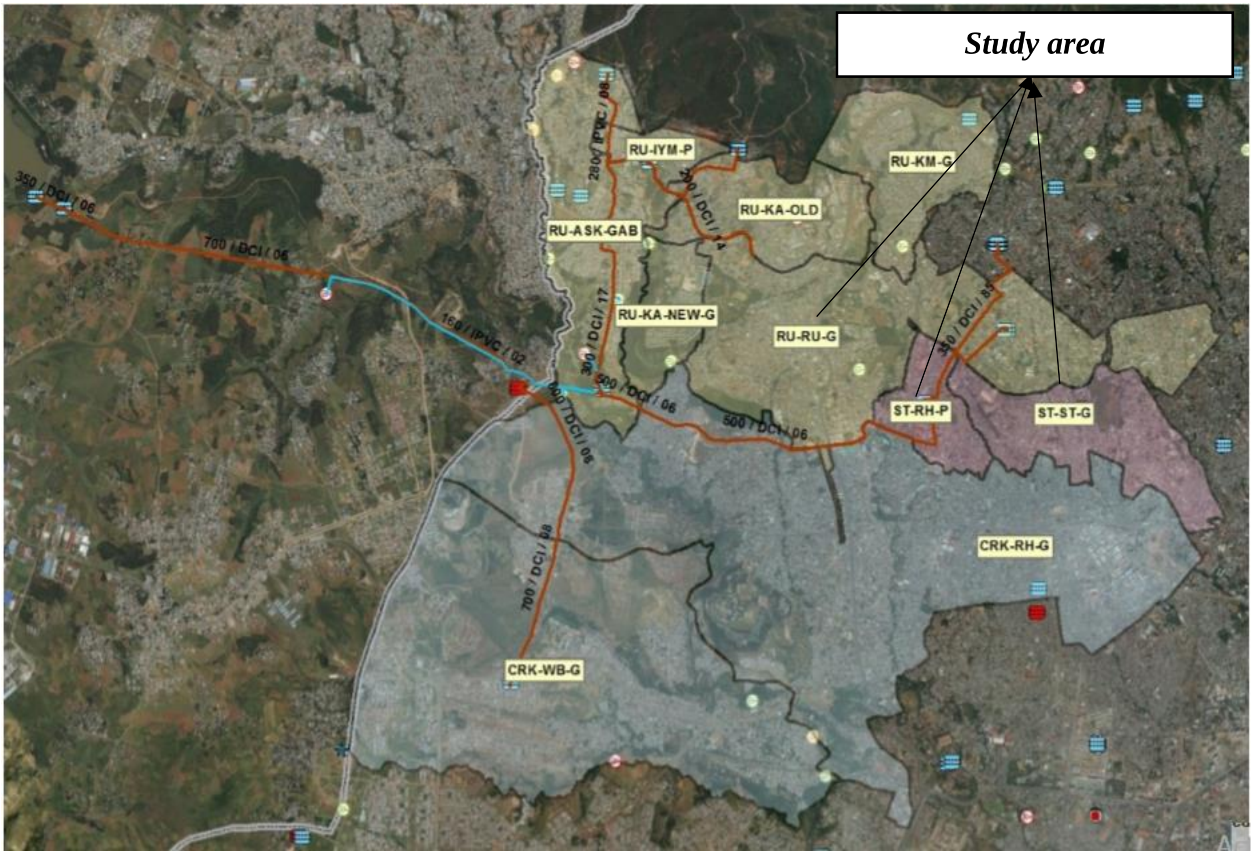

Figure 3.2 Location of the study area viewed on Google earth

Source: (AAWSA, WP1 draft final report, 2019)

3.2 Existing water supply network of the study area

3.2.1 Supply Source and Storage

The Ras Hailu reservoir (which is the principal recipient of the water that is being treated by the Gefersa WTP) is the main source of water for the three distribution zones selected for this study, and from which water is pumped to Rufael and St Paul storage tanks through DN350/DN300 pump mains, then the respective zones (RU-RU-G & ST-ST-G) are supplied by gravity, while zone ST-RH-P has a small area coverage and is supplied directly from the Ras Hailu reservoir through three small centrifugal pumps. Figure 3.3 (a) and Figure 3.3 (b) shows the current state of Ras Hailu reservoir and St Paul storage tanks.

(a)

(b)

Figure 3.3 Storage facilities: a) the two underground Ras Hailu reservoirs; and b) the two St Paul concrete tanks

3.2.2 Pumping Station

There are three pump stations in the selected distribution zones that convey water from Ras Hailu reservoir to Rufael storage tank, St Paul storages tank, and directly to the nearby areas. In pump station one (leading to the Rufael tank) there are two pumps (one operational and the other standby) each with a rating capacity of 320m^3/h and a head of 105m. Similarly, the second pump station (leading to the St Paul tank) has two pumps (one operational and the other standby) each with a rating capacity of 250m^3/h and 80m head. Unlike the two pump stations, the third pump station has three pumps (two pumps are in duty while the third pump is standby) that supply directly to nearby areas, each with a rating capacity of 62 m^3/h and 17m head. In order to get more acquainted with the Ras Hailu pump stations, the two pump stations are shown in the image below:

(a)

(b)

Figure 3.4 Ras Hailu pumping station: a) three centrifugal pumps that supply water to nearby areas; and b) the pump that pumps water into the St Paul tank

3.2.3 Distribution System Piping

The transmission and distribution system consist of a branch of mains with a total length in the system over 89 km. The system contains pipe ranging from DN 50 mm to DN 500 mm in diameter, but the majority of the system consists of 50 mm diameter pipes, followed by 63 mm diameter pipes. 7.9% (12 km) of the total pipelines in the system are distribution mains with diameters between DN 250 mm to DN 500 mm.

Table 3.2 shows the distribution of pipelines with varying diameters in the system, and Figure 3.5 represents a schematic of pipelines according to their diameters in the selected distribution zones.

Table 3.2 Distribution of Pipe Diameters in the Existing System

Pipe Diameter (mm)	Length (m)	Percentage (%)
50	23,443	29.2
63	15,085	22.32
65	1,330	1.7
75	2,370	3.44
90	4,207	5.22
100	4,989	6.12
110	9,298	10.84
150	6,444	5.23
200	10,267	8.03
250	199	0.4
300	7,228	4.46
350	3,507	2.04
400	465	0.9
500	290	0.1

The red lines represent the water pipelines in the system with diameters ranging from DN 250 mm to DN 500 mm. The rest in green represent pipes with diameters less than DN 250 mm.

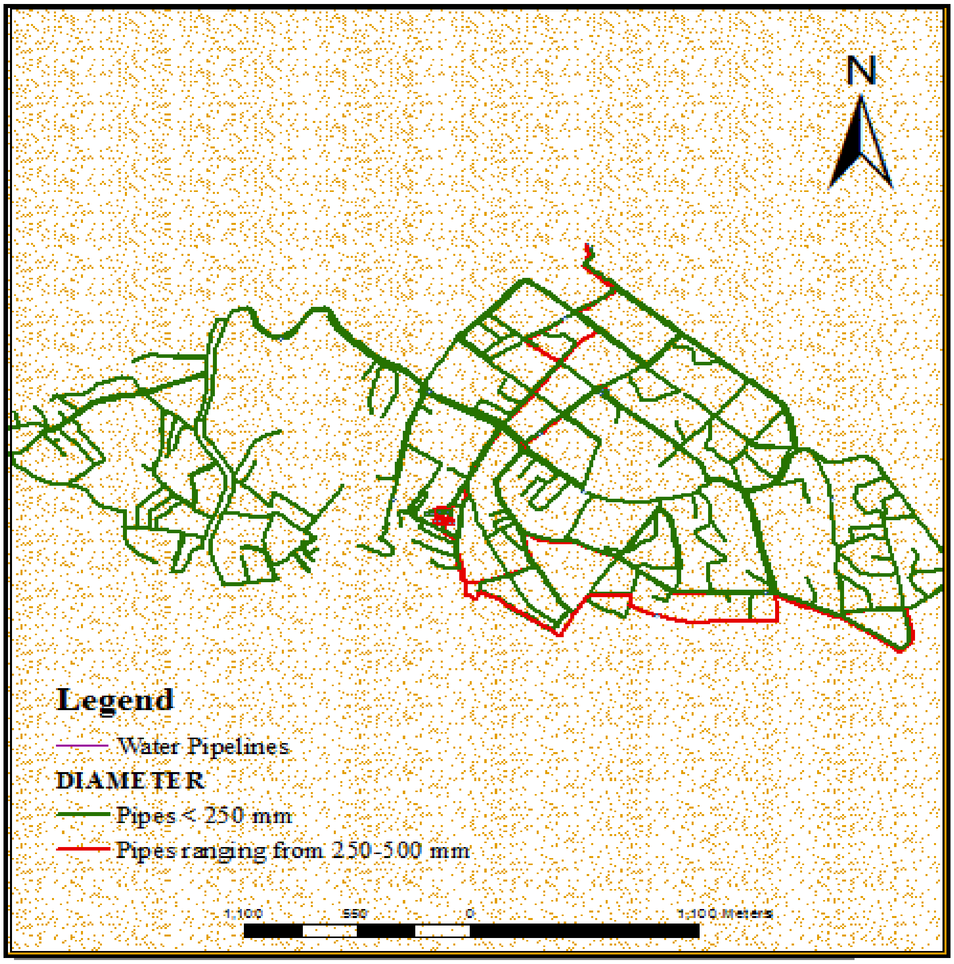

Figure 3.5 Pipelines in the system according to their diameter

Pipes throughout the distribution network mainly consist of Ductile Iron, Steel, Galvanized Steel, Polyethylene, and PVC. The total percentage of each material is approximately 29.35%, 0.15% 2.98%, 57.08%, and 10.44% respectively. The oldest pipes in the system were installed in 1955, and were made of ductile iron. 36% of the pipes present in the existing system were installed 40 years ago in 1975, and about 77% of these pipes are PVC.

Table 3.3 Distribution of pipe materials in the existing system

Pipe Material	Length (m)	Percentage (%)
Ductile Iron	26,108	29.35
Steel	134	0.15
Galvanized Steel	2,652	2.98
PVC	50,778	57.08
PE	9,282	10.44

The most widely used pipe material currently present in the system is PVC, but now in recent years HDPE (High Density Polyethylene) pipes have become more widely used in the system. Table 3.3 shows the composition of the various pipe materials in the existing system, and Figure 3.6 shows a schematic of the different pipe materials present in the system.

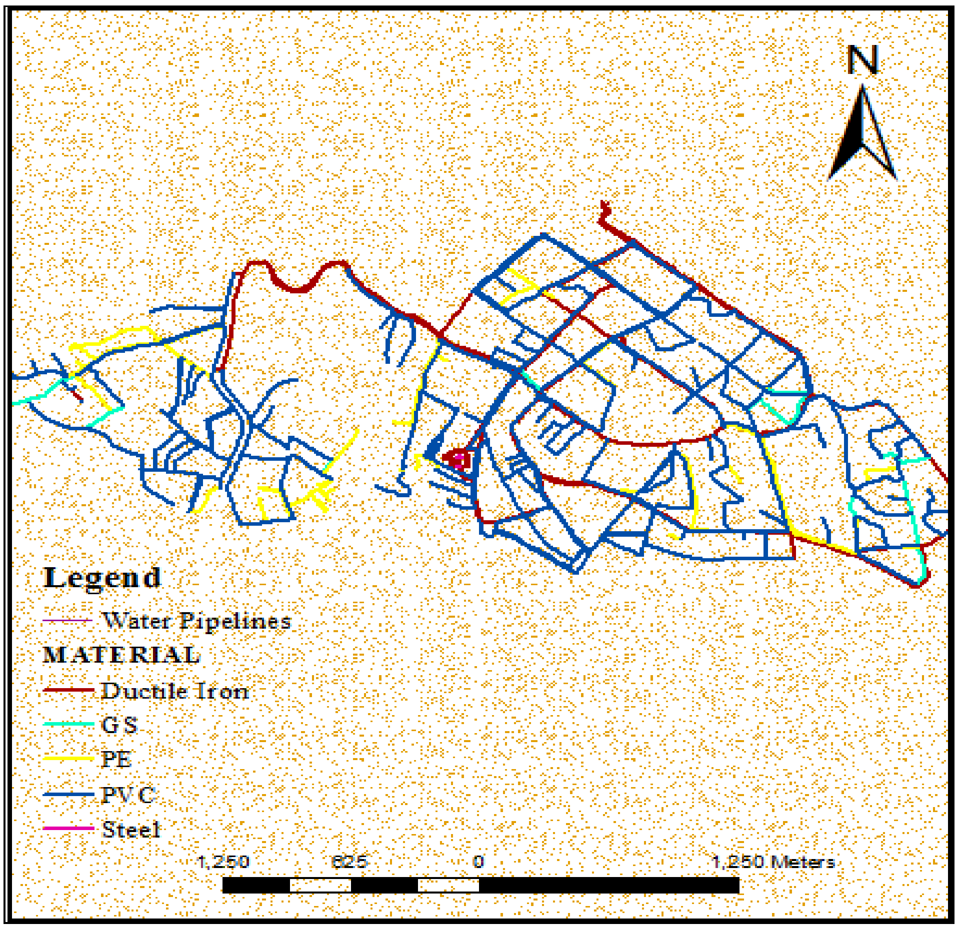

Figure 3.6 Schematic of various pipe materials in the system

3.2.4 Distribution System Valves

The selected WDN contains of 347 valves. In almost all pipelines in the existing system, gate valves have been installed to stop/allow the flow and to isolate specific areas during maintenance & new installations. On some pipelines, there are air valves to vent the air, even though most of them are out of operation. Apart from this, other types of valves such as pressure reducing valves and pressure sustaining valves are not in use in the selected network and are therefore not specified in the existing network model.

3.3 Rationale for selecting the study area

This study is conducted in three distribution zones that are found in the Rufael and Saint Paul sub branches as mentioned in the previous chapter. The choice of these distribution zones was basically based on the following reasons:

- Due to their proximity to one another
- Are interconnected hydraulically, as they have the same supply source (commonly supplied from the Ras Hailu dual purpose reservoir site)
- The term 'dual purpose' refers to the fact that the site also serves as a pump station. Due to this, it is more likely expected to be vulnerable to transients because pressure transients in distribution systems are usually most severe at pump stations.
- Additionally, the topography of the study area is undulating type in other words there is a variation in elevation. The highest point in the system is up to 2600m a.s.l. while the lowest is estimated to 2400m a.s.l, which implies locations in the system at higher elevation will have low operating pressure. This means that a transient producing event that occurs in close proximity to an area with significant elevation changes has a better opportunity at creating negative pressure in the more elevated portion of that distribution system (Fleming et.al. 2005).

3.4 Rationale for choosing modeling software

The paper aims to analyze the selected WDN in two operating modes (the engineering/steady mode and the transient mode). The engineering mode supports activities in the hydraulic analysis of a piping system. in this mode, either steady state flow condition analysis, can be carried out while the transient mode allows unsteady flow conditions to be investigated. Accordingly, among the many commercially available hydraulic modeling softwares WaterGEMS and HAMMER are chosen for the following reasons;

- Bentley Systems develop them both and therefore they have a lot in common regarding the representation of the objects like the use of links and nodes to represent a network.
- Both are integrated with geographic information systems (GIS), computer aided design programs (AutoCAD), and spreadsheets in order to facilitate model construction.
- Have a potential to handle a network of virtually unlimited size.
- The fact that they are both mutually exclusive, that is if there is a steady state model of a system in WaterGEMS, HAMMER can use that model file directly.
- Comparatively, are freely available as self-extracting executable files.

3.5 Data collection

The data collection process for this study was divided into two stages. The first was to take data from various bureaus to develop model database, and the second was to take pressure measurement from the selected sampling locations to determine if the model simulated was realistic. These two main data collection processes are presented in detail below.

For Model Development

Prior to the start of the study, officials from Addis Ababa Water and Sewerage Authority were contacted to verify that the basic information needed to generate a WDS model was available and to obtain a permit to use the data privately if available. Therefore, on this basis it was planned to gather up all relevant paper and electronic records from the appropriate department of AAWSA and conduct site inspections with an operator who can explain how the facility is operated under varying system conditions. Accordingly, the following information has been collected in order to more accurately reflect the real water distribution network.

Water Distribution Network Layout and Backbone Maps

The water distribution network layout for the entire city was obtained from the Water Distribution and System Control case team manager of AAWSA in the form of CAD file. The file contains data on network pipes such as diameter, material and construction year, location of reservoirs, valves, pumps and hydrants in the network. In addition, GIS maps of administrative boundaries were also obtained from AAWSA.

Information on Water Storage Facilities and Pumps

Attributes such as Base elevation, Minimum elevation, Initial elevation, and Maximum elevation, Diameter and Capacity for the system water tanks were also obtained from the Water Distribution and System Control Case Team of AAWSA and WP1 report (TROPICS Consulting Engineers, 2019). Information for each of the storage tanks in the system are summarized below in Table 3.4.

Table 3.4 Description of system storage facilities

Label	Capacity (m^3)	Diameter (m)	Base Elevation (m)	Minimum Elevation (m)	Initial Elevation (m)	Maximum Elevation (m)
Ras Hailu 1	2500	23.0.	2497.4	2497.4	2502	2503.4
Ras Hailu 2	2500	23.0.	2497.4	2497.4	2502	2503.4
St Paul 1	500	11.28	2546.5	2546.8	2551	2551.5
St Paul 2	500	11.28	2546.5	2546.8	2551	2551.5
Rufael New	2500	24.06	2592.9	2593.3	2597	2598.4
Rufael Old 1	500	11.76	2593.4	2593.7	2597	2597
Rufael Old 2	500	11.76	2593.4	2593.7	2597	2597

Another operational data required for input to the WDN model can include flow & head of a pump, pump speed, pump brake horsepower and related features. Such pump data was obtained from the AAWSA electromechanical department as well as from the WP1 report (TROPICS Consulting Engineers, 2020). The main data about the system pumps are presented in Table 3.5 as follows. However, it should be noted that, the names given to each pump are at the discretion of the author and not from the source.

Table 3.5 Description of system pumps

Label	Flow Q(m^3/h)	Lift H(m)	Pump Speed (rpm)	Power (KW)	Destination
RHPS1-P1	320	105	2960	160	Rufael
RHPS1-P2	320	105	2950	160	Rufael
RHPS2-P1	250	55.5	1463	75	Paul
RHPS2-P2	250	55.5	1463	75	Paul
RHPS3-P1	62	47	2940	18.5	Zone Network

Label	Flow Q(m^3/h)	Lift H(m)	Pump Speed (rpm)	Power (KW)	Destination
RHPS3-P2	62	47	2900	18.5	Zone Network
RHPS3-P3	62	47	2900	18.5	Zone Network

Elevation or Topographic Data

A 25m cell sized Digital terrain model (DTM) developed by the Integrated Land Management Information System Project Coordination Office was obtained from AAWSA to obtain ground elevations at the locations of the network model nodes. Similarly, a 1m interval contour map was also taken from the same office for comparison.

Water Consumption Data

In order to determine and allocate water demand to each supply junctions, a customer information system (CIS) database containing all information such as customer name, address, charge group (Domestic & Non-domestic), contract number, meter information (size, key, etc.) and meter-read water usage (actual monthly water consumption data) for 12 consecutive months (from July, 2019 to June, 2020) has been provided by the AAWSA, Information Technology Service (ITS) division. In connection with this, the geo-referenced customer meter data that contains coordinate data based on their physical location, such as an x-y coordinate for the entire city was obtained from the Water distribution case team of AAWSA.

Demand Patterns

The demand for water in a distribution system varies throughout the day. This variation in demand can be modeled using demand patterns. Demand patterns are simply time-varying multipliers applied to a given baseline demand. With this in mind, demand multipliers for Addis Ababa were adopted from the WP1 report (TROPICS Consulting Engineers, 2020) which are supposed to be representative of urban areas according to the Consultant's experience. (See Table 3.7 and 3.8)

Table 3.6 Domestic demand pattern

Time from start (hours)	3	6	9	12	15	18	21	24
Multiplier	0.4	0.8	1.2	1.1	1	1.4	1.2	0.7

Table 3.7 Non-domestic demand pattern

Time from start (hours)	2	4	6	8	10	12	14	16	18	20	22	24
Multiplier	0.3	0.3	1.4	1.4	1.4	1.4	1.4	1.4	1.4	1.4	0.3	0.3

Water Production Data

As Ras Hailu reservoir is considered to be the source of the system selected for this study, the total quantity of water that it receives from the GWTP should be known. Accordingly, the annual water production data of the Ras Hailu reservoir from July, 2019 to June, 2020 was taken from Operators working at the site in order to determine the amount of water that the Ras Hailu reservoir receives on a daily basis.

Firefighting Consumption Data

The annual water consumption for firefighting (from July, 2019 to June, 2020) in the selected area was provided by the Addis Ababa Fire Emergency Prevention and Rescue Authority Addis Ketema Branch Office (See Table 3.9).

Table 3.8 Monthly Water Consumption for Firefighting

Date	**Monthly Water Consumption for Firefighting (lit)**
Jul-19	8,000
Aug-19	4,000
Sep-19	6,000
Oct-19	59,000
Nov-19	46,000
Dec-19	63,000
Jan-20	111,500
Feb-20	120,000
Mar-20	45,500
Apr-20	154,000
May-20	71,000
Jun-20	27,000

For Model Calibration

Pressure had to be measured directly during a WDS analysis in order to calibrate a hydraulic model to enhance confidence in the model and provide a thorough understanding of the hydraulic system's behavior and performance. Based on this, pressure was measured by taking into account the following circumstances and procedures:

Sampling Locations

Nine representative sampling points for pressure measurements that reflect a variety of situations in the distribution network were selected primarily based on the hydraulic modeling output and the operational experience of the water utility technicians. Pressure measurements were collected using Metrolog P V2.15 data loggers installed at pressure measurement points (customer's meter near the supply nodes). These pressure measurement points are listed in Table 3.10 and their position is indicated on the GIS maps shown in Figure 3.7.

Table 3.9 Location of representative samples nodes and the corresponding sampling points

	Sample Junction Nodes					Sampling Points			
	No	**Label**	**x**	**y**	**z**	**Label**	**x**	**y**	**z**
For Calibration	1	J-8	468,000.46	1,000,578.05	2,523.96	4-Menta	467876.56	1000542.7	2525.63
	2	J-215	469,794.32	1,001,002.77	2,575.84	Rufael	469804.66	1000993.34	2571.06
	3	J-243	470,285.61	1,000,466.09	2,553.09	Paulos	470231.42	1000570.61	2554.36
	4	J-314	470,846.83	1,000,034.03	2,517.45	Enqulal Fabrika	470852.46	1000033.28	2515.62
	5	J-350	471,111.12	999,212.45	2,469.90	Chew Berenda	471131.8	999189.3	2469.91
	6	J-413	469,556.06	1,000,218.01	2,518.34	Medihanealem	469508.27	1000254.54	2519.56
For Validation	7	J-81	468,325.40	999,290.36	2,477.55	Kolfe	468337.57	999304.56	2476.89
	8	J-291	470,111.93	999,503.00	2,492.15	Pastor	470136.92	999808.55	2495.67
	9	J-178	469,925.48	999,036.85	2,476.37	Abebe Bikila Stadium	469942.49	999088.27	2478.53

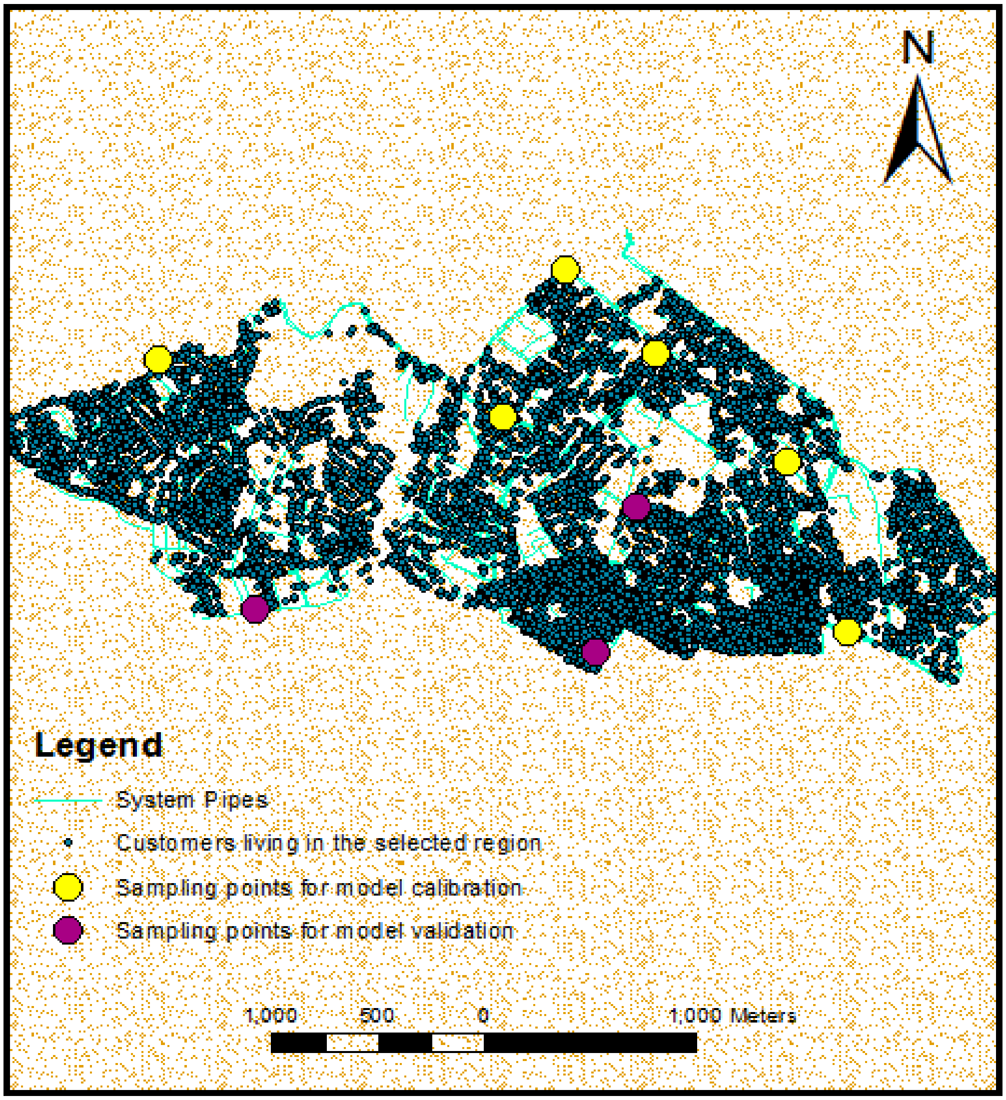

Figure 3.7 pressure measurement-sampling locations

It is recalled that pressure tests were conducted at customer's meter locations, yet various studies have shown that measuring pressures at such a location can lead to pressure fluctuations due to head loss in the service line as flow changes especially when usage is sporadic.

In the face of all this, one of the reasons why the required pressure measurements were taken from the customer's meter rather than transmission mains, hydrants, etc. was a safety issue (in order to regularly inspect and safeguard the measuring equipment, sampling locations must be properly secured). As a result, individual housing was selected and the head loss between these sampling points and supply main nodes had been considered in order to compensate for losses up to mains.

The implementation of the field survey for each sampling sites included the following stages;

- Reprogramming and tagging of data loggers that will be used to measure pressure from the selected nine sampling points in the office.
- Simultaneous installation of these nine data loggers on the selected nine representative sampling points on the same day for a period of 24-hours.
- Removal of loggers and downloading of measurement data.

Note that taking measurements at two measurement points had to be repeated due to the sudden run out of water on the day they are scheduled to receive it. Thus, these two points were recorded theoretically under different boundary conditions (water levels at tanks Rufael and St. Paul) than the remaining seven points, but practically the boundary conditions were similar in each day. This is because the dynamics of the daily pumping of water to these water tanks from Ras Hailu reservoir and the release of water from these tanks to the local residents is fairly the same in each day, and significant variation of water levels in the tanks between two different days within the measurement period is not expected to warrant a different boundary condition for the analysis. As a result, the assumption that all nine points have a similar boundary condition is fairly accurate. Furthermore, according to office engineers who record and monitor daily water level fluctuations in these tanks, there is no discernible variation in water level between the two days in a week or two weeks (as long as there is no significant change in the pumping and consumption pattern), further attesting the assumption of a fairly consistent boundary condition.

Sampling Size

There was a report released by the AWWA Engineering and Computer Applications Committee in 1999 G.C. This report was titled ECAC Calibration Guidelines Report and presents a set of criteria for model calibration. These criteria are summarized below in Table 3.11 (copied directly from the report).

Table 3.10 ECAC Draft Calibration Criteria for Modeling

Intended Use	Level of Detail	Time of Simulation	Number of Pressure Readings	Accuracy of Pressure Readings	Number of Flow Readings	Accuracy of Flow Readings
Low-Range Planning	Low	Steady-State or EPS	10% f Nodes	±5 psi for 100% Readings	1% of pipes	± 10%
Design	Moderate to High	Steady-State or EPS	5% - 2% of Nodes	±2 psi for 90% Readings	3% of Pipes	± 5%
Operations	Low to High	Steady-State or EPS	10% - 2% of Nodes	±2 psi for 90% Readings	2% of Pipes	± 5%
Water Quality	High	EPS	2% of Nodes	±3 psi for 70% Readings	5% of Pipes	± 2%

The number of pressure readings is related to the level of detail as illustrated in the table below.

Level of Detail	Number of Pressure Readings
Low	10% of Nodes
Moderate	5% of Nodes
High	2% of Nodes

However, another report released by AWWA in 2012 emphasized that the criteria included in the ECAC Calibration Guidelines Report were so controversial in content that it couldn't be approved by the committee and therefore shouldn't be considered as true calibration standards. Nevertheless, the (ECAC, 1999) report was used as a starting point for this study. Accordingly, the question of how many samples should be taken from the network in relation to the intended use of the model to be developed was answered as follows.

- Intended use: - for transient analysis
- No of supply nodes (Junctions) in the network: - 433
- Minimum No. of pressure readings: - 2% of supply nodes (junctions)
- Accordingly, the sample size should be: - 9 junctions (in context of this study, 9 customer meters representing the junctions were sampled for both calibration and validation purpose)

Equipment Preparation

A pressure data logger has been used to measure the pressure in the selected sampling points since AAWSA currently uses pressure data loggers for measuring and monitoring pressure in the WDS. Thus prior to use these devices in the field, a preliminary test was conducted to determine whether the loggers are working properly and ensure that their current state was adequate for field testing. Then the next step would be programming and tagging all the properly working data loggers in the office following the procedures outlined below to ensure that the data obtained from the field were valid for its intended purpose.

- Installation of PMAC Lite software (designed for this purpose) on a personal computer
- Connecting a Personal Computer to communication connector on logger via a data cable
- Once the logger has been connected to a computer, PMAC Lite software was opened and all the relevant information such as installation address, installation date, removal date, and measurement file name were entered in the data entry field of a logger that contains some of the logger configuration parameters.
- Finally, the logger became reprogrammed, meaning that the oldest day of data was deleted and new data was stored in its place.

It is also important to note here that tee pipes (to keep customers from running out of water on the day of the pressure measurement) and connecting hose (to connect the customers meter to pressure data loggers) were also required for the field work. The field data collection process is shown in Figure 3.8 below.

Other Considerations

Water shifting schedule: Through discussion with senior technicians working at AAWSA and reviewing their water shifting schedule, efforts have been made to determine which villages would receive water on a daily basis to adjust the field survey date accordingly.

Availability of assisting personnel: another important thing to consider was to make sure that the field workers were available to assist with testing.

Preliminary exploratory survey: It was important to conduct an exploratory survey to ensure if the selected sites were indeed suitable for testing purpose.

Figure 3.8 Field data collection process

3.6 Model Development

3.6.1 General

Before the transient analysis was possible, a calibrated extended period simulation (EPS) model was necessary to provide initial and boundary conditions for the transient simulation. Therefore, a hydraulic model which is representative of the current water distribution system was created using WaterGEMS a proprietary program (developed by Bentley systems, USA). WaterGEMS allows users to create a model of a system comprised of pipe links and nodes (junction, storage tanks & reservoir nodes). The program can be used to simulate numerous different scenarios in the system and analyzing the network through an iterative process utilizing the mass balance concept. The process provides results for pressures, flow, velocities, and hydraulic grade lines in pipes and nodes throughout the system.

3.6.2 Development of network database

Prior to performing the calculation, the input file or the data needed for the calculation has to be prepared. According to a 2012 AWWA report, the information required to create an accurate model is divided into four categories. These are geographical, facilities, operational and demand data. Thus, before these data were compiled and entered into the hydraulic model, the network database was prepared in the following order.

- Delineating the selected water distribution zones from the entire city water network map developed in AutoCAD format by setting up distribution zone boundaries as a background.
- Geo referencing and projecting the maps by making CAD .dwg file readable in Arc GIS in order to facilitate the development of a digital model of a pipe layout with actual length.
- GIS shapefiles for the water network components (pipes, service reservoirs, storage tanks and pumps) and appurtenances (gate valves, fire hydrants, air valves & end caps) along with their attribute information were created on the geo referenced maps.
- Exporting the new created GIS shapefiles into the hydraulic modeling software using the Model Builder tool available in the WaterGEMS software. A synchronization relationship was created between the Pipes and Point GIS files and the Pipes and Junctions elements of the hydraulic modeling software file.
- Checking for the connectivity errors (errors in the conversion process from the created GIS shapefiles to the pipe and node elements in the hydraulic model). These errors result in

certain pipes or nodes being entirely disconnected from the rest of the distribution network. They are unnoticeable at the normal zoom level so that it would take a great deal of time to check each pipe or node manually for connectivity. But the goodness is that WaterGEMS have a built-in tool called "Network Navigator" which helps to identify and resolve such kind of issues by highlighting system components which were completely disconnected. Accordingly, some pipelines and facilities were redrawn to resolve model connectivity issues.

3.6.3 Compilation of data

Once the shapefiles for the selected systems have been prepared in this way, the data (facilities data, elevation data, and demand data) that must be supplied for the various components included in a water distribution network model will be developed either on the GIS or hydraulic modeling software (WaterGEMS) database. Table 3.12 lists information for input to the hydraulic model and detail explanation for some of these parameters is also provided below in the next sub sections.

Table 3.11 Some of the information required to model network components

Component	Properties	Remark
Pipes	ID Label Start node End node Diameter Length Roughness coefficient Wave speed	For Transient Analysis
Junctions	ID Label Elevation Demand Demand Pattern	
Reservoir	ID Label Elevation Elevation (Inlet/Outlet Invert)	For Transient Analysis
Tanks	ID Label Base Elevation Minimum Elevation Initial Elevation Maximum Elevation Diameter	

Component	Properties	Remark
Pumps	ID Label Head-discharge curve Pump inertia Efficiency Rotational speed	 For Transient Analysis " "
Valves	ID Label Valve type Elevation	

3.6.3.1 Physical Facilities Data

Facilities data for the system include the geometric descriptions and hydraulic attributes of pipes, pumping facilities, storage facilities, and other control facilities. System facilities require proper geometric data and hydraulic data. Distribution system geometry includes the connectivity, length, and diameter of pipes within the distribution system and within specific facilities. Hydraulic data for input to the model can include pump type and curve, valve type and characteristics, and pipe roughness characterization (AWWA, 2012).

Pipe Data

Model attributes for pipelines include the pipeline diameter, length, material, roughness, and wave speed. Some are described as follows;

Pipe diameters: - one of the data required for hydraulic model calculation is the nominal diameter which was obtained directly from the polyline (pipes) shapefile which created from the AutoCAD map. But note that this information on pipe diameters only reflects the size of the pipe at the time of installation. This means that it does not represent the current state of a pipe since the diameter of a pipe can be significantly reduced over time because of corrosion and other related factors. To encapsulate this, the actual diameter of the pipe is difficult to measure, so the nominal diameter is commonly used in the modeling and the roughness coefficient will often account for the diameter discrepancy (Walski et.al, 2003).

Pipe length: - the length of a pipe should reflect the whole distance that water flows from one node to the next (Walski et.al, 2003). For this study, the scaled length for each of the pipes in the network was obtained from the previously developed GIS shapefile piping layer. Therefore, it can be said that the model developed for this study is almost entirely a scaled model. But there are too many nodes at the pump station and reservoir sites in the selected system, so the researcher is forced to selectively depict these portion of the system schematically.

Pipe Initial Roughness Coefficients: - another necessary input to the hydraulic model is a pipe roughness coefficient. Pipe roughness coefficients can be estimated based on material, age, and diameter in order to account the head loss in a pipe due to friction forces and are assigned to the model as Hazen Williams C-factors. The higher the C-factor the smoother the pipe, which means less energy loss on that pipe and conversely, low C-factor is assigned to rougher pipes. Since this model or the model to be developed is yet uncalibrated, the C-factors were assigned to each pipes based on typical initial C-factors (refined through model calibration) for both new and older pipe of different materials. Accordingly, the initial C-factors were adopted from (Wood, 1991) for each pipe based on material and age as shown in Table 3.13 below.

Table 3.12 Typical Hazen-William C-Factor Coefficients

Pipe Material	Age (years)	Diameter	C Factor
Cast iron	New	All sizes	130
	5	>380 mm (15in)	120
		>100 mm (4in)	118
	10	>600 mm (24in)	113
		>300 mm (12in)	111
		>100 mm (4in)	107
	20	>600 mm (24in)	100
		>300 mm (12in)	96
		>100 mm (4in)	89
	30	>760 mm (30in)	90
		>400 mm (16in)	87
		>100 mm (4in)	75
	40	>760 mm (30in)	83
		>400 mm (16in)	80
		>100 mm (4in)	64
Ductile iron	New		140
Polyvinyl chloride	Average		140

Pipe Material	Age (years)	Diameter	C Factor
Asbestos cement	Average		140
Wood stave	Average		120

Pipe Wave Speed: - is one of the parameter needed to define the system during the construction of a transient model. It depends on the properties of the pipe & the water (i.e., the more rigid the pipe, the faster the wave speed). Based on this assumption, the HAMMER software used to analyze the transient event in this study has a tool called wave speed calculator that will derive the wave speed for each pipe in the model using the following Korteweg equation (also mentioned above).

$$a = \sqrt{\frac{\frac{E_v}{\rho}}{1+\frac{DE_v}{eE}\Psi}} \quad \ldots\ldots\ldots\ldots\ldots\ldots (26)$$

Where; a is the wave speed (m/s); Ev is the bulk modulus of elasticity (Pa); ρ is liquid density (kg/m3); D is the pipe diameter (mm); e is the pipe wall thickness (mm); E is the Young's Modulus; and Ψ is the pipeline support factor.

Note that explaining each of the properties in this equation in detail is not part of this study but it is clear from the equation that one of the properties required to calculate the wave speed of a pipe is wall thickness. However, since, it is difficult to obtain a specified wall thickness for each pipe material, wall thickness values that are believed to be in line with the current situation have been assigned to each pipe by reviewing various literatures written by various researchers in the past.

Junction Nodes Data

Junction nodes have been created at the point where two or more pipelines intersect, pipe data such as diameter, age, or material changes and at a single pipe's end (typically referred to as a dead end). Junctions play a crucial role in the hydraulic modeling of a water distribution system because customer demands are typically represented at these points. In general, the only physical feature defined at a junction node is its elevation and how this elevation data is structured as an input to the hydraulic model will be explained in detail in section 3.6.3.2.

Pump Data

Pump Characteristic Curve: - Pumps add energy to water to lift it from lower to higher levels. For a fixed rotational speed, a pump has a unique relationship between the head it can deliver and the flow rate it can supply. The curve showing this relationship is known as the head discharge curve, and it typically has a concave downward shape. The set of curves showing head, efficiency, and power as a function of flow rate are known as a pump's characteristic curves (Larry W. mays, 1999).

The pump database in the hydraulic model was populated with a pump curve for each pump in the system. As mentioned in the previous section, the total dynamic head and the corresponding flow information required to create the pump curve were obtained from the most recent pump test results which were carried out by the Consultant's staff of TROPICS Consulting Engineers PLC. Pumps are modelled by specifying the design head-flow point to which the modelling software adapts a typical pump curve. As an example, the pump curve of one of the pumps in the system is shown in Figure 3.9.

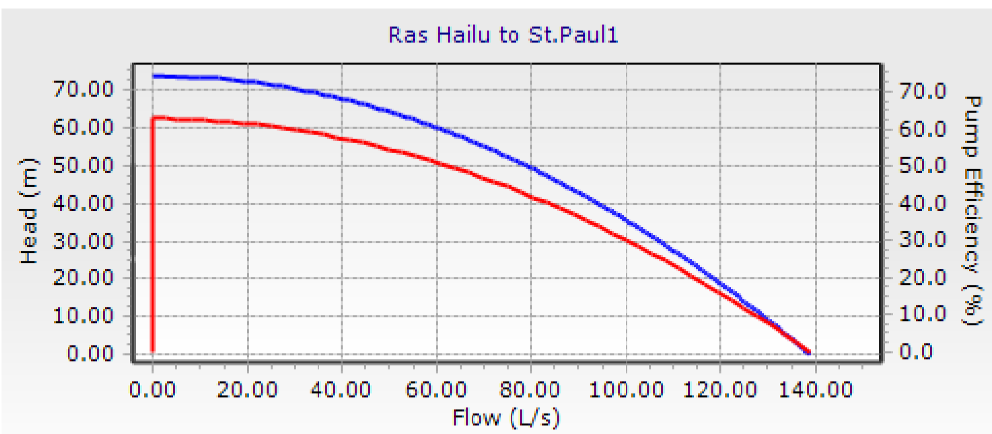

Figure 3.9 Pump curve for design operating point

Pump Brake Horsepower & Speed: - prior to running the surge model, pump brake horsepower (the power required to drive a pump) and pump speed (the rotational speed of the impeller) were also required to be inputted into the model in order to calculate the combined pump, shaft, and motor inertia for each of the respective elements. HAMMER uses inertia to track the rate at which a pump spins up or down when a power is added or removed. These values were provided directly by the pump manufacturer and available in the AAWSA electromechanical department for various purposes.

Water Storage Facilities Data

Hydraulic model elements representing water storage facilities are either tanks or reservoirs. These elements are used to store and release water as demands vary throughout the day within the water system network (AWWA, 2012).

In order for the developed model to accurately represent the actual system on the ground, important parameters such as diameter, base elevation, and water levels must be met for each of the storage tanks in the system. Such geometric inputs for these storage elements were mainly obtained from a recent study conducted by TROPICS Consulting Engineers and AAWSA, in which some of the participating staffs were able to collect these data through site visits.

Note that, in WaterGEMS the water level in a tank can be described based on either the water level above base elevation or hydraulic grade line elevation which is the elevation measured from the global datum (base elevation) plus the water levels. For this study the second operating range, type was adopted and attention should be paid to storage tanks elevation as it is used to define the HGL. Accordingly, the obtained elevation data for storage tanks was rechecked and supplemented by the researcher through site visits and inspections using a global positioning system (GPS).

3.6.3.2 Elevation Data

Node Elevation is one of an important input parameter for a hydraulic model. At this point in the process, the created junction nodes have the Geographical (x, y) coordinates but does not have elevation/Cartesian (z) coordinate. so they must be exported back to ArcGIS using the export tool available in the WaterGEMS software in order to access this elevation data for each node. Once the nodes have been successfully imported into ArcGIS, ground elevation data available in the form of Digital Terrain Models (DTMs) must be added to the map by defining both the DTM and junction node layers to the same projection system. This makes the DTM sets to appear behind the junction node shapefile as shown in Figure 3.10.

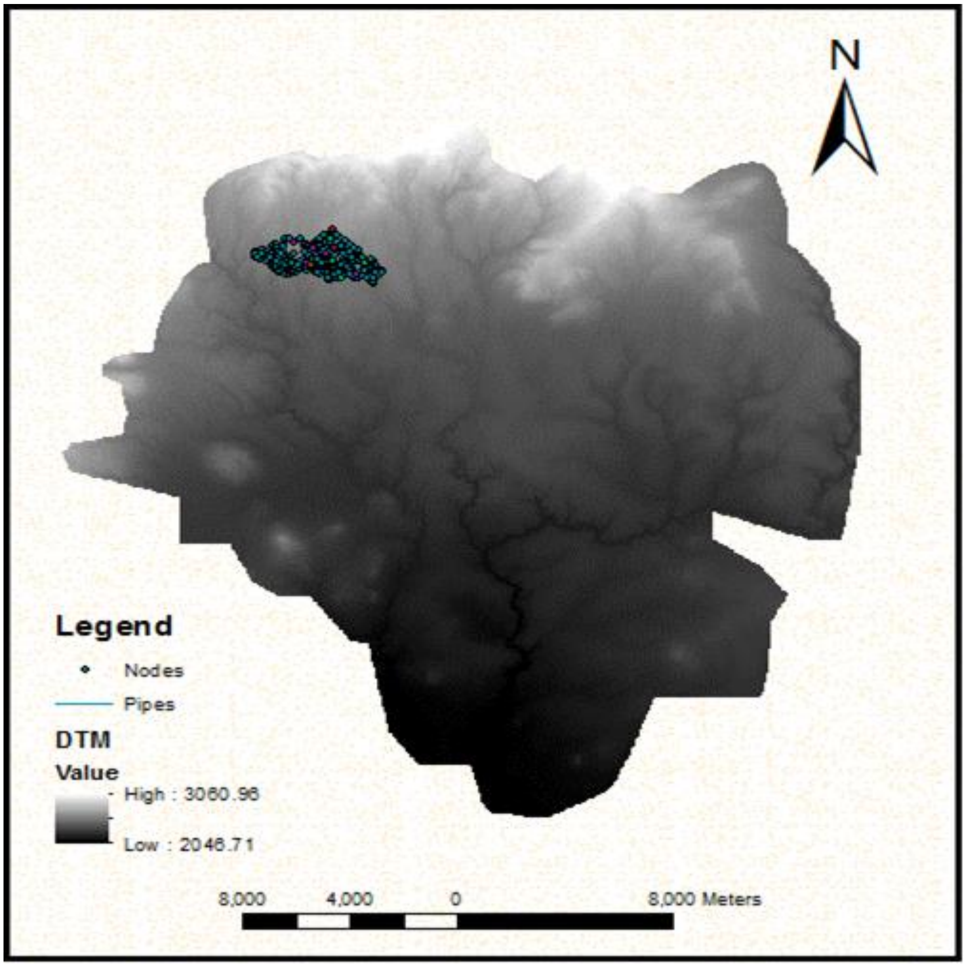

Figure 3.10 System nodes with overlain Digital Terrain Model of Addis Ababa

After verifying that the entire system has been covered by DTM, this digital terrain model was extrapolated to obtain elevations for all junction nodes and various system components (with the exception of storage facilities). Accordingly, the "Functional Surface" tool, which is built into ArcGIS, was used to extract ground elevations to all nodes based on their coordinates. Once the elevations have been extracted to the nodes, a simple copy and paste function of the values into the hydraulic model data table will complete the process of assigning elevation data to the system. Note that the main reason why DTM is preferred over other elevation techniques for modeling junctions for this study was that the elevation extracted from it was approximately the same as the elevation recorded by GPS for some of the components in the system and it is therefore believed to provide relatively accurate pressure to the system since the hydraulic model uses this elevation to calculate pressure at a given location.

3.6.3.3 Operational Data

Operational data consist of facility status changes involved in the day-to-day running of a water system to successfully deliver water to utility customers. Operational data are generally classified as two main types: (1) automated controls and (2) manual controls.

Automated controls are programmed into the utility SCADA system for automatic water system operations such as pump and valve control logic. Most modeling software packages include a control scheme that replicates the behavior of a SCADA system. The model automatically changes valve position or pump status in response to changes in pressure, flow, water level, or time at determined points in the model.

Manual controls are typically used to represent operator intervention over the system. It is often challenging to develop hydraulic model control logic for manual controls because the set point to trigger a change in facility status is not predefined. Typically, the modeler will replicate the manual control using time-based controls based on when the SCADA system showed the change of facility status occurring. This approach to emulate manual controls may be suitable for model calibration, but it is typically not recommended for analysis (AWWA, 2012).

Based on the recommendations of this AWWA report, it was not necessarily to create a system-specific controls for the selected system. This is due to the fact that automated type system controls (programmable logical controls) have not yet been implemented and its day-to-day operations are still manually operated based on the operator experience.

3.6.3.4 Demand Data

Amount of water exiting the system (demand) data were added to the hydraulic model attribute after system layout has been established and facilities data have been accurately attributed. In order to determine an average daily demand for the system one must evaluate all respective water system uses that contribute to the model output. These quantities include customer's demand (domestic and non-domestic), unaccounted for water, and firefighting. The procedures for assigning such a demand to each junction nodes in the system are briefly described as follows:

Customers demand

It is the amount of water required to meet the non-emergency needs of system users, and it is often the metered percentage of total water usage (Walski et al., 2003). This customer usage information (billing record) for each household was acquired from AAWSA for a period of 12 consecutive months from July, 2019 to June, 2020 for the purpose of generating a baseline or an average daily demand. The obtained billing data covers the water usage for nearly 161,615 registered customer accounts under three (Addis ketema, Gullele, and Arada) AAWSA branch offices. However, georeferenced customer consumption data (customer meter coordinate data) was needed to determine how many of these 161,615 registered AAWSA subscribers were living in the region selected for this study. Fortunately, AAWSA currently possess such data.

Accordingly, the whole Addis Ababa customer meter coordinate data that obtained from AAWSA in EXCEL format was imported into the GIS database in order to create GIS point shapefile. Once the shapefile was created, the spatial location of each service connections can be displayed on the GIS user interface as shown in Figure 3.11 below.

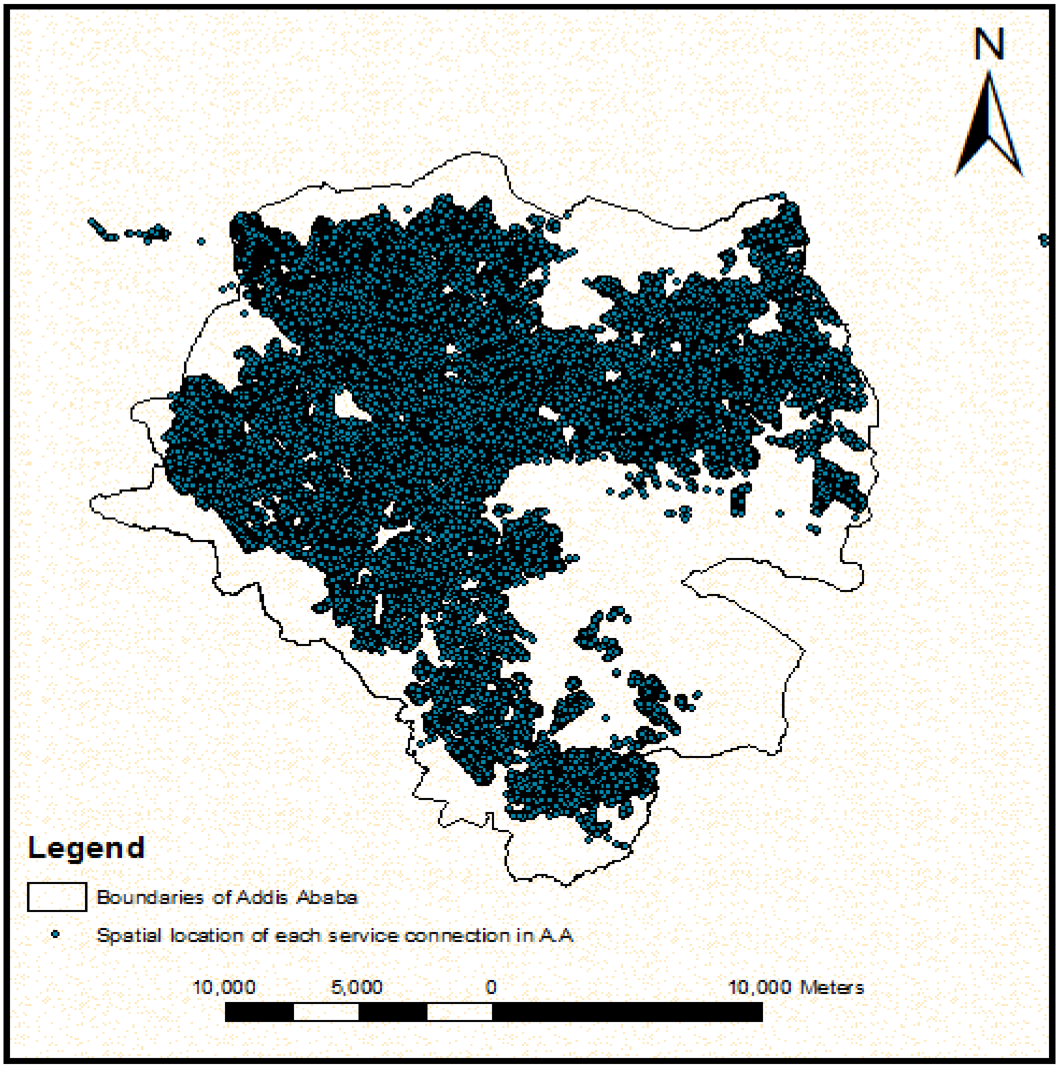

Figure 3.11 Spatial location of AAWSA customer's in Addis Ababa

Subsequently, 22,996 customers who had settled in the study area were separated from the total number of customers in the city and are categorized according to their consumption type as either domestic or non-domestic (see Figure 3.12). It has to be noted that AAWSA currently considers three consumption categories; namely domestic, non-domestic and public fountain. But, public fountain demand is neglected in this study as the percentage of people using tap outside compound shared by multiple households (public fountains) in the area is less than 0.5%.

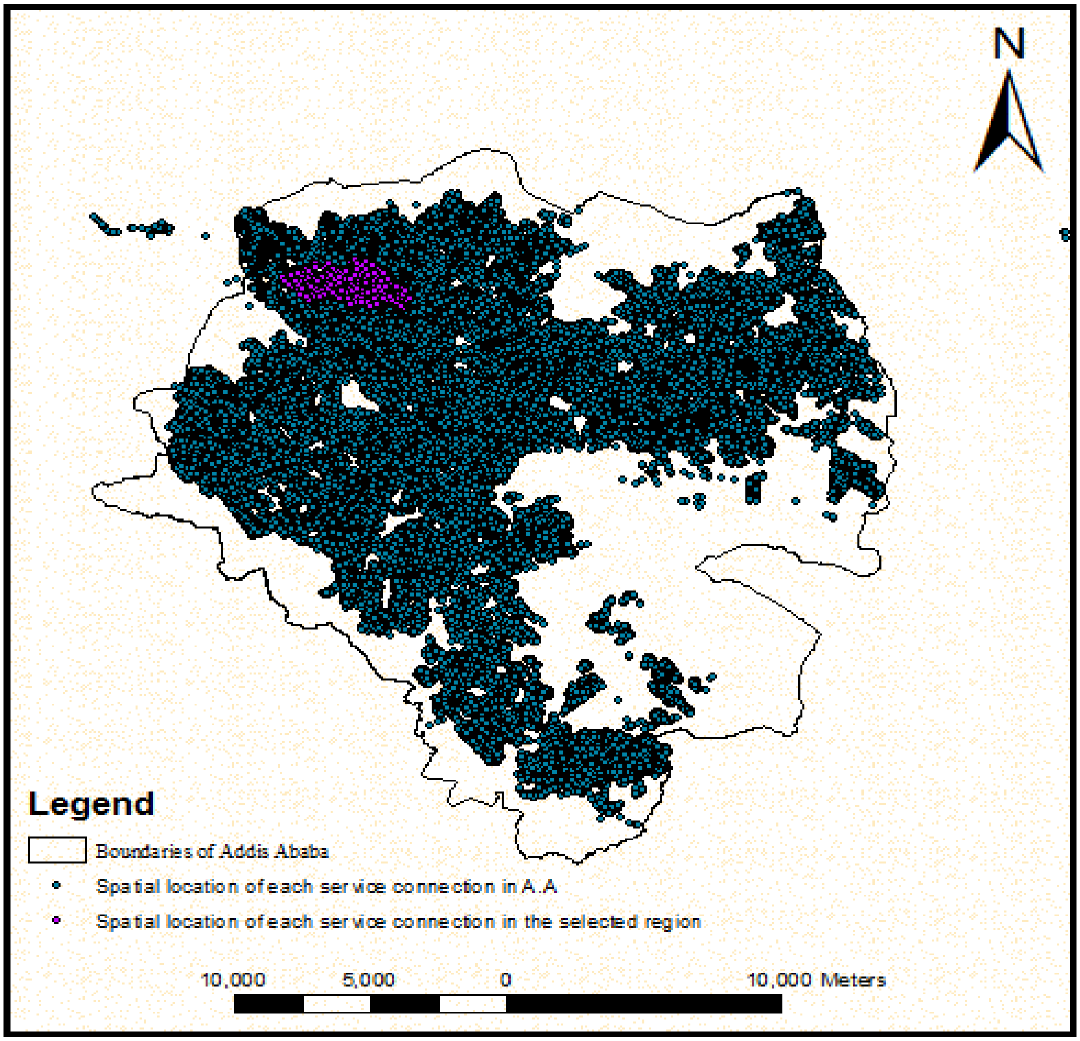

Figure 3.12 Spatial location of AAWSA customer's (customers in the selected WDS highlighted in purple)

After customers in the selected area were identified in this way, their attribute was exported back to EXCEL in order to determine their daily demand by cross referencing their spatial location with their associated monthly consumption data obtained from the CIS database. Then, the actual daily water consumption as well as the spatial representation of where that consumption occurred have been prepared in geometrical form as GIS shapefile.

Once the daily demand of customers along with their spatial locations have been set up in this way, the next task was importing the data into the hydraulic modeling software WaterGEMS to allocate this demand to each junction nodes in the system. The process of assigning such a demand to each junction nodes began with generating a Thiessen polygon in order to easily define the service areas of demand nodes (to answer the question of which demand node was closest to which inhabitants). Since each customer within a Thiessen polygon for a junction is nearer to that node than any others, it is assumed that customers within a particular Thiessen polygon are supplied by the same demand node. Accordingly, the demand from each household within each polygon can then be aggregated to that polygon's node and this was done by using the 'customer meter aggregation' option of the LoadBuider tool of the WaterGEMS software.

Unaccounted-for water (UFW)

It is the percentage of overall consumption that's lost owing to system leakages, theft, unmetered services, and other factors (Walski et al., 2003). In order to determine the total amount of water that has been lost in the system, water production data was needed in addition to consumption data. Accordingly, the annual water production data of the Ras Hailu reservoir was taken from operators working at the site in order to determine the amount of water that the Ras Hailu reservoir receives on a daily basis. Thus far, the average daily distribution from Ras Hailu reservoir to users is 15,000 m^3/day and the average daily water consumption of customers is 9055.03 m^3/day. Therefore, the amount of water that is lost due to one of the above reasons was calculated according to the equation below:

$$UFW\,\% = \frac{\textbf{Water produced} - \textbf{Water consumed}}{\textbf{Water produced}} * \mathbf{100} \ldots\ldots\ldots\ldots\ldots\ldots\ldots\ldots (27)$$

From the result obtained, the system experiencing a loss that accounted for approximately 39.63% of the total water production. Since it was difficult to identify specific areas that deal with high and low losses, the obtained amount was simply distributed evenly across all the junctions in the system.

Fire Fighting Demand

It is the water provided during fire emergencies. As mentioned in section 3.5 above, the annual water consumption for firefighting in the selected area was obtained from the Addis Ababa Fire Emergency Prevention and Rescue Authority Addis Ketema Branch Office and according to the data, the institute used 715,000 liters of water for the period of record. This annual water consumption was then converted into daily water consumption (although it is estimated that not every day there is a fire hazard) and distributed equally among each hydrant in the system. Another thing to note here is that in the event of a fire breaks out, water is wasted when firefighters try to draw water from the hydrants or when the hydrants collapses. But, the amount of water wasted in such a way is so small that it was neglected.

3.7 Model Analysis

After the basic network model inputs have been developed as described above, the next task was to carefully enter these inputs into the model and compute it with the desired type of analysis. The thing to note here is that, the overall goal of this thesis is to perform a hydraulic transient analysis. yet, a standard transient analysis typically relies on a previously constructed steady state/extended period model that contains all system characteristics pertaining to pipes, elevations, and boundary conditions. Accordingly, the following analyses were performed as part of this study: 1) steady state analysis, 2) extended period simulation, 3) transient analysis. The process by which these three analyses were performed is described below, and the results from these analyses will be discussed in more detail in the next chapter.

3.7.1 Steady-state Analysis

With respect to transient analysis, a steady-state analysis must be performed prior to analyzing the effect of a transient event on a system. This analysis focused on steady state hydraulics where the fluid momentum was not considered and the effects of all changes in the operation have stopped. Based on this assumption, for the typical average day demand, the model has been run in steady state in which the demand at each node remains unchanged within 24 hours as the simulation solves for pressure and flow.

3.7.2 Extended-period Analysis

Although the steady-state model provides results on flows and pressures in the system, it doesn’t allow the system to change over time. Therefore, extended-period model was needed to further analyze system response (i.e., pressure and flow changes) to external demands over a predefined period of time, as pumps cycle on and off, and as tank levels change using a series of steady state simulations linked with differential equation describing storage tank dynamics. In order to ensure the model would be representative of the real system flow dynamics over an extended-period of time, a demand curve was applied to the model to represent the average hourly demand fluctuations throughout a typical day.

If we look at a typical community lifestyle, there is a low water demand throughout the night while most people are sleeping. There is a rise in demand around 7 am when most people are waking up to take shower and get ready for their work day and drop slightly most of the time during the day. Another spike is observed from 6-8 pm when people are home from work and using water for various household tasks and then drops considerably over the course of the night. But, this is quite different for non-domestic areas (industry and commercial establishments) this means that most commercial establishments are open during the day and their water demand is expected to be high. Therefore, this demand curve was generated in a hydraulic model using demand multipliers which were developed by TROPICS Consulting Engineers, 2020. As an example, a typical diurnal curve for a residential area is shown in Figure 3.13

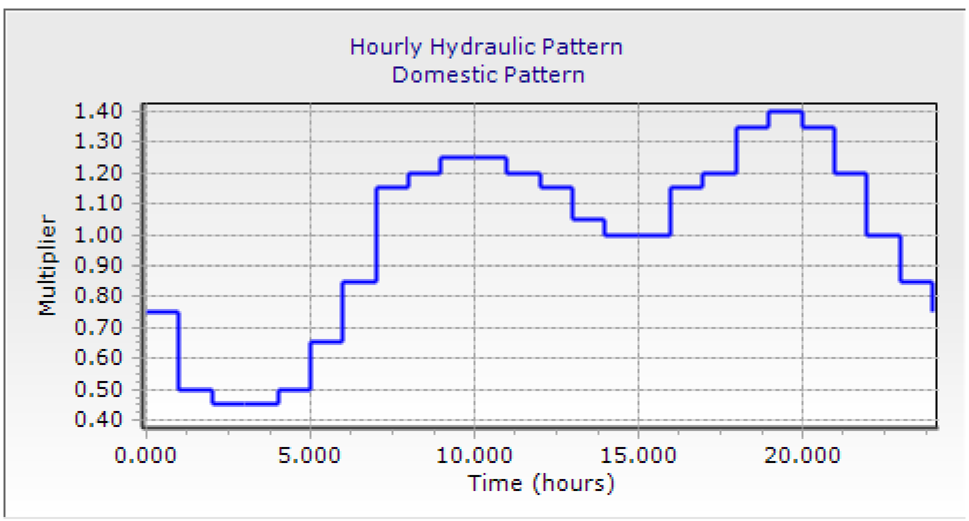

Figure 3.13 Domestic demand 24-hr pattern

So on this basis, the system has been simulated for 24-hours with a computational time interval of one-hour and the time of the day in which the simulation began was 12:00AM.

3.7.3 Hydraulic Transient Analysis

To perform a transient analysis, additional input to the EPS model was required, including: wave speed) for all the network pipelines, and pump data such as speed & inertia. To assure that the transient model was initially balanced, a 10 second transient analysis was performed with no transient producing events specified. Once this was ensured, a transient event was defined and simulated for the system as outlined below.

3.7.3.1 Initiation of transient event

In order for a water distribution system to be analyzed for its risk regarding to transient events, a transient event must first be modeled. Although there are many different transient events (such as: pump & valve operations, rapid changes in demand conditions, etc.) occurring in the system at any given time, transient events related to a pumping operation specifically a pump shutdown due to a power outage (i.e. a pump trip) have been modeled for this study since power outage is a recurring phenomenon in the area.

Now that the pump shutdown has been defined as a transient event for this study, it is possible to analyze the system response to the transients. The transient analysis was done through HAMMER CONNECT Edition software in special two scenarios. These are 1) pump shutdown without surge protection device to see where the trouble areas are for the system & determine the severity, and 2) pump shutdown by adding surge protection devices to provide an acceptable level of protection against system failure.

3.7.3.2 Modeling approach used to simulate transient producing event

The following assumption were incorporated while setting up the transient model in HAMMER.

- In this study the initial conditions were calculated using an EPS run, so it was necessary to select the time step at which the transient analysis would begin. Accordingly, the transient simulation began at the 19 th hour when the flow supplied to the system is high.
- Shut down simulation only performed for pumps that are on at this period.
- Time of initial transient was predefined or that the transient was specified to start at time t = 5 seconds, while the system was at steady-state for the first 5 seconds.
- The check valve on each pump (RHPS1 & RHPS2) has been modeled to be closed instantly after the reverse flow is detected.
- The check valve on each pump (RHPS1 & RHPS2) has been modeled to be open instantly after the specified valve opening pressure threshold is exceeded.
- Check valves are not equipped for the RHPS3 pumps, so they were modeled accordingly.

- The transient analysis was specified to run over a 120 second analysis period. This means that results were calculated for a 120 second period following the pump shutdown.
- The results were then displayed graphically and in tabular form to show how the network and individual pieces of the system performed over the course of the analysis.

3.7.3.3 Modeling approach used to simulate surge protection devices

Although detailed in the next chapter, the transient analysis indicates that severe transients may exist in the system. Thus, double acting air valves and hydropneumatic tank have been considered as solution techniques to alleviate the transient conditions. Accordingly, the following approaches were used to simulate such protection devices.

To model air vacuum valve

- Are placed directly in series with the main pipeline to view air pocket formation.
- Volume of air near the valve at the start of the simulation should be zero.
- The air/vacuum valve should be appropriately sized to reduce negative pressures in the systems. Based on this, the air inlet orifice ranges from 1-3 inches in order to allow free entry of air into the pipeline and the outlet orifice ranges from ~ ½ intake size to full intake size in order to allow discharge of air out of the air valve upon increase in pipeline pressure.

To model a hydropneumatic tank

- Located just downstream from the pump station to keep the water column moving after a pump shutdown.
- Sized appropriately for the water to supply the demands and dampen the transient wave for at least the minimum time the pump was off.
- Starting liquid volume (initial liquid volume) of the tank is assumed to two-thirds of total volume of a tank.
- Hydropneumatic tank with a bladder (more specifically the area where air/gas is contained) is preferable.
- Gas preset pressure (the pressure inside the gas bladder) is assumed to be one-third of the pump head.
- Initial hydraulic grade of a hydropneumatic tank must be defined. When initial conditions were calculated, the hydropneumatic tank was treated as a junction as if there was no tank

present and therefore the resulting HGL at the tank location was used as the initial hydraulic grade of the tank.

- Diameter of the tank inlet orifice (the size of the opening between the gas vessels and the main pipeline) should be smaller than the main pipeline.

3.8 Model calibration and validation

The modeler cannot presume that the model is an accurate mathematical description of the system just because the required data has been obtained and entered into a hydraulic simulation software package. The hydraulic modeling software simply solves the continuity and energy equations using the data provided; thus, the quality of the data will determine the quality of the output. A hydraulic model's correctness is determined by how well it has been calibrated; hence a calibration analysis should always be performed before using it for decision-making.

- The definition of calibration in itself is described in the AWWA, 2012 report as it is the process of comparing the results of model simulations to actual field data and making corrections and adjustments to the model to achieve close agreement between computer-predicted values and field measurements. Pressures, flow rates and reservoir water levels are common comparison values. Pipe roughness factors, demand at nodes, and the position of isolation valves (closed or open), control valve settings, pump curves, and demand patterns are some of the parameters that are commonly altered in the meantime (USEPA, 2005).

In this study, the EPS model was calibrated using field data on pressure as described the previous section and adjust (pipe roughness factor) to better match the actual behavior of a water distribution system since it has significant influence on system pressures. The calibration process was done through the Darwin Calibrator feature, which is a built-in tool in WaterGEMS and results obtained from it were crosschecked whether it really meets the criteria set by (Walski, 1983).

(Walski, 1983) states that for a good data set/ a model user should be able to achieve an average difference between predicted and observed head of ±5 ft. (1.5 m) to a maximum difference of ±15 ft. (5.0 m). With a poor data set, an average difference of ±10 ft. (3.1 m) to a maximum difference of ±30 ft. (10 m) is a reasonable target.

- On the other hand, validation is the steps that follows calibration and uses a separate set of field data than that for which it was calibrated in order to ensure that the model is well calibrated. The calibrated model is regarded validated if the model results (visually) substantially approximate the field findings for an adequate time period. Significant discrepancies suggest the need for more calibration (AWWA, 2005).

For this study, validation was performed manually using the correlation coefficient equation (R) method. The correlation coefficient indicates the strength of linear relationship between the model outputs and observed values. The correlation coefficient is derived by dividing the covariance of the two variables by the product of their standard deviations, this is given by

$$\boldsymbol{R} = \frac{\sum(\boldsymbol{x}-\overline{\boldsymbol{x}})(\boldsymbol{y}-\overline{\boldsymbol{y}})}{\sqrt{\sum(\boldsymbol{x}-\overline{\boldsymbol{x}})^{2}\sum(\boldsymbol{y}-\overline{\boldsymbol{y}})^{2}}} \quad \text{...(28)}$$

Where:

R is the correlation coefficient;

X and Y are the observed and computed pressure values;

$\bar{x}$ and $\bar{y}$ are mean value of observed and computed pressure;

The value of the correlation coefficient ranges from −1 to +1. If R = 0, there is no linear relationship between the simulated and observed values, while if R =1 or −1, there is a prefect positive or a perfect negative linear relationship between the variables (Zlatanovic et al. 2017).

4. RESULTS AND DISCUSSION

This chapter includes an in-depth discussion of the findings of the primary simulations (hydraulic and transient) performed for the specified system.

4.1 Steady-state Analysis

Steady state analysis was required to ensure that the layout of the system was properly configured and that no disconnected nodes were present in the system, but the results that were obtained from this analysis were instantaneous and can be representative of the system perhaps only for a few hours or for a few minutes because any real water distribution systems may not always be in a true steady state condition. As a result, this analysis was only intended to serve as a foundation for an extended period simulation model.

4.2 Extended-period Analysis

The initial reason for simulating the system over an extended period, as discussed in the earlier sections, was to understand the hydraulic dynamics of a system. Furthermore, in order to examine the transient behavior of a system, a highly calibrated and verified hydraulic model was required; hence, EPS was favored over steady state simulation for calibrating the system. As a result, the operation of a system was analyzed over a 24-hour period, allowing to see how the nodal demand and tank level (the amount of water entering and exiting tank) fluctuates in 24 hours, while also calculating pressure for each junction node as well as flow, velocity, & headloss for each pipe. At this point in the process, however, the EPS model findings are based on the data provided as an input. Although the input data was designed to be as accurate and realistic as feasible, it was necessary to calibrate the model with field data to verify whether the model output matched the real system on the ground. As a result, the EPS model was calibrated and validated as follows.

4.2.1 Model calibration

As described in detail in the preceding chapter, the calibration process began by collecting pressure measurements at selected locations. The process of collecting such a data provides an opportunity to understand the operation of the real system at a specified number of locations and times.

For achieving calibration, the Darwin Calibrator of WaterGEMS was used. In order to calibrate a model, Darwin Calibrator makes adjustments to the pipe roughness and demand till get the model results to match the field measurements. Nevertheless, the only parameter that was adjusted during the calibration process was the pipe roughness value (Hazen-Williams C-Factors). Note that the nodal demand was not modified during the calibration process since it was the actual meter data averaged over the year.

Bentley systems, in a guideline for its user's, stated that if a system has a lower fitness value during calibration, it can be said that the system has calibrated well. With this in mind, the selected system has been calibrated (See figure 4.1 for more).

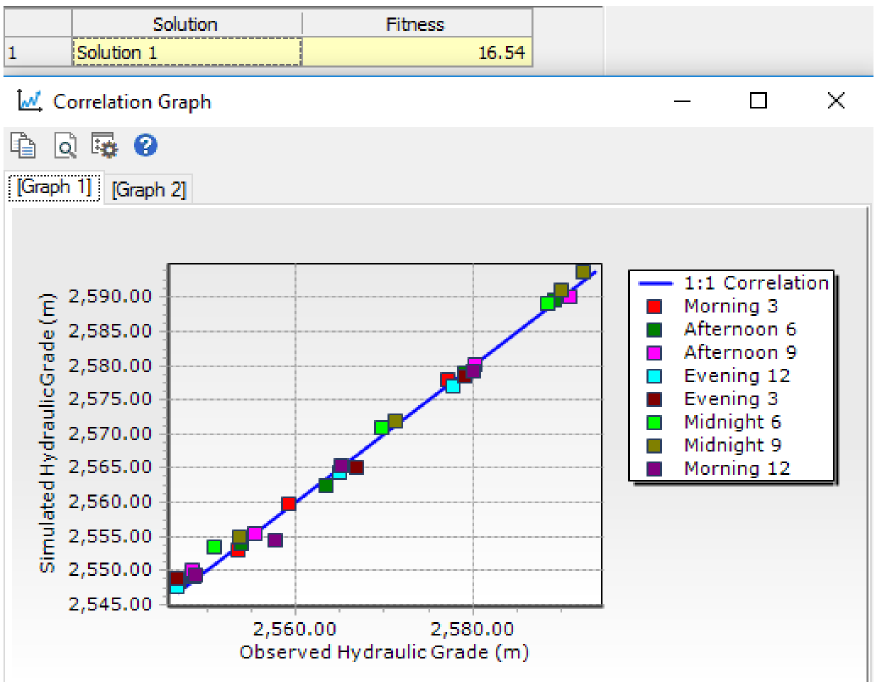

Figure 4.1 calibration result from Darwin calibrator of WaterGEMS

Once the system has been calibrated using a Darwin calibrator, the system model was re-run again for 24 hours using the adjusted parameter (the new Hazen-Williams C factors). According to the results of the simulation, the following technique was used to determine the extent to which the simulated values differed from those observed on the ground and to determine whether the variance fell within the criteria set by (Walski, 1983). Results are shown in table 4.1 below.

Table 4.1 Comparison of simulated pressure results with field-measured data

Time (hr.)	Sample nodes	X	Y	Z	Observed Pressure (mH_2O)	Simulated Pressure (mH_2O)	Discrepancy b/n observed and simulated (mH_2O)
9:00 AM	J-8	468000.51	1000577.97	2533.2	35.36	36.33	-0.97
	J-215	469794.15	1001002.44	2567.95	12.32	14.04	-1.72
	J-243	470285.54	1000465.8	2550.62	24	25.59	-1.59
	J-314	470846.63	1000034.16	2515.67	45.21	47.96	-2.75
	J-350	471111.02	999212.44	2472.79	77.08	78.91	-1.83
	J-413	469555.94	1000217.72	2518.88	35.25	34.62	0.63
12:00 PM	J-8	468000.51	1000577.97	2533.2	39.44	38.78	0.66
	J-215	469794.15	1001002.44	2567.95	13.35	14.26	-0.91
	J-243	470285.54	1000465.8	2550.62	26	26.27	-0.27
	J-314	470846.63	1000034.16	2515.67	43.17	48.23	-5.06
	J-350	471111.02	999212.44	2472.79	78.76	79.53	-0.77
	J-413	469555.94	1000217.72	2518.88	35.69	35.56	0.13
3:00 PM	J-8	468000.51	1000577.97	2533.2	40	42.5	-2.5
	J-215	469794.15	1001002.44	2567.95	15.1	14.91	0.19
	J-243	470285.54	1000465.8	2550.62	27.07	27.97	-0.9
	J-314	470846.63	1000034.16	2515.67	47.34	51	-3.66
	J-350	471111.02	999212.44	2472.79	78.58	84.01	-5.43
	J-413	469555.94	1000217.72	2518.88	37.19	37.52	-0.33
6:00 PM	J-8	468000.51	1000577.97	2533.2	32	32.93	-0.93
	J-215	469794.15	1001002.44	2567.95	21.6	24.12	-2.52
	J-243	470285.54	1000465.8	2550.62	24.7	24.15	0.55
	J-314	470846.63	1000034.16	2515.67	47.5	47.27	0.23
	J-350	471111.02	999212.44	2472.79	76.9	78.14	-1.24
	J-413	469555.94	1000217.72	2518.88	29.85	33.63	-3.78
9:00 PM	J-8	468000.51	1000577.97	2533.2	34.98	36.72	-1.74
	J-215	469794.15	1001002.44	2567.95	10.2	13.32	-3.12
	J-243	470285.54	1000465.8	2550.62	26	25.21	0.79
	J-314	470846.63	1000034.16	2515.67	49.51	47.71	1.8

Time (hr.)	Sample nodes	X	Y	Z	Observed Pressure (mH_2O)	Simulated Pressure (mH_2O)	Discrepancy b/n observed and simulated (mH_2O)
	J-350	471111.02	999212.44	2472.79	76.9	79.08	-2.18
	J-413	469555.94	1000217.72	2518.88	37.06	35.09	1.97
12:00 AM	J-8	468000.51	1000577.97	2533.2	62.42	65.7	-3.28
	J-215	469794.15	1001002.44	2567.95	18.4	19.21	-0.81
	J-243	470285.54	1000465.8	2550.62	35.3	36.05	-0.75
	J-314	470846.63	1000034.16	2515.67	52.29	53.32	-1.03
	J-350	471111.02	999212.44	2472.79	81.14	83.34	-2.2
	J-413	469555.94	1000217.72	2518.88	42	43.68	-1.68
3:00 AM	J-8	468000.51	1000577.97	2533.2	68.52	71.18	-2.66
	J-215	469794.15	1001002.44	2567.95	20.13	22.23	-2.1
	J-243	470285.54	1000465.8	2550.62	36.8	42.36	-5.56
	J-314	470846.63	1000034.16	2515.67	70.92	74.2	-3.28
	J-350	471111.02	999212.44	2472.79	93.9	101.93	-8.03
	J-413	469555.94	1000217.72	2518.88	44.2	47.6	-3.4
6:00 AM	J-8	468000.51	1000577.97	2533.2	41.9	46.16	-4.26
	J-215	469794.15	1001002.44	2567.95	19.87	21.41	-1.54
	J-243	470285.54	1000465.8	2550.62	27	32.33	-5.33
	J-314	470846.63	1000034.16	2515.67	47.7	54.68	-6.98
	J-350	471111.02	999212.44	2472.79	78.98	85.88	-6.9
	J-413	469555.94	1000217.72	2518.88	38.52	36.88	1.64
						Average	**-1.98**

As it can be seen from the table above, the mean difference between the actual pressure and the pressure computed is -1.98, which is the acceptable level of agreement between measurements and model outputs that meets Walski's calibration criteria (average difference of ±1.5m to a maximum of ± 5.0) for a good data set.

4.2.2 Model validation

To ensure that the model was correctly calibrated, the calibrated model was run and results were compared to a "different set of field data" from the one used to calibrate the model using the correlation coefficient equation (R) approach.

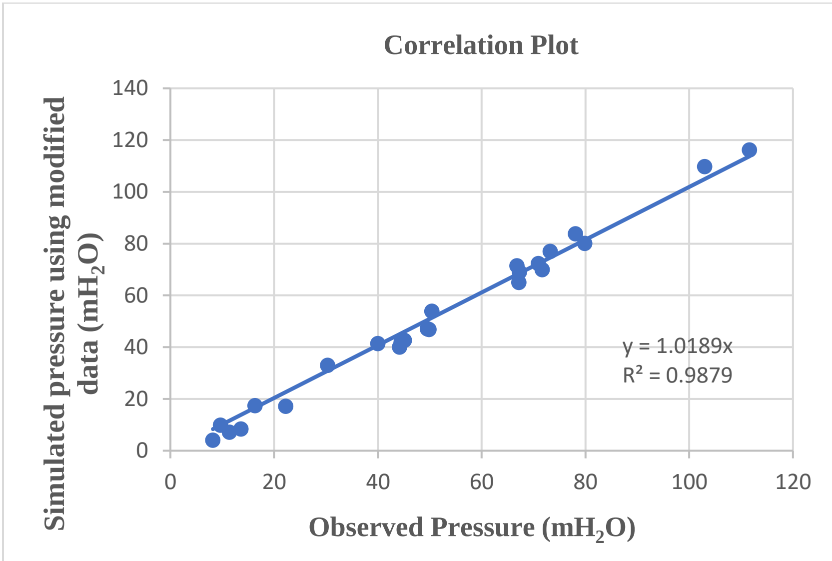

Figure 4.2 Correlation between the two variables (observed and simulated pressure)

As shown in the graph above, the best-fit equation derived from the observed and simulated pressures gives simulated pressure of 0m pressure head when the observed pressure head is zero. This is the y-intercept. We know that the perfect fit should have a slope of one which is Y = X, but here my curve gives a slope of 1.018, which shows that there is a little bit overestimation. i.e., the model somehow understates the actual pressure in the system by a value of 1.018m. For example, the overestimation for a maximum observed pressure head of 110m would be about 1.98m and the overestimation for a minimum observed pressure head of 9m would be about 0.16m. Thus, the margin of error in the estimation of the simulated pressure is within the range of 0.16m to 1.98m, and this is very reasonable.

In general, all of the methods utilized thus far indicate that the model is properly calibrated. As a result, because the model is now considered calibrated, the EPS model findings are thought to replicate the system on the ground. Accordingly, the current EPS model outputs (system pressure & velocity) that will affect the subsequent transient analysis as well as the overall performance of a system are provided below. It should be noted that the pressure findings were chosen as the most essential aspect in this investigation.

System Pressure

Despite the fact that there are no globally accepted or established norms for the specification of pressure standards, countries adopt their own pressure standards that they deem suitable for their systems. As a result, the former minister of water resources indicated in a 2006 study titled "urban water supply design requirements" that the minimum and maximum operating pressures in the distribution network should be 15m and 60m, respectively. Although the MoWR's standards are still accepted by AAWSA, it was noted in a discussion with experts in the bureau that the maximum allowable pressure could be up to 80m depending on some factors. Accordingly, in this study the acceptable range of pressures in the network was taken at 15m to 80m. Pressures of 15m and above are considered adequate to fully satisfy consumer demands. Pressures greater than 80m are considered excessive and a liability in terms of network integrity and leakage losses. With this in mind, the outputs from the model are presented in two cases as follows:

System pressure at high consumption hour: - demand is typically high especially in the morning (6AM-8AM) and early evening (6 PM-8 PM). The pressure observed at the junction nodes during these hours is summarized in Table 4.2 as follows:

Table 4.2 Actual nodal pressure distribution during peak consumption hour

Pressure (mH_2O)	No. of Junction nodes	Percentage (%)
>80	8	1.85
70-80	21	4.85
60-70	33	7.62
50-60	69	15.93
40-50	72	16.63
30-40	80	18.48
15-30	118	27.25
>15	32	7.39
Total	**433**	**100**

As shown in Table 4.2 above, about 7.39% of nodes were found to be below the minimum desirable pressures 15m during high consumption hour, while 8 junction nodes (1.85% of the total junction nodes in the system) were found above the maximum allowable pressure of 80m. The remaining 90.76% of the junction nodes were found to be within the allowable pressure range of 15m-80m.

Also, very large pressure differences have been obtained in the network, with highest pressures reaching 104m and approximately zero pressures occurring at some nodes. This is related to large ground elevation differences within the system, which reach 145m.

System pressure at low consumption hour: - normally, demand is low at mid night (12AM-5AM). The pressure observed at the junction nodes during these hours is summarized in Table 4.3 as follows:

Table 4.3 Actual nodal pressure distribution during low consumption hour

Pressure (mH_2O)	No. of Junctions nodes	Percentage (%)
>80	174	40.18
70-80	87	20.09
60-70	62	14.32
50-60	29	6.7
40-50	27	6.24
30-40	11	2.54
15-30	21	4.85
>15	22	5.08
Total	**433**	**100**

As can be seen from the table above, about 5.08% of nodes were found to be below the minimum required pressure 15m during low consumption period, and 40.18% of junction nodes were recorded above the maximum allowable pressure 80m. The remaining 54.74% of junction nodes were found to be within the allowable pressure range 15m-80m.

As a summary of the results, most of the junction nodes where the pressure is very low during both high and low consumption hours are located downstream of the pumps. This is because once the tanks have been filled, the pumps that supply water to the tanks are intentionally shutdown, and this in turn results in low pressure at the downstream side of the pumps (Walski et al., 2003). It also has been observed that very few junction nodes in the network are under low pressure due to their pipe size and higher elevation. As a result of the findings, the majority of the junction nodes with very low pressure during both high and low consumption hours are located downstream of the pumps. This is due to the fact that when the tanks have been filled, the pumps that deliver water to the tanks are purposefully cut down, resulting in low pressure at the downstream side of the pumps. It has also been discovered that because to their smaller pipe size and higher elevation, only few junction nodes in the network are under low pressure. On the other hand, as indicated in Table 4.3 above, nearly half of the nodes in the system are subjected to excessive pressure during the low consumption hour. This is primarily due to a decrease in demand at night. In contrast, the majority of nodes in a near perfect loop receive optimum pressure that does not exceed the minimum or maximum permitted pressure range.

Note that, the lower the initial steady state pressure is, the lower the minimum pressure will be when a low-pressure surge is generated.

System Velocity

Regarding velocity, similarly, there is no universal consensus on the maximum velocity that should exist in a water main. However, when inspecting designs for permissible velocities some engineers consider 0.6m/s as the minimum and 1.5m/s as the maximum allowable velocity, while others believe that the maximum could be up to 2.4m/s, and still others take 3.1m/s as the maximum flow velocity. As can be understood from several publications as well as from experts in AAWSA, the acceptable velocity for the study area ranges from 0.6m/s (since the system is looped, it is also worth noting that there may be sections of the pipeline where the velocity is zero) to 2m/s.

Accordingly, only no more than ten of the total distribution and transmission lines in the network were exceeded the maximum velocity allowed. The highest velocity in the network was observed at the high consumption hour, which is 2.96 m/s.

The overall results suggest that, there are some important technical issues in the network that need to be addressed such as existence of undersized pipes and spatial distribution of disproportional mains. However, improving the system is not part of this study. The purpose of this study is simply to conduct a transient analysis of the system in its current state (without improvement) based on the results obtained so far and see how it will react to the resulting transient event. But this does not mean that the HAMMER software used for transient analysis does not require any modification of the system. This means that the parameters for all pipes, such as pipe length and diameter, as well as the estimated velocity, must be verified to ensure that they are correct and that the headloss over the pipe is predicted; otherwise, they must be rectified. As a result, the lengths of several of the system's pipelines have been changed. The reason for this is that, regardless of the initial conditions friction method, HAMMER uses the Darcy-Weisbach friction method during a transient simulation, resulting in pipes that are much shorter than expected with excessive headloss producing a really large Darcy-Weisbach friction factor (f), which is not valid for that friction method.

4.3 Hydraulic Transient Analysis

As described extensively in the previous chapters, for this study a pump shutdown due to a power outage (a pump trip) have been modeled as the initiated transient event by considering the time of a day in which a system would be highly impacted if such an event occurred. Often, the system is thought to be vulnerable to such an event when storage tanks are being filled, when there is a high demand, when pumping is at maximum level and all storage tanks deliver water to their respective distribution zones (Fleming et al., 2005). So in the context of the study area, this time is in the afternoon between 5 pm and 7 pm. Accordingly, the transient simulations took place during a simultaneous failure of three pumps that were pumping water through three pumping pipelines to Rufael tank, St Paul tank, and directly to nearby areas. Furthermore, simulations were conducted by considering the various surge protection devices. A brief overview of these pumping pipelines as well as their response to sudden shutdown of the three pumps is presented as follows.

Pumping pipeline 1: - The water drawn from the Ras Hailu reservoir is transported to the Rufael tank via this major pipeline. It has a total length of more than 2 km (2090m), is made of ductile iron pipe with an inner diameter of 350 mm, and has a total head difference of 102m. Furthermore, because this pipeline is straight and has no bumps as indicated in the pipeline profile below in Figure 4.3, the utility has not placed any surge protection devices under the guise that it will not be subjected to transient pressures, which it is. However, the pump has a check valve at the discharge.

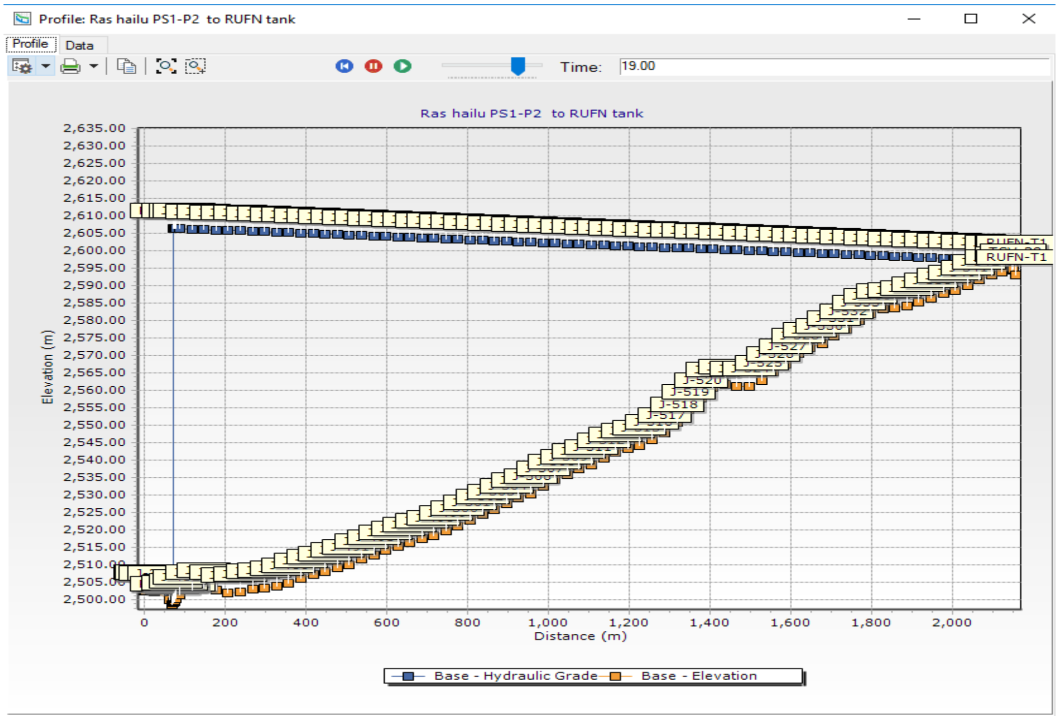

Figure 4.3 Profile of pumping pipeline from Ras Hailu PS1 to Rufael tank

Pumping pipeline 2: - Water is transported from Ras Hailu pump station 2 to the St Paul tank. It is 1.4km (1404m) long, made of ductile iron pipe with an inner diameter of 300 mm, and has a total head difference of 59 m. This pipeline, like the pumping main 1, is devoid of any surge protection equipment. However, the pump linked to it has a check valve at its outlet to prevent back flow. The pipeline profile is depicted in Figure 4.4.

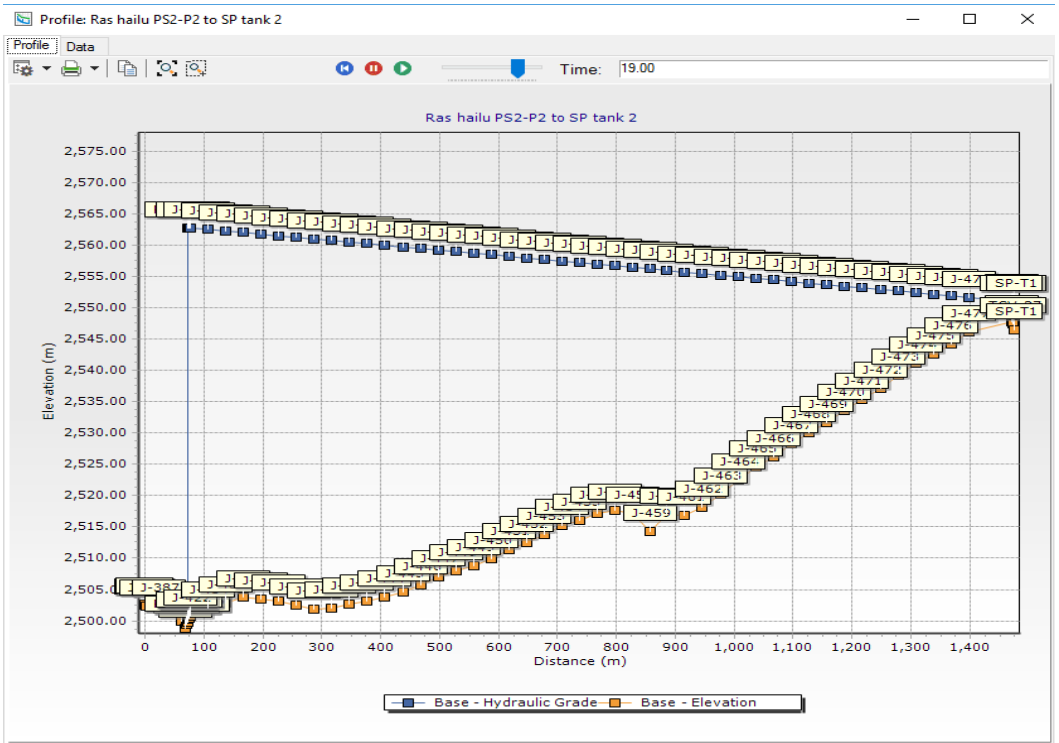

Figure 4.4 Profile of pumping pipeline from Ras Hailu PS2 to St Paul tank

Pumping pipeline 3: - It gathers water from three tiny pumps at Ras Hailu pump station 3 and distributes it to surrounding communities. The pipeline leaves the pump station via a 150mm Ductile iron pipe and travels up to 620 meters before distributing water to the remainder of the distribution system via PVC pipes. Furthermore, unlike the two pumping mains, the pump that pumps water into the distribution system via this pipeline does not have a check valve due to its low head and limited area coverage. The pipeline profile is depicted in Figure 4.5.

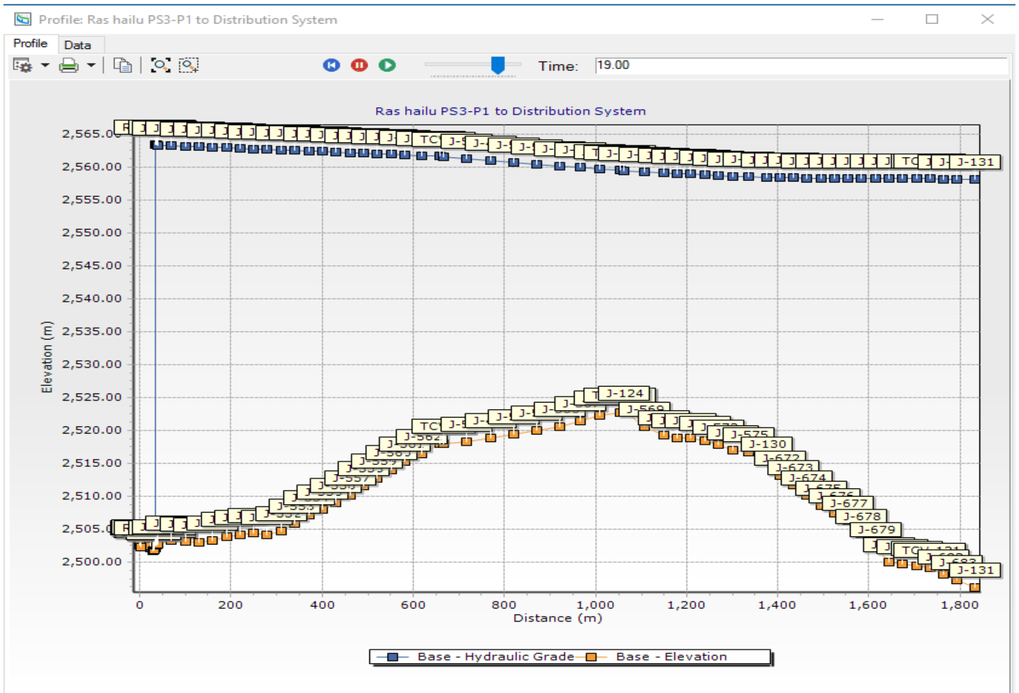

Figure 4.5 Profile of pumping pipeline from Ras Hailu PS3 to distribution system

If said so briefly about pumping mains, the results of the hydraulic transient study done on the simultaneous failure of three pumps at each pump station are as follows:

4.3.1 Analysis without Surge-Protection Devices

Transient pressures due to an emergency power breakdown have been simulated in this section without any protection devices in service to establish how vulnerable the system is to transient pressures. The simulation was centered primarily on the three pumping mains, and the responses of the three pumping pipelines, as well as their respective distribution zones, to such a phenomenon are shown below:

4.3.1.1 Pumping pipeline 1 response to sudden pump shutdown

First, to give a little insight into the graph, the profile's top section reveals any air or vapor volume that has occurred during the simulation. The green line is indicating the ground elevation of pipes. The black shows the starting hydraulic grade, while the red & blue lines shows the maximum, and the minimum hydraulic grade envelopes over the course of the transient simulation. Accordingly, the envelopes of the calculated maximum and minimum hydraulic grade line along the pumping pipeline 1 profile are shown on Figure 4.6.

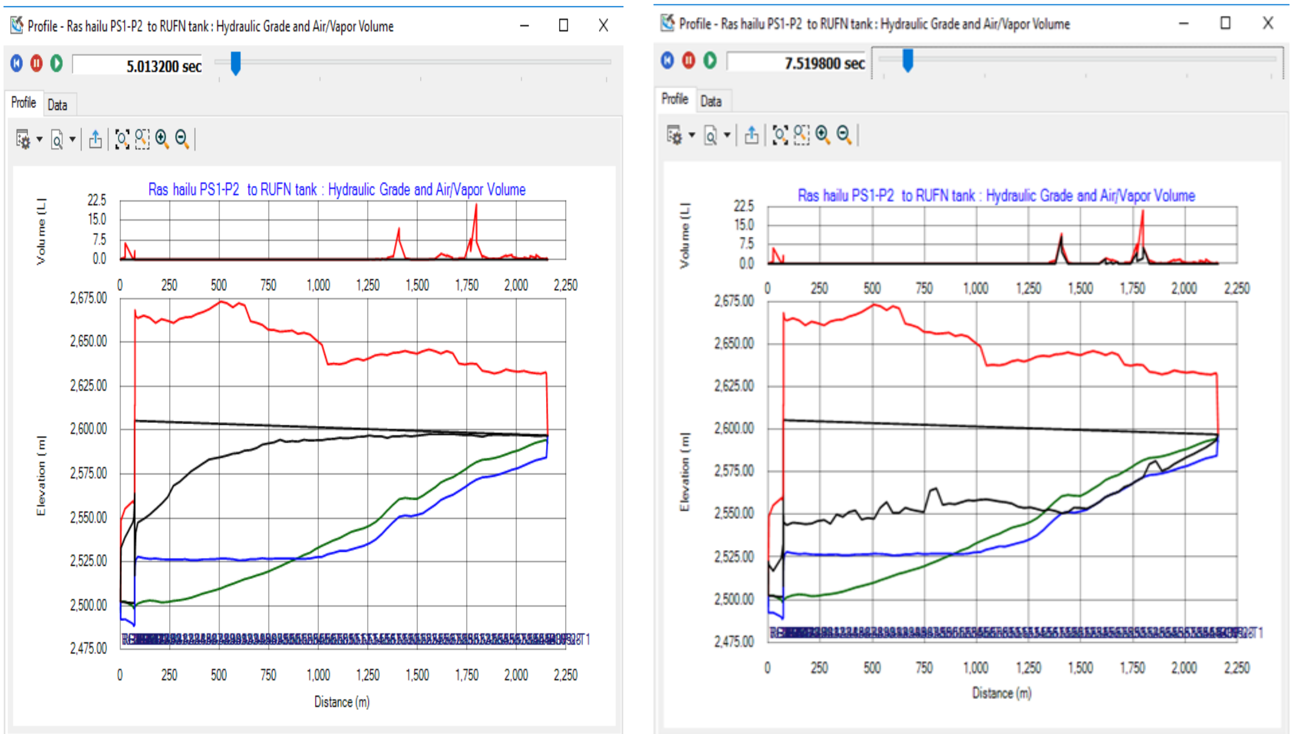

(a) (b)

Figure 4.6 Maximum and Minimum head envelopes for pumping pipeline 1, following the power failure of RHPS1-P2

The system was at steady-state for the first 5 seconds of the transient simulation. After 5 seconds, the pump shuts down and the wave starts propagates downstream as shown in figure 4.6 (a). As the wave travels downstream, it pretty quickly drops below upstream pressure as it reaches high point at a distance about 1,750 m. At this point the pressure goes below vapor pressure and cause a vapor pocket to form as shown in figure 4.6 (b), which may result in vaporous cavitation in a long part of the pipeline.

Likewise, the profile for the pumping pipeline 1 shows that a significant vapor cavity (shown as vapor volume on the downstream end of the pipeline profile) forms at the local high point of the pipeline (J-406). This is clearly seen in the P66:J406> time history graph below.

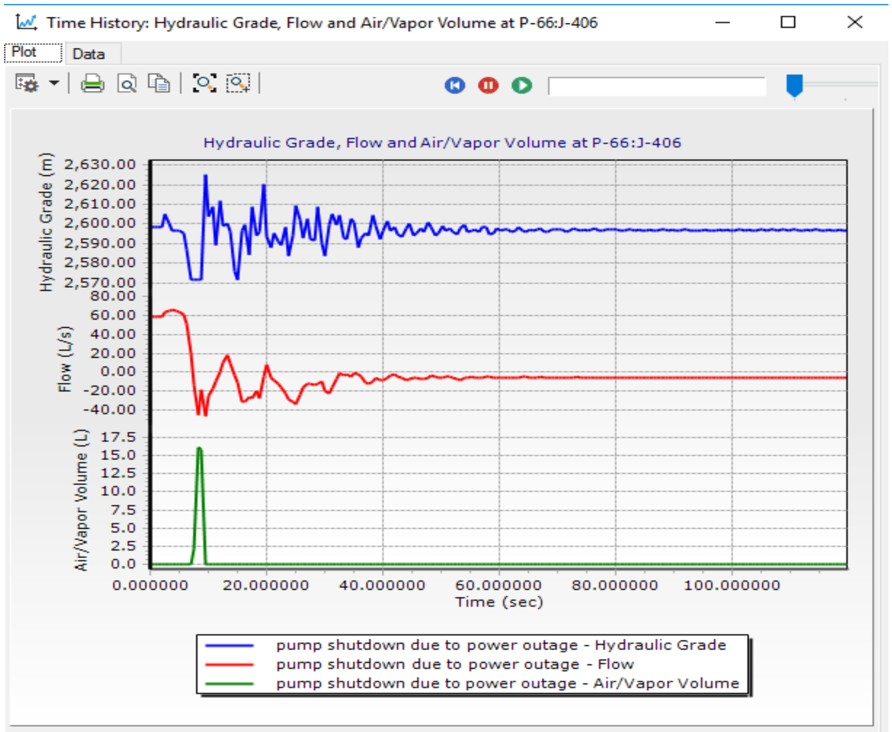

Figure 4.7 Graphic Time history showing the formation of vapor cavity at P66:J406>

After a certain time, the vapor pockets that have formed would collapse when the pipeline pressure increases due to more flow entering the region than leaving it and could create pressure spikes that may damage (rupture) the pipeline due to the re-pressurization of the pipeline by a flow reversal or a reflected transient pressure wave (Carmona-paredes et al., 2019).

4.3.1.2 Pumping Pipeline 2 response to sudden pump shutdown

Considering the response of the pumping main 2 to the transient phenomena, it can be said that it is better able to withstand transient pressures than the two pumping pipelines, and this is may be due to the fact that its pump inertia is relatively higher than the two pumping pipelines. To reinforce this hypothesis, (Walski et al., 2003) states pumps with higher inertias can help manage transients by moving water through the pump for a longer duration as they decelerate slowly.

However, the transient event in the system does not seem to have caused so much damage to the main pipeline, but this does not mean that the pumping pipeline itself and the distribution zone benefiting from it should not be protected against transient pressures. The maximum and minimum hydraulic grade lines along the pumping pipeline 2 profile are shown on Figure 4.8.

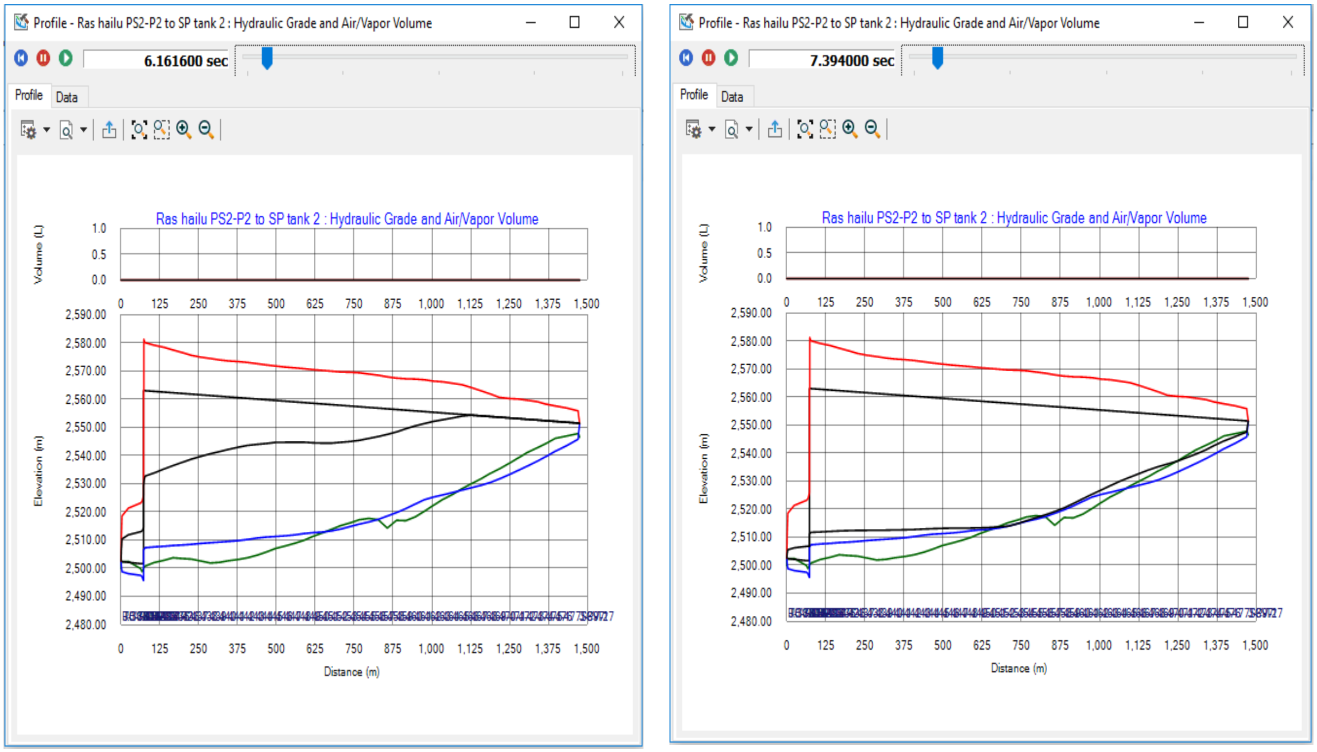

(a) (b)

Figure 4.8 Maximum and Minimum head envelopes for pumping pipeline 2, following the power failure of RHPS2-P2

It can be observed from Figure 4.8 (b) that the pipeline will experience negative pressures at some high points since the minimum head envelop intersects the physical elevation of the pipeline. But since the transient pressure is not less than vapor pressure and doesn't reach the vaporization level, the vapor pocket has not been created in the pipeline. This indicates that cavitation and wall column separation are temporarily not created along this pipeline.

4.3.1.3 Pumping Pipeline 3 response to sudden pump shutdown

As noted above, this pumping pipeline convey water directly to the distribution zone, and transient analysis results show that most parts of the distribution system are highly susceptible to negative transient pressure. This is mainly due to the fact that there is no check valve for the pump and also no surge protection devices for the main pipeline. Another concern is that most of the pipes in the system are PVC pipes aged 50 years and older and are more likely being exposed to collapse. Once again, the (Walski et al., 2003) reinforces this notion by saying: Steel, PVC, HDPE, and thin-wall ductile iron pipes are all prone to collapse due to vapor separation, but any pipe that has been fatigued by repeated exposure to these events is at risk of failure. The envelopes of the calculated maximum and minimum hydraulic grade line along the pipeline profile are shown on Figure 4.9 below.

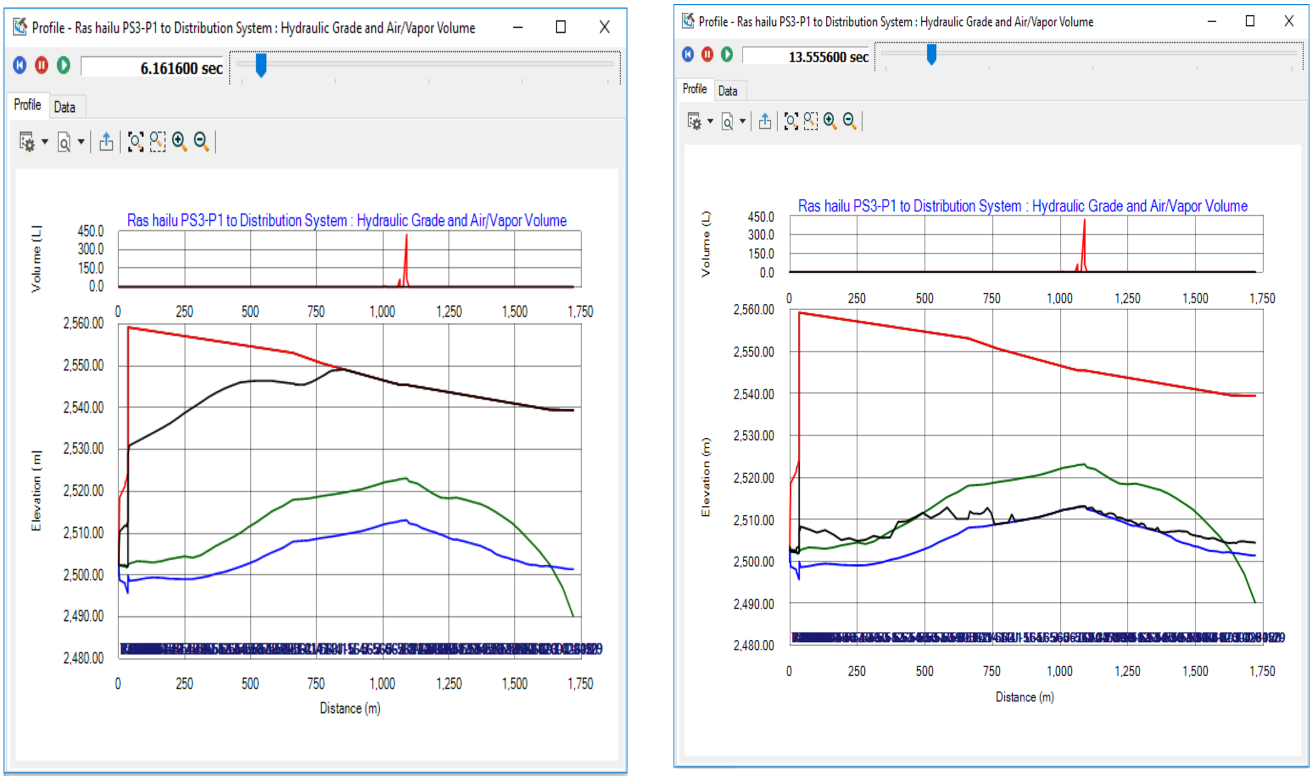

(a) (b)

Figure 4.9 Maximum and Minimum head envelopes for pumping pipeline 3, following the power failure of RHPS3-P1

As shown in Figure 4.9 (a), the failure at the pump creates a downsurge wave travels down the right side to the end of the system. Likewise, as can be seen from the animated pipeline profile presented in Figure 4.9 (b), the minimum hydraulic grade is below the pipeline elevation until it reaches the end of the system, this means that the pumping main itself as well as the distribution zone that receives water through this pipeline are highly susceptible to negative pressure. Moreover, the minimum head envelope reveal that the transient pressure has been reduced to vapor pressure at the highest point (perhaps about 1,050 meters downstream of the pump station), and as a result, a vapor pocket has been created.

4.3.1.4 System response to sudden pump shutdown

In this study, the so-called 'system (water distribution system)' is basically three distribution zones that receive water through the three pumping mains we have seen so far. These are 1) RU-RU-G, which receives water from the Rufael tank via pumping pipeline 1, 2) ST-ST-G, which receives water from the St Paul tank via pumping pipeline 2, & 3) ST-RH-P, which receives water directly from the Ras Hailu reservoir and distribute it to nearby areas via pumping pipeline 3. Accordingly, the complete set of system results for the hydraulic transient analysis is summarized in the following parameters: 1) Average steady-state pressure (the static pressure before the transient event was initiated), 2) Maximum pressure (the highest pressure reached during the transient event), 3) Minimum pressure (the lowest pressure reached during the transient event), and 4) Minimum pressure below vapor pressure (a point where cavitation occurs).

So, to better define these parameters and identify problematic areas, results should be displayed as either in tabular format or graphically by color-coding the desired pipes. However, the graphical display of results in HAMMER is limited as compared to that of GIS. Therefore, all the results were sent to GIS in order to color-code results graphically using HAMMER software export tool. The results of each of the parameters were color-coded onto the system schematics for better visual assessment and presented in Figures 4.10 – 4.13 below. Similarly, in order to see how many pipes in the system exceed the high- and low-pressure threshold in tabular format, use Appendix A to C.

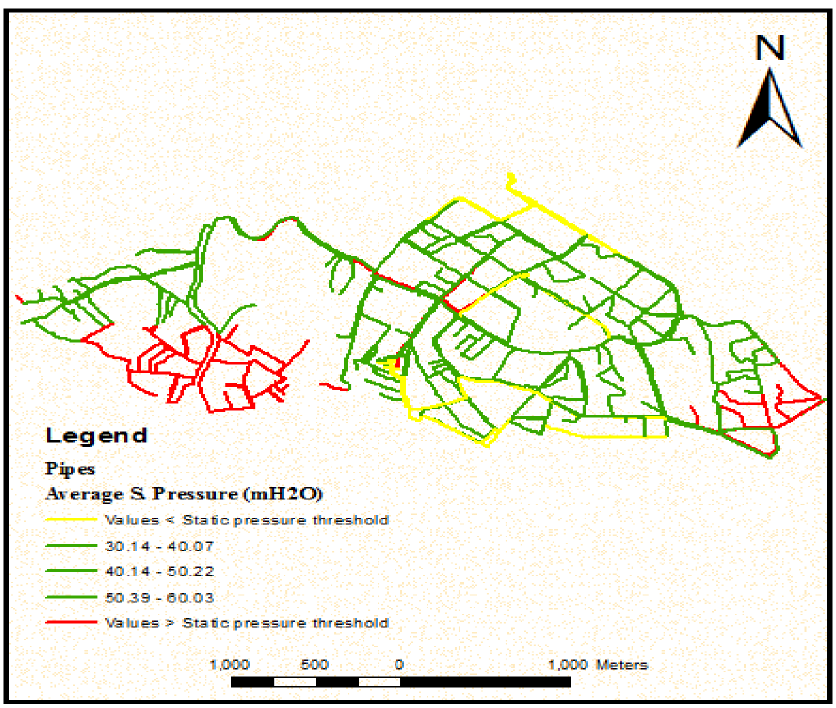

Figure 4.10 Average static pressure

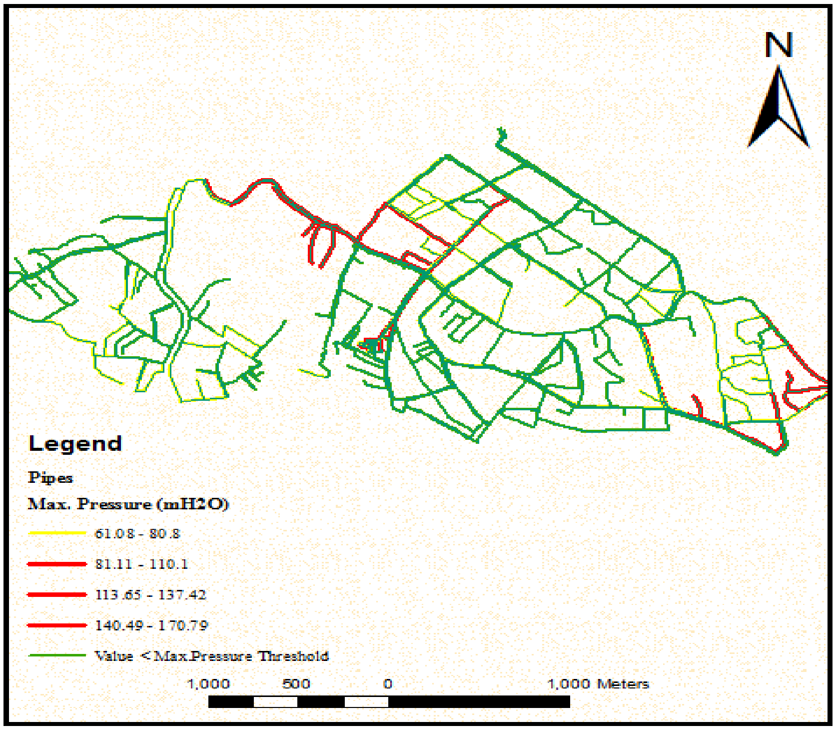

Figure 4.11 Maximum transient pressure

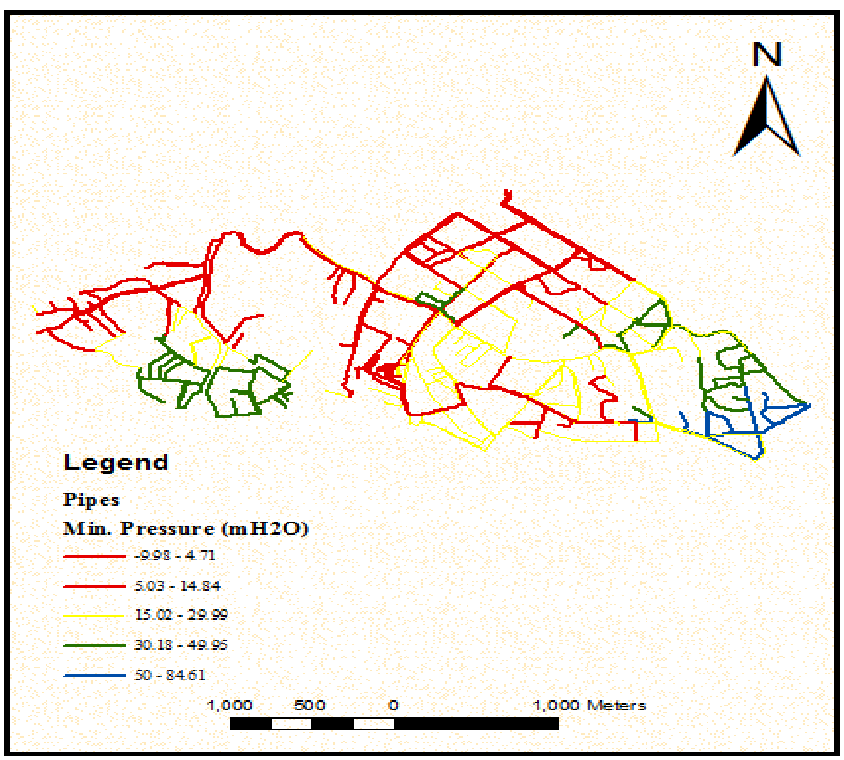

Figure 4.12 Minimum transient pressure

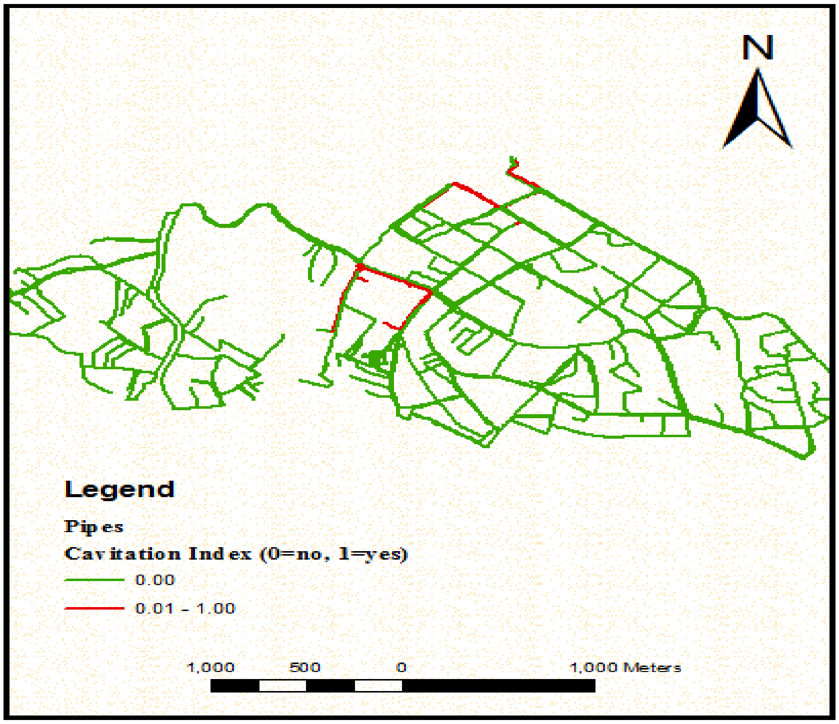

Figure 4.13 Pipes that accommodate cavitation

Now as shown above, results were displayed graphically on a schematic of the water distribution network and were color coded for easy visual inspection. From the results it can be observed that the system (all the three distribution zones) was/were predicted to experience low and negative pressure transients, maximum transient pressures were found especially in areas of close proximity where the transient event was initiated, and it has also been observed that vapor pockets are created on some pipes (about 7% of the system) when a complete loss of pumping power was simulated.

Accordingly, of the three distribution zones in the system, the ST-RH-P was found to be highly vulnerable to low and negative pressures transients due to its proximity to the pump station and due to the lack of any surge protection device in the zone. Prior to the transient event, almost 94% of the system had an average static pressure, but after the transient event was initiated, 85% of the system was found to be highly susceptible to negative and low-pressure transients.

Similarly, the RU-RU-G distribution zone was operated at an average steady state pressure of less than 60 mH_2O before a transient event (complete loss of pumping power) occurred, however, significant pressure has been observed in low-lying areas, such as Tero and Kolfe. On the other hand, with a complete loss of pumping power the system was predicted to experience negative and low pressures in more than 80% of the system and it is speculated that this may be mainly due to the fact that most of areas in the distribution zone are located more than a kilometer away from their respective source Rufael storage tank, that there are dead end pipes in the distribution zone, and that there are some areas that have had relatively low static pressure in the past.

Distribution zone ST-ST-G, on the other hand, was found to be less susceptible to low and negative pressures, while high pressure was observed in the area around St. Yohannes church due to its lowest elevation and due to its high standard operating pressures.

To summarize, it appears that additional surge protection devices were required to keep the system from experiencing difficulties caused by pressure transients. Thus, the next step was to pick protective equipment to manage pressure transients and then, re-simulate the system using Bentley HAMMER to assess the effectiveness of the selected devices, which is explained in the following section.

4.3.2 Analysis with Surge-Protection Devices

There are no general rules or universally applicable guidelines for eliminating an objectionable pressure in a water distribution system. Any surge protection devices and/or operating strategies must be chosen accordingly. The final choice will be based on the initial cause and location of the transient disturbance(s), the system itself, the consequences if remedial action is not taken, and the cost of the protection measures (AWWA, 2005).

So in this study, a double acting air valves and a hydropneumatic tank (also known as a gas vessel or air chamber) were installed at local high points in the system and on the downstream side of the pumps in order to alleviate transient pressures as well as to control future hydraulic transients that may occurs in the event of a sudden power outage. Accordingly, the results obtained from the three pumping mains as well as the whole system by taking into account these surge protection devices are discussed below.

4.3.2.1 Pumping Pipeline 1 response to surge protection devices

As can be seen from the previous analysis (analysis without surge protection devices), Pumping Pipeline 1 has been exposed to some form of sub-vapor pressure and negative pressures since 1,070m from the pump station to the end of the system. Therefore, with the intention of alleviating this problem, Air valves with an air-inflow orifice diameter of 80mm & an air-outflow orifice diameter of 40mm have been installed at the high points of the pipeline. However, as shown in

Figure 4.14 (a) below, the addition of Air valves does not provide adequate protection. Sub-atmospheric pressure and cavitation occurs at the downstream end of the system, due to the high point.

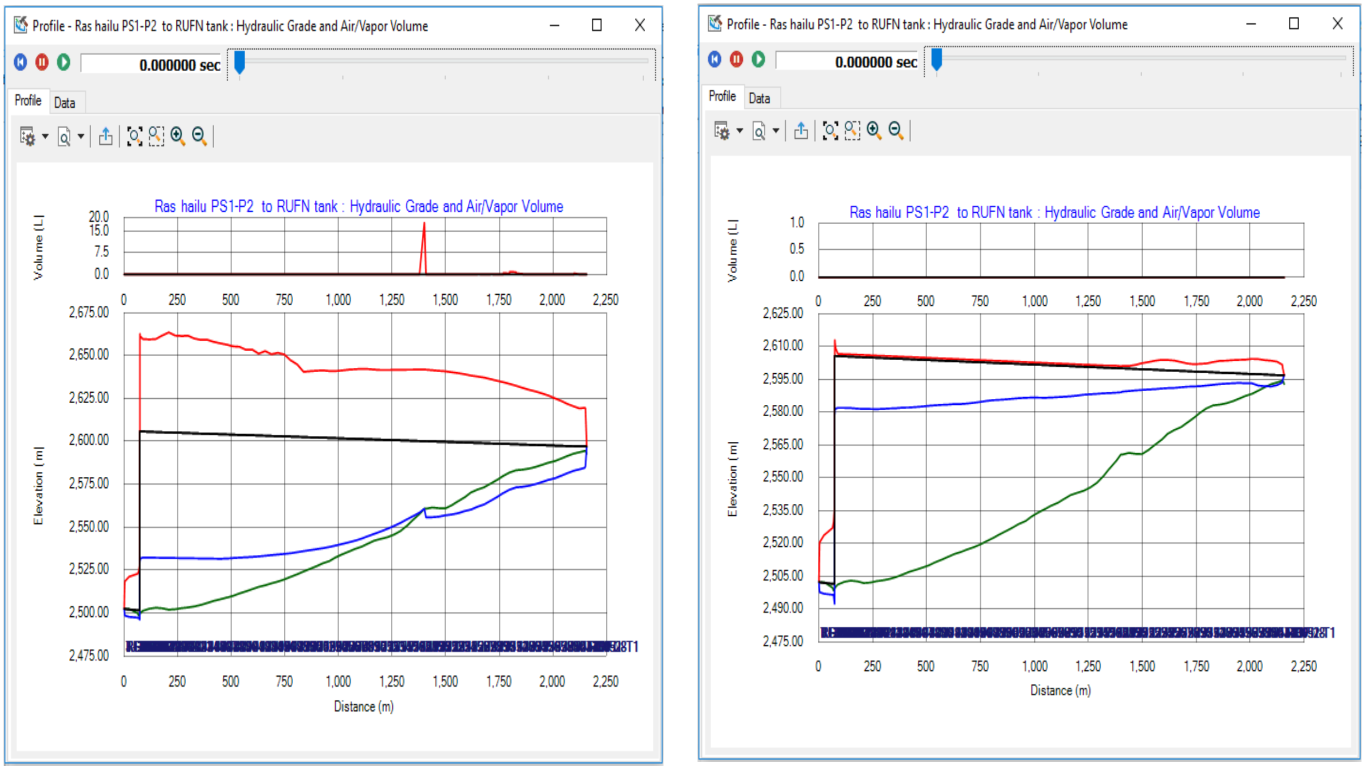

(a) (b)

Figure 4.14 The envelope along Pumping Pipeline 1 a) with Air valves at high points; and b) with both Air valves and Hydropneumatic tank

Therefore, in order to eliminate the occurrence of cavitation and reduces negative pressures that previously existed along the pipeline, a hydropneumatic tank just downstream of the pump station was added. The results show that the proposed control devices have been found to be a good solution to protect the system against severe transient pressures. It can be observed in Figures 4.14 (b) that, the maximum head along the pumping pipeline were considerably reduced and the minimum head along the pipeline were uplifted to within acceptable limits. In this case, the cushioning effect produced by the hydropneumatic tank absorbed the transient pressures waves considerably. Thus, it can be stated that these devices have a beneficial effect over the entire the pumping pipeline system.

4.3.2.2 Pumping Pipeline 2 response to surge protection devices

Unlike Pumping Pipeline 1, this pumping pipeline was less susceptible to transient pressure. It should be noted, however, that negative pressures were created on certain pipeline segments. It is therefore believed that this situation can be remedied by installing double acting air valves with an air-inflow orifice diameter of 80mm and an air outflow orifice diameter of 40mm and this can be clearly seen in Figure 4.15 below:

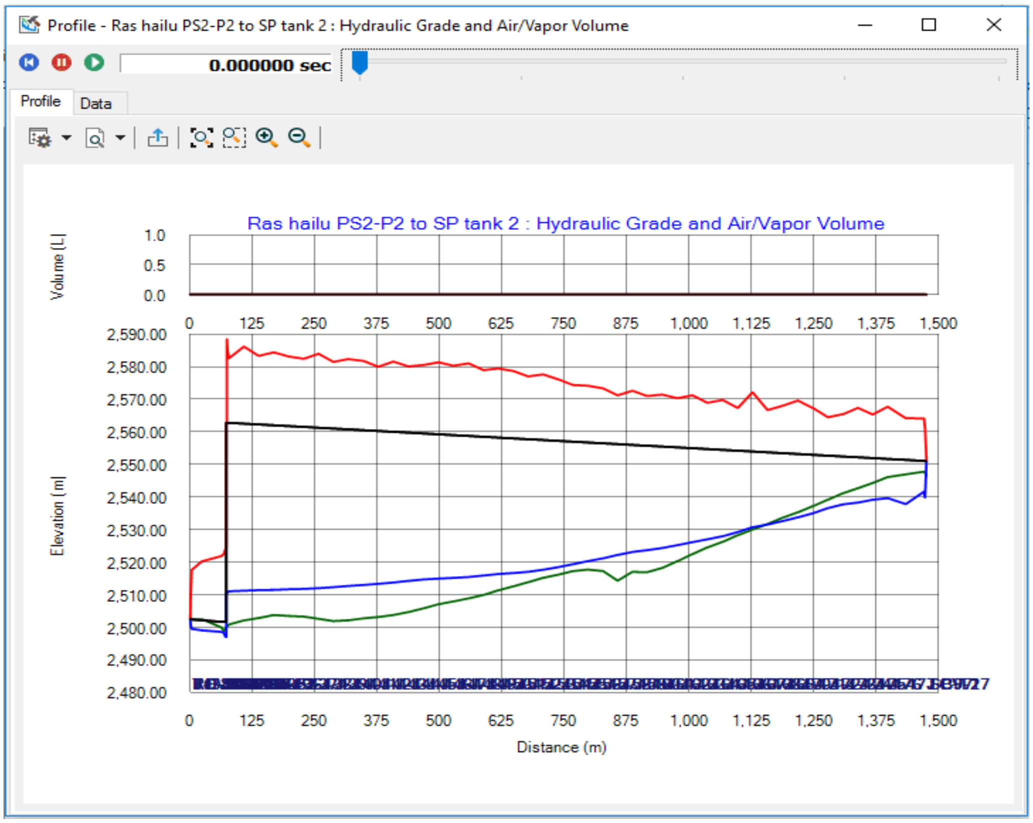

Figure 4.15 The envelope along pumping pipeline 2 with Air valves

As can be seen from the figure, although the proposed control devices did not completely eliminate all the negative pressures on the pipeline (this is because the last segments of the pipeline are still vulnerable to sub-atmospheric pressure), but they did significantly reduce them. It is worth mentioning here is that the air valves can limit the pressure from dropping below zero. However, pressure can still become sub-atmospheric some distance to either side of the air valve. Thus, to the authors' knowledge, the sub-atmospheric pressures exerted on the last segments of the pipeline can now be tolerated, unless the transient pressures at this point go down to the vapor pressure and form vapor cavity which may lead to cavitation and water column separation.

4.3.2.3 Pumping Pipeline 3 response to surge protection devices

It will be recalled that, as stated in the previous section, this pumping pipeline is highly vulnerable to hydraulic transients. To reduce this risk, air valves with an air-inflow orifice diameter of 40mm and an air-outflow orifice diameter of 20mm have been installed at the high points of the pipeline. However, given the limited capacity of the air valves to fully withstand the transients created on the pipeline, it was found necessary to install hydropneumatic tank at the downstream of the pump station. Check out the profile below.

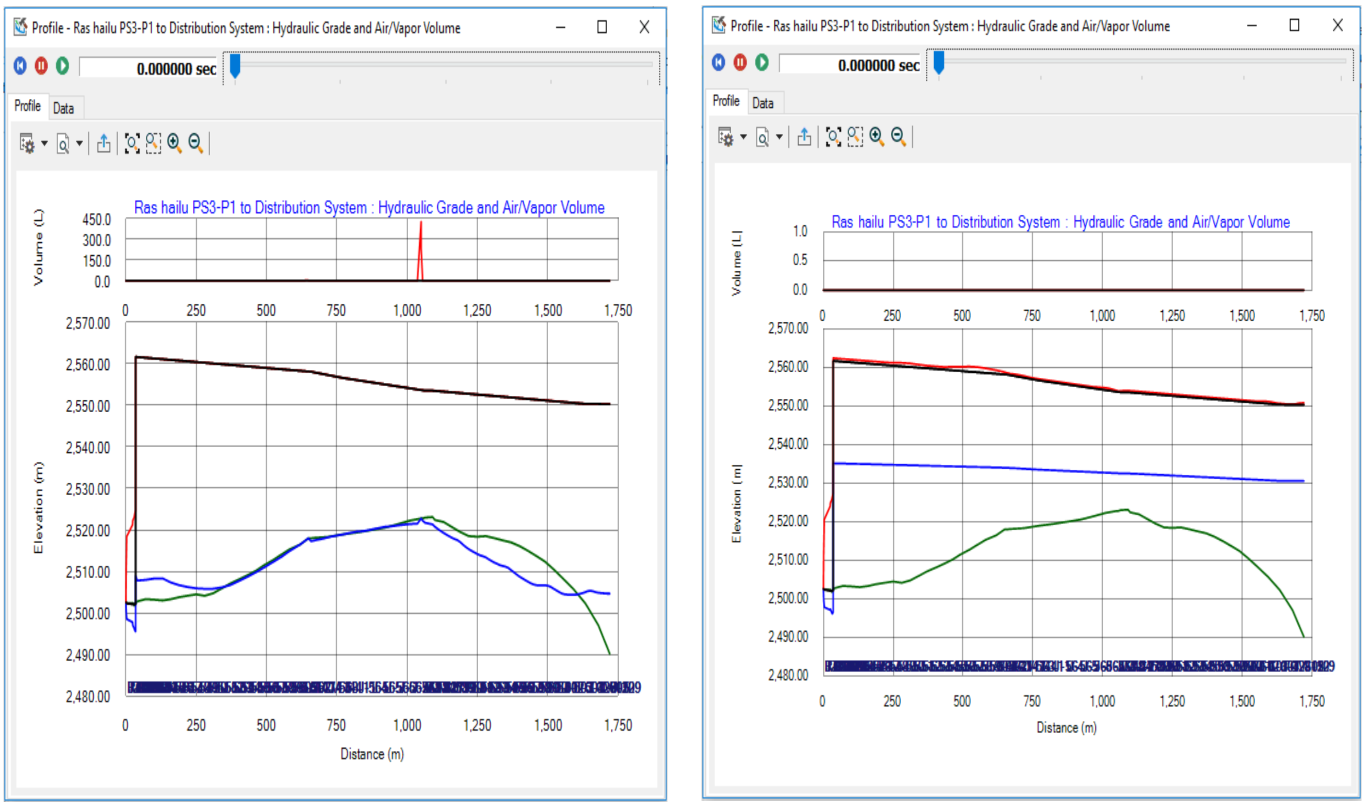

(a) (b)

Figure 4.16 The envelope along pumping pipeline 3 a) with Air valves at high points; and b) with both Air valves and Hydropneumatic tank

Figure 4.16 (a) shows that the air valves alone are not sufficient to protect the system from the transient phenomenon, due to the negative pressures experienced by the pipeline at some high points. while from Figure 4.16 (b) it is observed that by installing the hydropneumatic tank at the discharge header of the pump station, the minimum head along the pipeline was considerably uplifted and thus no negative pressures occur anywhere along the pumping pipeline. Therefore, it can be stated that installing hydropneumatic tank at the discharge header of the pump station & air valve at high points were effective at preventing transient pressures in this pipeline.

4.3.2.4 System response to surge protection devices

In general, the establishment of surge protection devices on the pumping pipeline has enabled the system to reduce its exposure to negative and sub-vapor pressure and to operate more than 90% of the system at a steady state pressure of less than 80 mH2O. To support this with an image see Figure 4.17 below. Similarly, in order to see how many pipes in the system exceed the high- and low-pressure threshold after surge protection devices in tabular format, use Appendix D & E.

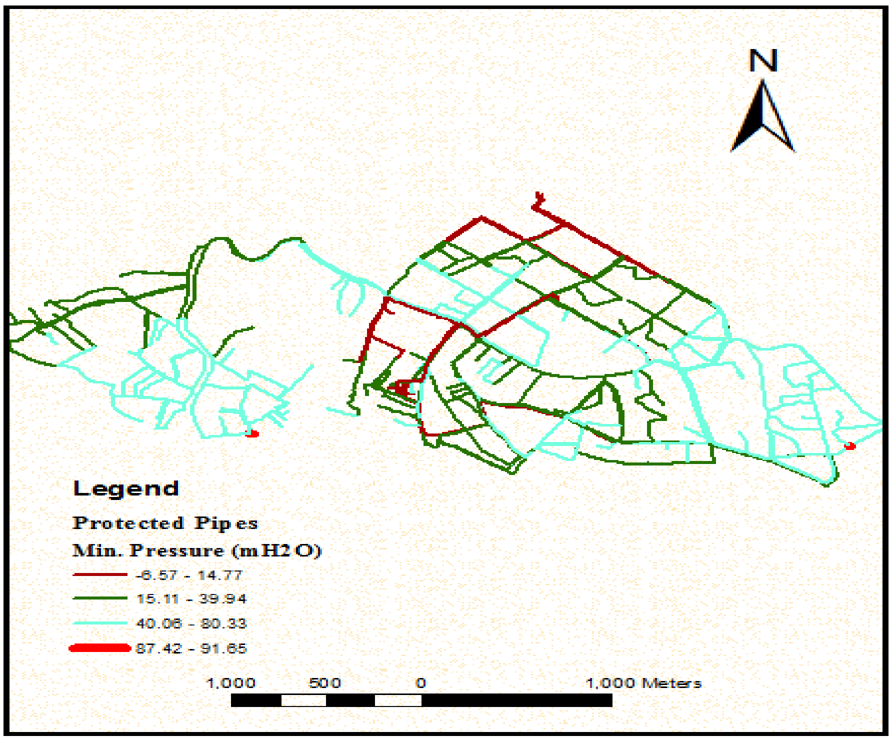

Figure 4.17 Minimum transient pressure after the establishment of surge protection devices

As can be seen from the figure, most parts of the system that used to have the lowest pressure in the previous analysis (without surge protection devices) have been able to operate within the permissible limit. This, in turn, indicates that, if the system is equipped with such protection devices, it will increase the efficiency of its day-to-day operation and streamline its overall service.

5. CONCLUSIONS AND RECOMMENDATIONS

This chapter provides a concluding remark based on the major findings of the study and also provides recommendation for the work to be done in the future in this regard.

5.1 Conclusion

As previously stated, the primary goal of this research is to examine system's response to the most common transient phenomenon pump shutdown caused by a sudden power outage (since it is a recurring phenomenon in the area) using a transient modeling software HAMMER. Accordingly, a transient simulation was conducted and the following major conclusions have been drawn based on major findings.

- Areas that are located more than a kilometer away from their respective source were found to be more vulnerable to low and negative pressures transients.
- Distribution system that receive water directly from the pump or in other word, areas near the pump station were found to be more susceptible to low and negative pressure transients.
- Areas that have had relatively low initial steady state pressure were also more likely to be exposed to negative sub-atmospheric and/or sub-vapor pressure.
- The Moment of inertia of the rotating parts (pump & motor) also has a significant impact on system's response to transients when a pump is suddenly stopped. It assists the motor, pump rotating parts to decelerate slowly, and continues transporting water through the pump for a long time following a power outage.
- Pipes close to the pumping stations where the power outage occurred have experienced significant pressure fluctuations. This is because when pumps supplying water were suddenly shutdown, negative pressure waves start propagate down to the downstream boundary, then the reflected pressure wave is an overpressure wave that can cause serious damage to the pumps. However, to prevent this from occurring, the check valves fitted on the pumps are closed before this positive pressure waves reaches and this situation, in turn, doubles and reflects the incoming positive pressure wave on them. At this point, nearby pipes exceed the maximum allowable pressure.
- The addition of closed hydropneumatic tanks just downstream of the pump station would prevent negative surges from occurring in the respective distribution zones after a power outage. Note that, since the pipelines downstream of the pump stations were less than 14

inches, it was sufficient to install $5m^3$ & $3m^3$ of hydropneumatic tanks to reduce pressure surges when a power outage occurred.

- Similarly, air valves with an air inflow orifice diameter of 20-80mm and air outflow orifice diameter of 15-40mm were able to reduce the sub-atmospheric and sub-vapor pressures exerted on high points in the piping system.

5.2 Recommendations

The following recommendations are made for the respective water utility (AAWSA) to consider as part of their surge mitigation program as well as for their future work in relation to hydraulic transients:

- Rejecting the hypothesis that hydraulic transients have little or no adverse impact onto the system, special attention should be paid to system equipment that are directly related to the creation and control of hydraulic transients. Therefore, a computer-based transient analysis should be performed to determine the impact of hydraulic transients on the overall system.
- Vulnerable areas are identified based on the transient model and should be given priority in terms of maintenance and leak detection.
- It is also advisable to install surge mitigation devices that are considered effective in terms of system characteristic itself, initial cause & location of disturbance, and the cost of the protection devices to be installed in all systems that are considered vulnerable to hydraulic transients. For example, installing hydropneumatic tanks near pump stations and air valves at high points in the piping system are more likely to be effective for other areas with similar configurations to the area studied.
- In a newly designed system, it is important to note that transient conditions are likely to be reduced by implementing the appropriate system flow control operations such as installing pumps that have relatively high inertia and prolonging valve opening &valve closing times.
- Although not included in this study, a field-monitoring program needs to be conducted over a long period in order to better understand the impact of surge in the system.

Generally, in order to determine the extent to which transients can damage pipes and the entire system components, and knowingly to protect against the potential risk of such incidents, the author acknowledges that this research needs to be expanded and improved either by the authority or by other stakeholders in the future.

REFERENCES

Abnet, G., Erena, B., Imam, M., Tsion, L., and Yonas, A. (2017) city profile Addis Ababa, Report prepared in the SES (Social Inclusion and Energy Management for Informal Urban Settlements) project, funded by the Erasmus+ Program of the European Union.

Antonaropoulos, Z and A. P., and Associates S. B. (2019). Consultancy Service for Existing Water Network Management Assessment, WP1 draft final Report. Tropical Consulting Engineers PLC. AAWSA Water and Sanitation Development and Rehabilitation Project Office.

AWWA. (2012). Computer Modeling of Water Distribution Systems. Manual of Water Supply Practices- M32. Denver: American Water Works Association.

Boulos, P. F., Wood, D. J., Lingireddy, S., Karney, B. W., & McPherson, D. L. (2005). Numerical methods for modeling transient flow in distribution systems. American Water Works Association,AWWA, 97(7), 104–115.

Boulos, P.F., Karney, B.W., Wood, D.J., and Lingireddy, S., (2005). Hydraulic Transient Guidelines for Protecting Water Distribution Systems. Journal AWWA, May 2005.

Carmona-Paredes, R. B., Pozos-Estrada, O., Carmona-Paredes, L. G., Sánchez-Huerta, A., Rodal-Canales, E. A., & Carmona-Paredes, G. J. (2019). Protecting a pumping pipeline system from low pressure transients by using air pockets: A case study. Water (Switzerland), 11(9).

Chaudhry, M. Applied hydraulic transients. Van Nostrand Reinhold Co, New York, 1987.

D.Starczewska, R. C. and J. B. (2015). Occurrence of transients in water distribution networks. Procedia Engineering, 119, 1473–1482.

D.Starczewska, R. C. and J. B. (2016). Pressure transients in water distribution networks: understanding thei rcontribution to pipe repairs, University of Sheffield Sheffield, UK.

Elias, Y., and Laura, S. (2018). The Transformation of Addis Ababa: A Multiform African City by Cambridge Scholars Publishing.

El-Turki, A. (2013). Modeling of Hydraulic Transients in Closed Conduits. Colorado State University Fort Collins, Colorado, 19–53.

EPA. (2003). Cross-Connection Control Manual. United States Environmental Protection Agency Office of Water Office of Ground Water and Drinking Water.

Fecser, N., Krecht, R., & Kuti, R. (2019). Analysis of Transient Phenomena in Water Supply Networks. International Journal of Latest Engineering and Management Research (IJLEMR).

Federal Democratic Republic of Ethiopia Ministry of Water Resource (2006) 'Urban water supply design criteria', Water Resources Administration Urban Water Supply and Sanitation Department, pp. 1–60.

Fleming, K. K., Gullick, R. W., Dugandzic, J. P., & Lechevallier, M. W. (2005). Susceptibility of Potable Water Distribution Systems to Negative Pressure Transients. New Jersey Department of Environmental Protection Division of Science, Research & Technology.

Friedman, M., L. Radder, S. Harrison, D. Howie, M. Britton, G. Boyd, H. Wang, R. Gullick, M. LeChevallier, D. Wood. And J. Funk (2004). Verification and Control of Low-Pressure Transients in Distribution Systems; AWWA Research Foundation, Denver, CO.

Getinet, E. (2019). Evaluation of Addis Ababa Water Supply System Using Integrated Approach, Dissertation for the Degree of Doctor of Philosophy in Environmental Planning, Ethiopian Institute of Architecture, Building Construction and City Development Addis Ababa University

Gullick, R., LeChevallier, M., Svindland, R., and Friedman, M. Occurrence of transient low and negative pressures in distribution systems. Journal of American Water Works Association, 96 (11):52–66, 2004.

Gullick, R. W., Lechevallier, M. W., Case, J., Wood, D. J., Funk, J. E., & Friedman, M. J. (2005). Application of pressure monitoring and modelling to detect and minimize low pressure events in distribution systems. IWA, 65–81.

Hassan, A., Chowdhury, R., & Khan, D. M. (2011). Aspect and necessity of hydraulic transient analysis in water distribution system in Dhaka. 4th Annual Paper Meet and 1st Civil Engineering Congress, 978–984.

Hoagland, S., Schal, S., Ormsbee, L., and Bryson, S. (2015). Classification of Water Distribution Systems for Research Applications; Proc. EWRI Congress 2015

Hoagland, S. W. H. (2016). Transient-Based Risk Analysis of Water Distribution Systems. University of Kentucky.

Ivo Pothof and B. Karney. (2016). Guidelines for Transient Analysis in Water Transmission and Distribution Systems. Intech, i(tourism), 13.

Jalal, M. M. (2008). « Performance Measurement of Water Distribution Systems (WDS). A critical and constructive appraisal of the state-of-the-art ». University of Toronto, 157.

Jung, B. S., Boulos, P. F., Wood, D. J., & Bros, C. M. (2009). A Lagrangian wave characteristic method for simulating transient water column separation. Journal / American Water Works Association, 101(6), 64–73.

Jung, B. S., Karney, B. W., & Asce, M. (2006). Hydraulic Optimization of Transient Protection Devices Using GA and PSO Approaches. Journal of Water Resources Planning and Management.

Karney, B. W., & McInnis, D. (1990). Transient analysis of water distribution systems. Journal / American Water Works Association, 82(7), 62–70.

Kodikara, J., Rathnayaka, S., Shannon, B., & Rajeev, P. (2015). Monitoring of pressure transients in water supply networks. Water Resources Management, 30(2), 471–485.

Kroon, J., Stoner, M., and Hunt, W. Water Hammer: Causes and Effects. Journal of American Water Works Association, 76(11):39–45, 1984.

LeChevallier, M. W., Gullick, R. W., Karim, M. R., Friedman, M., & Funk, J. E. (2004). The potential for health risks from intrusion of contaminants into the distribution system from pressure transients. Journal of Water and Health, 1(1), 3–14.

El-Turki, A. (2013). Modeling of Hydraulic Transients in Closed Conduits. Colorado State University Fort Collins, Colorado, 19–53.

M. Elbashir and S. Amoah (2007). Hydraulic Transient in a Pipeline Using Computer Model to Calculate and Simulate Transient, Division of Water Resources Engineering Department of Building and Environmental Technology Lund University, Sweden.

Rathnayaka, R., Robert, D. J., Rajeev, P., & Kodikara, J. A review of the pressure transient effects on water distribution main failures. International Conference on Structural Engineering & Construction Management, (September 2015), 129–143.

Statistical, Economic and Social Research and Training Centre for Islamic Countries (SESRIC) (2015). Correlation and Regression Analysis.

Starczewska,D.,Collins,R.,andBoxall,J. Occurrence of transients in water distribution networks. Proceeding of the 13th International Conference of Computing and Contol for the Water Industry, CCWI. Leicester, 00:1–11, 2015.

Tapomoy Guha. (2019). Transient analysis of a piped water network using hammer software : a case study of south mizoram. Jadavpur University, India, (June).

Walski, T.M., Chase, D.V., Savic, D.A., Grayman, W., Beckwith, S., and Koelle, E. (2003). Advanced Water Distribution Modeling and Management.

Walski. (1983). Technique for calibrating network models, Article in Journal of Water Resources Planning and Management

Wood, Don J. (2005). Water hammers Analysis-Essential and Easy (and Efficient). ASCE, 1123-1131

Wood, D.J., Comprehensive Computer Modeling of Pipe Distribution Networks, Civil Engineering Software Center, College of Engineering, University of Kentucky, Lexington, KY, 1991.

Zlatanovic, L., Moerman, A., Hoek, J. P. Van Der, Vreeburg, J., Blokker, M., Zlatanovic, L.Vreeburg, J. (2017). Development and validation of a drinking water temperature model in domestic drinking water supply systems. Urban Water Journal, 9006, 1–7.

APPENDICES

Appendix A: Transient Analysis results without Surge Protection Equipment (Pipes exceeded the maximum pressure threshold during the analysis)

S.No.	Label	Diameter (mm)	Material	Wave Speed (m/s)	Pressure (Start) (m H2O)	Pressure (Max. Transient) ($m H_2O$)	Pressure (Min. Transient) ($m H_2O$)	Velocity (m/s)	Velocity (Max. Transient) (m/s)	Velocity (Min. Transient) (m/s)
1	P-111	300	Ductile Iron	1,192.76	119.63	170.79	25.26	0.98	0.44	-0.23
2	P-108	300	Ductile Iron	1,192.76	119.63	168.61	22.89	0.98	1.28	-0.25
3	P-96	300	Steel	1,192.76	119.73	168.09	25.79	0.98	0.44	-0.28
4	P-97	300	Steel	1,192.76	118.77	167.67	23.79	0.98	0.29	-1.28
5	P-149	200	Steel	1,200.59	117.52	167.45	25	1.27	1.12	-0.43
6	P-148	200	Ductile Iron	1,200.59	113.4	167.45	26.04	1.27	1.11	-0.36
7	P-9	350	Ductile Iron	1,162.73	118.77	164.32	25.79	1.44	1.06	-0.4
8	P-191	150	Ductile Iron	1,221.70	-0.2	163.4	-9.98	0.15	0.94	-0.62
9	P-24	350	Ductile Iron	1,162.73	105.71	162.95	15.42	1.03	0.7	-0.42
10	P-23	350	Ductile Iron	1,162.73	104.38	162.95	16.93	1.03	0.7	-0.48
11	P-11	350	Ductile Iron	1,162.73	117.52	162.36	23.63	1.03	0.7	-0.51
12	P-10	350	Ductile Iron	1,162.73	115.99	162.36	24.67	1.03	0.7	-0.51
13	P-22	350	Ductile Iron	1,162.73	107.01	161.8	17.65	1.03	0.7	-0.54
14	P-14	350	Ductile Iron	1,162.73	115.14	160.95	24.17	1.03	0.7	-0.55
15	P-13	350	Ductile Iron	1,162.73	115.6	160.95	24.2	1.03	0.7	-0.54
16	P-12	350	Ductile Iron	1,162.73	115.12	160.6	23.63	1.03	0.7	-0.53

S.No.	Label	Diameter (mm)	Material	Wave Speed (m/s)	Pressure (Start) (m H2O)	Pressure (Max. Transient) (m H_2O)	Pressure (Min. Transient) (m H_2O)	Velocity (m/s)	Velocity (Max. Transient) (m/s)	Velocity (Min. Transient) (m/s)
17	P-25	350	Ductile Iron	1,162.73	102.63	160.59	13.93	1.03	0.7	-0.41
18	P-21	350	Ductile Iron	1,162.73	108.25	160.57	18.52	1.03	0.7	-0.56
19	P-18	350	Ductile Iron	1,162.73	113.32	160.07	21.23	1.03	0.7	-0.58
20	P-17	350	Ductile Iron	1,162.73	112.43	160.07	22.66	1.03	0.7	-0.58
21	P-20	350	Ductile Iron	1,162.73	111.24	160.04	19.36	1.03	0.7	-0.58
22	P-19	350	Ductile Iron	1,162.73	109.78	160.04	20.16	1.03	0.7	-0.58
23	P-15	350	Ductile Iron	1,162.73	115.03	159.79	23.42	1.03	0.7	-0.57
24	P-16	350	Ductile Iron	1,162.73	114.06	159.74	23.08	1.03	0.7	-0.58
25	P-27	350	Ductile Iron	1,162.73	101.09	158.08	10.76	1.03	0.7	-0.39
26	P-26	350	Ductile Iron	1,162.73	99.49	158.08	12.02	1.03	0.7	-0.41
27	P-28	350	Ductile Iron	1,162.73	97.85	155.53	10.44	1.03	0.7	-0.46
28	P-105	300	Ductile Iron	1,192.76	69.22	148.16	-9.98	0.52	0.81	-0.21
29	P-29	350	Ductile Iron	1,162.73	96.61	145.59	9.34	1.03	0.7	-0.49
30	P-102	300	Ductile Iron	1,192.76	69.52	143.74	-9.98	0.52	0.47	-0.18
31	P-30	350	Ductile Iron	1,162.73	95.13	143.58	8.8	1.03	0.7	-0.51
32	P-92	300	Ductile Iron	1,192.76	68.99	142.86	-9.98	0.52	0.81	-0.22
33	P-31	350	Ductile Iron	1,162.73	93.81	141.35	7.13	1.03	0.7	-0.52
34	P-936	300	Ductile Iron	1,192.76	65.83	140.49	-9.98	1.04	0.41	-0.91
35	P-937	300	Ductile Iron	1,192.76	66.96	140.49	-9.98	1.04	0.41	-0.91
36	P-32	350	Ductile Iron	1,162.73	92.25	137.42	5.77	1.03	0.7	-0.52
37	P-93	300	Ductile Iron	1,192.76	68.6	137.15	-9.98	0.52	0.19	-0.51
38	P-33	350	Ductile Iron	1,162.73	90.39	135.62	4.45	1.03	0.7	-0.54
39	P-935	300	Ductile Iron	1,192.76	64.51	133.83	-9.98	1.04	0.44	-0.91
40	P-34	350	Ductile Iron	1,162.73	88.64	133.26	2.74	1.03	0.7	-0.55

S.No.	Label	Diameter (mm)	Material	Wave Speed (m/s)	Pressure (Start) (m H2O)	Pressure (Max. Transient) (m H_2O)	Pressure (Min. Transient) (m H_2O)	Velocity (m/s)	Velocity (Max. Transient) (m/s)	Velocity (Min. Transient) (m/s)
41	P-930	300	Ductile Iron	1,192.76	64.17	132.99	-9.98	1.04	0.43	-0.92
42	P-931	300	Ductile Iron	1,192.76	64.79	132.99	-9.98	1.04	0.43	-0.92
43	P-35	350	Ductile Iron	1,162.73	86.66	131.94	1.3	1.03	0.7	-0.56
44	P-934	300	Ductile Iron	1,192.76	64.39	131.79	-9.98	1.04	0.46	-0.91
45	P-927	300	Ductile Iron	1,192.76	61.34	131.78	-9.98	1.04	0.43	-0.91
46	P-928	300	Ductile Iron	1,192.76	62.35	131.78	-9.98	1.04	0.43	-0.91
47	P-925	300	Ductile Iron	1,192.76	58.49	131.56	-9.98	1.04	0.45	-0.9
48	P-926	300	Ductile Iron	1,192.76	60.03	131.56	-9.98	1.04	0.43	-0.91
49	P-36	350	Ductile Iron	1,162.73	84.79	130.74	-0.55	1.03	0.7	-0.58
50	P-929	300	Ductile Iron	1,192.76	63.16	128.47	-9.98	1.04	0.43	-0.92
51	P-932	300	Ductile Iron	1,192.76	64.47	128.4	-9.98	1.04	0.46	-0.92
52	P-190	150	Ductile Iron	1,221.70	-0.07	127.89	-9.98	0.15	1.25	-0.84
53	P-110	300	Ductile Iron	1,192.76	119.65	127.86	-4.44	0.98	0.41	-0.05
54	P-933	300	Ductile Iron	1,192.76	64.21	127.84	-9.98	1.04	0.46	-0.91
55	P-37	350	Ductile Iron	1,162.73	82.94	127.3	-2.19	1.03	0.7	-0.59
56	P-38	350	Ductile Iron	1,162.73	80.91	126.23	-3.26	1.03	0.7	-0.59
57	P-39	350	Ductile Iron	1,162.73	79.3	123.98	-4.75	1.03	0.7	-0.59
58	P-696	50	Ductile Iron	517.57	71.71	123.2	6.86	0.07	0.62	-0.55
59	P-924	300	Ductile Iron	1,192.76	56.83	122.53	-9.98	1.04	0.46	-0.91
60	P-923	300	Ductile Iron	1,192.76	55.58	122.03	-9.98	1.04	0.46	-0.91
61	P-922	300	Ductile Iron	1,192.76	54.27	120.07	-9.98	1.04	0.48	-0.91
62	P-915	300	Ductile Iron	1,192.76	43.13	118.86	-9.98	1.04	0.64	-0.92
63	P-916	300	Ductile Iron	1,192.76	44.64	118.86	-9.98	1.04	0.63	-0.92
64	P-40	350	Ductile Iron	1,162.73	76.77	118.72	-6.3	1.03	0.71	-0.58

S.No.	Label	Diameter (mm)	Material	Wave Speed (m/s)	Pressure (Start) (m H2O)	Pressure (Max. Transient) (m H_2O)	Pressure (Min. Transient) (m H_2O)	Velocity (m/s)	Velocity (Max. Transient) (m/s)	Velocity (Min. Transient) (m/s)
65	P-920	300	Ductile Iron	1,192.76	51	118.4	-9.98	1.04	0.5	-0.91
66	P-921	300	Ductile Iron	1,192.76	52.8	118.4	-9.98	1.04	0.49	-0.91
67	P-914	300	Ductile Iron	1,192.76	42.26	117.59	-9.98	1.04	0.65	-0.91
68	P-919	300	Ductile Iron	1,192.76	49.36	116.59	-9.98	1.04	0.54	-0.91
69	P-918	300	Ductile Iron	1,192.76	47.7	115.35	-9.98	1.04	0.55	-0.91
70	P-698	50	Ductile Iron	517.57	69.86	115.18	7.19	0.08	0.62	-0.43
71	P-107	300	Ductile Iron	1,192.76	119.65	114.77	17.79	0.98	1.28	0
72	P-41	350	Ductile Iron	1,162.73	74.7	114.19	-6.33	1.03	0.71	-0.58
73	P-150	200	Ductile Iron	1,200.59	82.71	113.65	33.23	1.27	1.12	-0.43
74	P-917	300	Ductile Iron	1,192.76	45.97	110.1	-9.98	1.04	0.58	-0.91
75	P-192	150	Ductile Iron	1,221.70	-0.91	106.3	-9.98	0.15	0.38	-0.44
76	P-700	50	Ductile Iron	517.57	69.45	106.28	8.43	0.1	0.57	-0.09
77	P-913	300	Ductile Iron	1,192.76	42.32	106.16	-9.98	1.04	0.65	-0.91
78	P-194	150	Ductile Iron	1,221.70	-0.64	105.75	-9.98	0	0.39	-0.45
79	P-157	200	Ductile Iron	1,192.76	82.2	105.34	31.25	0.24	0.75	0.17
80	P-151	200	Ductile Iron	1,200.59	82.2	105.27	36.46	1.02	0.63	-0.68
81	P-152	200	Ductile Iron	1,200.59	82.16	105.26	38.43	1.02	0.63	-0.68
82	P-153	200	Ductile Iron	1,200.59	82.1	104.89	40.39	1.02	0.63	-0.69
83	P-154	200	Ductile Iron	1,200.59	81.86	103.98	41.72	1.02	0.63	-0.69
84	P-155	200	Ductile Iron	1,200.59	81.58	102.51	33.67	0.62	0	-0.95
85	P-161	200	Ductile Iron	1,200.59	81.58	101.86	32.7	0.4	1	0.07
86	P-42	350	Ductile Iron	1,162.73	72.86	101.53	-7.11	1.03	0.7	-0.58
87	P-43	350	Ductile Iron	1,162.73	70.96	100.36	-7.31	1.03	0.71	-0.57
88	P-912	300	Ductile Iron	1,192.76	44.86	99.85	-9.98	1.04	0.7	-0.92

S.No.	Label	Diameter (mm)	Material	Wave Speed (m/s)	Pressure (Start) (m H2O)	Pressure (Max. Transient) (m H_2O)	Pressure (Min. Transient) (m H_2O)	Velocity (m/s)	Velocity (Max. Transient) (m/s)	Velocity (Min. Transient) (m/s)
89	P-44	350	Ductile Iron	1,162.73	69.36	98.72	-9.23	1.03	0.71	-0.52
90	P-45	350	Ductile Iron	1,162.73	67.2	97.63	-9.98	1.03	0.71	-0.51
91	P-911	300	Steel	1,192.76	41.78	97.56	-9.98	1.04	0.71	-0.92
92	P-46	350	Steel	1,162.73	65.12	97.51	-9.98	1.03	0.71	-0.5
93	P-876	50	Steel	517.57	93.45	97.49	74.5	0.7	-0.19	-0.44
94	P-47	350	Steel	1,162.73	63.81	97.29	-9.98	1.03	0.71	-0.5
95	P-101	300	Steel	1,192.76	69.92	96.86	-9.98	0.52	0.42	-0.03
96	P-875	50	Steel	517.57	93.49	96.12	84.61	0.7	-0.18	-0.47
97	P-158	200	Steel	1,192.76	76.93	96.02	13.37	0.24	0.77	0.18
98	P-461	75	Steel	501.98	73.29	95.84	67.84	0.29	0.02	-0.19
99	P-48	350	Ductile Iron	1,162.73	62.56	95.46	-9.98	1.03	0.71	-0.49
100	P-49	350	Steel	1,162.73	60.74	95.2	-9.98	1.03	0.71	-0.49
101	P-50	350	Steel	1,162.73	58.35	94.76	-9.98	1.03	0.72	-0.48
102	P-910	300	Steel	1,192.76	41.49	94.29	-9.98	1.04	0.73	-0.92
103	P-695	50	Steel	517.57	71.09	93.33	7.02	0.07	0.65	-0.5
104	P-195	150	Steel	1,221.70	0.37	92.5	-9.98	0	0.48	-0.59
105	P-51	350	Steel	1,162.73	55.03	92.34	-9.98	1.03	0.72	-0.48
106	P-340	100	Steel	473.38	69.3	92.21	7.59	0.03	0.29	-0.28
107	P-193	150	Steel	1,221.70	0.04	91.39	-9.98	0.15	0.49	-0.6
108	P-392	100	Steel	1,329.46	85.42	90.95	76.58	0.13	0.04	0.02
109	P-864	50	Steel	517.57	96.87	90.95	76.44	0.01	0.42	0.33
110	P-877	50	Steel	517.57	86.58	90.44	65.5	0.88	-0.54	-1
111	P-909	300	Steel	1,192.76	39.79	90.01	-9.98	1.04	0.76	-0.92
112	P-162	200	uPVC	1,200.59	74.46	89.44	27.5	0.12	0.67	0.2

S.No.	Label	Diameter (mm)	Material	Wave Speed (m/s)	Pressure (Start) (m H2O)	Pressure (Max. Transient) (m H_2O)	Pressure (Min. Transient) (m H_2O)	Velocity (m/s)	Velocity (Max. Transient) (m/s)	Velocity (Min. Transient) (m/s)
113	P-887	50	uPVC	517.57	86.58	89.4	73.12	0.12	0.48	0.11
114	P-888	50	Ductile Iron	517.57	86.4	89.33	60.16	0.12	0.47	0.1
115	P-746	50	Ductile Iron	517.57	57.49	88.47	9.49	0.25	1	-0.63
116	P-908	300	uPVC	1,192.76	37.33	88.44	-9.98	1.04	0.76	-0.92
117	P-52	350	uPVC	1,162.73	51.13	88.33	-9.98	1.03	0.71	-0.47
118	P-339	100	Ductile Iron	473.38	69.01	87.34	7.65	0.05	0.43	-0.38
119	P-338	100	uPVC	473.38	68.77	87.08	8.65	0.09	0.83	-0.53
120	P-163	200	Ductile Iron	1,200.59	70.89	86.63	22.57	0.12	0.67	0.2
121	P-53	350	Ductile Iron	1,162.73	47.44	86.18	-9.98	1.03	0.72	-0.46
122	P-697	50	Ductile Iron	517.57	69.3	86.12	7.22	0.08	0.62	-0.43
123	P-699	50	Ductile Iron	517.57	69.01	86.06	8.43	0.1	0.57	-0.14
124	P-175	200	Ductile Iron	1,200.59	42.79	85.81	7.49	0.28	0.29	-0.41
125	P-907	300	Ductile Iron	1,192.76	34.77	85.8	-9.98	1.04	0.7	-0.91
126	P-164	200	Ductile Iron	1,200.59	65.94	85.55	6.88	0.09	0.55	0.13
127	P-745	50	Steel	517.57	56.97	85.53	9.78	0.25	0.96	-0.38
128	P-878	50	Steel	517.57	82.73	85.22	65.93	0.88	-0.51	-0.97
129	P-241	150	Steel	1,221.70	82.42	85.22	49.95	0.1	-0.04	-0.18
130	P-851	50	Steel	517.57	86.64	83.68	80.28	0.3	0.79	0.73
131	P-54	350	Steel	1,162.73	44.05	83.55	-9.98	1.03	0.72	-0.53
132	P-55	350	Steel	1,162.73	43	83.55	-9.98	1.03	0.72	-0.54
133	P-643	63	Steel	330.71	46.93	83.49	37.61	0.32	0.11	0
134	P-646	63	Steel	330.71	86.64	83.49	75.76	0.09	-0.46	-0.56
135	P-758	50	Steel	517.57	73.47	83.43	46.46	0.01	0.31	-0.3
136	P-852	50	Steel	517.57	86.79	83.41	66.95	0.3	0.79	0.73

S.No.	Label	Diameter (mm)	Material	Wave Speed (m/s)	Pressure (Start) (m H2O)	Pressure (Max. Transient) (m H_2O)	Pressure (Min. Transient) (m H_2O)	Velocity (m/s)	Velocity (Max. Transient) (m/s)	Velocity (Min. Transient) (m/s)
137	P-244	150	Steel	1,243.14	61.3	83.09	-9.98	0.15	0.58	-0.32
138	P-56	350	Ductile Iron	1,162.73	43.1	83.03	-9.98	1.03	0.72	-0.54
139	P-404	90	Ductile Iron	475.81	55.56	83	10.23	0.08	0.43	-0.25
140	P-57	350	Ductile Iron	1,162.73	42.91	82.5	-9.98	1.03	0.72	-0.53
141	P-58	350	Ductile Iron	1,162.73	40.75	82.08	-9.98	1.03	0.72	-0.55
142	P-865	50	Ductile Iron	517.57	79	81.76	72.12	0.3	0.42	0.34
143	P-393	100	Ductile Iron	1,329.46	87.18	81.76	71.37	0.09	0.08	0.05
144	P-906	300	Ductile Iron	1,192.76	32.28	81.74	-9.98	1.04	0.7	-0.91
145	P-754	50	Ductile Iron	517.57	65	81.67	17.02	0.39	0.94	-0.92
146	P-863	50	Ductile Iron	517.57	81	81.11	75.52	0.37	0.96	0.87
147	P-862	50	Ductile Iron	517.57	80.86	80.8	75.63	0.44	1.09	1
148	P-159	200	Ductile Iron	1,200.59	61.71	80.79	10.36	0.24	0.75	0.18
149	P-59	350	Ductile Iron	1,162.73	38.02	80.66	-9.98	1.03	0.72	-0.55
150	P-861	50	Ductile Iron	517.57	79.4	80.29	75.36	0.44	1.09	0.99
151	P-860	50	Ductile Iron	517.57	79.27	80.03	75.14	0.36	-2.1	-2.32
152	P-239	150	Ductile Iron	1,221.70	79.4	80.03	67.14	0.07	0.01	-0.05
153	P-168	200	Ductile Iron	1,200.59	34.44	80.03	32.58	0.04	0.22	0.17

Appendix B: Transient Analysis results without Surge Protection Equipment (Pipes rated below the minimum pressure threshold during analysis)

S.No.	Label	Diameter (mm)	Material	Wave Speed (m/s)	Pressure (Start) (m H2O)	Pressure (Max. Transient) (m H_2O)	Pressure (Min. Transient) (m H_2O)	Velocity (m/s)	Velocity (Max. Transient) (m/s)	Velocity (Min. Transient) (m/s)
1	P-191	150	Ductile Iron	1,221.70	-0.2	163.4	-9.98	0.15	0.94	-0.62
2	P-105	300	Ductile Iron	1,192.76	69.22	148.16	-9.98	0.52	0.81	-0.21
3	P-102	300	Ductile Iron	1,192.76	69.52	143.74	-9.98	0.52	0.47	-0.18
4	P-92	300	Ductile Iron	1,192.76	68.99	142.86	-9.98	0.52	0.81	-0.22
5	P-936	300	Ductile Iron	1,192.76	65.83	140.49	-9.98	1.04	0.41	-0.91
6	P-937	300	Ductile Iron	1,192.76	66.96	140.49	-9.98	1.04	0.41	-0.91
7	P-93	300	Ductile Iron	1,192.76	68.6	137.15	-9.98	0.52	0.19	-0.51
8	P-935	300	Ductile Iron	1,192.76	64.51	133.83	-9.98	1.04	0.44	-0.91
9	P-930	300	Ductile Iron	1,192.76	64.17	132.99	-9.98	1.04	0.43	-0.92
10	P-931	300	Ductile Iron	1,192.76	64.79	132.99	-9.98	1.04	0.43	-0.92
11	P-934	300	Ductile Iron	1,192.76	64.39	131.79	-9.98	1.04	0.46	-0.91
12	P-927	300	Ductile Iron	1,192.76	61.34	131.78	-9.98	1.04	0.43	-0.91
13	P-928	300	Ductile Iron	1,192.76	62.35	131.78	-9.98	1.04	0.43	-0.91
14	P-925	300	Ductile Iron	1,192.76	58.49	131.56	-9.98	1.04	0.45	-0.9
15	P-926	300	Ductile Iron	1,192.76	60.03	131.56	-9.98	1.04	0.43	-0.91
16	P-929	300	Ductile Iron	1,192.76	63.16	128.47	-9.98	1.04	0.43	-0.92
17	P-932	300	Ductile Iron	1,192.76	64.47	128.4	-9.98	1.04	0.46	-0.92
18	P-190	150	Ductile Iron	1,221.70	-0.07	127.89	-9.98	0.15	1.25	-0.84
19	P-933	300	Ductile Iron	1,192.76	64.21	127.84	-9.98	1.04	0.46	-0.91
20	P-924	300	Ductile Iron	1,192.76	56.83	122.53	-9.98	1.04	0.46	-0.91
21	P-923	300	Ductile Iron	1,192.76	55.58	122.03	-9.98	1.04	0.46	-0.91

S.No.	Label	Diameter (mm)	Material	Wave Speed (m/s)	Pressure (Start) (m H2O)	Pressure (Max. Transient) (m H_2O)	Pressure (Min. Transient) (m H_2O)	Velocity (m/s)	Velocity (Max. Transient) (m/s)	Velocity (Min. Transient) (m/s)
22	P-922	300	Ductile Iron	1,192.76	54.27	120.07	-9.98	1.04	0.48	-0.91
23	P-915	300	Ductile Iron	1,192.76	43.13	118.86	-9.98	1.04	0.64	-0.92
24	P-916	300	Ductile Iron	1,192.76	44.64	118.86	-9.98	1.04	0.63	-0.92
25	P-920	300	Ductile Iron	1,192.76	51	118.4	-9.98	1.04	0.5	-0.91
26	P-921	300	Ductile Iron	1,192.76	52.8	118.4	-9.98	1.04	0.49	-0.91
27	P-914	300	Ductile Iron	1,192.76	42.26	117.59	-9.98	1.04	0.65	-0.91
28	P-919	300	Ductile Iron	1,192.76	49.36	116.59	-9.98	1.04	0.54	-0.91
29	P-918	300	Ductile Iron	1,192.76	47.7	115.35	-9.98	1.04	0.55	-0.91
30	P-917	300	Ductile Iron	1,192.76	45.97	110.1	-9.98	1.04	0.58	-0.91
31	P-192	150	Ductile Iron	1,221.70	-0.91	106.3	-9.98	0.15	0.38	-0.44
32	P-913	300	Ductile Iron	1,192.76	42.32	106.16	-9.98	1.04	0.65	-0.91
33	P-194	150	Ductile Iron	1,221.70	-0.64	105.75	-9.98	0	0.39	-0.45
34	P-912	300	Ductile Iron	1,192.76	44.86	99.85	-9.98	1.04	0.7	-0.92
35	P-45	350	Ductile Iron	1,162.73	67.2	97.63	-9.98	1.03	0.71	-0.51
36	P-911	300	Steel	1,192.76	41.78	97.56	-9.98	1.04	0.71	-0.92
37	P-46	350	Steel	1,162.73	65.12	97.51	-9.98	1.03	0.71	-0.5
38	P-47	350	Steel	1,162.73	63.81	97.29	-9.98	1.03	0.71	-0.5
39	P-101	300	Steel	1,192.76	69.92	96.86	-9.98	0.52	0.42	-0.03
40	P-48	350	Ductile Iron	1,162.73	62.56	95.46	-9.98	1.03	0.71	-0.49
41	P-49	350	Steel	1,162.73	60.74	95.2	-9.98	1.03	0.71	-0.49
42	P-50	350	Steel	1,162.73	58.35	94.76	-9.98	1.03	0.72	-0.48
43	P-910	300	Steel	1,192.76	41.49	94.29	-9.98	1.04	0.73	-0.92
44	P-195	150	Steel	1,221.70	0.37	92.5	-9.98	0	0.48	-0.59
45	P-51	350	Steel	1,162.73	55.03	92.34	-9.98	1.03	0.72	-0.48
46	P-193	150	Steel	1,221.70	0.04	91.39	-9.98	0.15	0.49	-0.6

S.No.	Label	Diameter (mm)	Material	Wave Speed (m/s)	Pressure (Start) (m H2O)	Pressure (Max. Transient) (m H_2O)	Pressure (Min. Transient) (m H_2O)	Velocity (m/s)	Velocity (Max. Transient) (m/s)	Velocity (Min. Transient) (m/s)
47	P-909	300	Steel	1,192.76	39.79	90.01	-9.98	1.04	0.76	-0.92
48	P-908	300	uPVC	1,192.76	37.33	88.44	-9.98	1.04	0.76	-0.92
49	P-52	350	uPVC	1,162.73	51.13	88.33	-9.98	1.03	0.71	-0.47
50	P-53	350	Ductile Iron	1,162.73	47.44	86.18	-9.98	1.03	0.72	-0.46
51	P-907	300	Ductile Iron	1,192.76	34.77	85.8	-9.98	1.04	0.7	-0.91
52	P-54	350	Steel	1,162.73	44.05	83.55	-9.98	1.03	0.72	-0.53
53	P-55	350	Steel	1,162.73	43	83.55	-9.98	1.03	0.72	-0.54
54	P-244	150	Steel	1,243.14	61.3	83.09	-9.98	0.15	0.58	-0.32
55	P-56	350	Ductile Iron	1,162.73	43.1	83.03	-9.98	1.03	0.72	-0.54
56	P-57	350	Ductile Iron	1,162.73	42.91	82.5	-9.98	1.03	0.72	-0.53
57	P-58	350	Ductile Iron	1,162.73	40.75	82.08	-9.98	1.03	0.72	-0.55
58	P-906	300	Ductile Iron	1,192.76	32.28	81.74	-9.98	1.04	0.7	-0.91
59	P-59	350	Ductile Iron	1,162.73	38.02	80.66	-9.98	1.03	0.72	-0.55
60	P-905	300	Ductile Iron	1,192.76	30.2	79.52	-9.98	1.04	0.7	-0.92
61	P-901	300	Ductile Iron	1,192.76	21.19	79.09	-9.98	1.04	0.7	-0.92
62	P-902	300	Ductile Iron	1,192.76	23.53	79.09	-9.98	1.04	0.69	-0.92
63	P-60	350	Ductile Iron	1,162.73	35.46	77.47	-9.98	1.03	0.72	-0.53
64	P-904	300	Ductile Iron	1,192.76	27.75	77.44	-9.98	1.04	0.69	-0.92
65	P-900	300	Ductile Iron	1,192.76	19.14	77.02	-9.98	1.04	0.71	-0.92
66	P-245	150	Ductile Iron	1,243.14	61.39	76.65	-9.98	0.15	0.58	-0.42
67	P-103	300	Ductile Iron	1,192.76	1.38	74.89	-9.98	0.52	0.81	-0.12
68	P-61	350	Ductile Iron	1,162.73	32.25	73.19	-9.98	1.03	0.72	-0.53
69	P-62	350	Ductile Iron	1,162.73	30.27	72.96	-9.98	1.03	0.72	-0.55
70	P-903	300	Ductile Iron	1,192.76	25.64	72.88	-9.98	1.04	0.7	-0.92
71	P-104	300	Ductile Iron	1,192.76	69.61	72.38	-9.98	0.52	0.81	-0.02

S.No.	Label	Diameter (mm)	Material	Wave Speed (m/s)	Pressure (Start) (m H2O)	Pressure (Max. Transient) (m H_2O)	Pressure (Min. Transient) (m H_2O)	Velocity (m/s)	Velocity (Max. Transient) (m/s)	Velocity (Min. Transient) (m/s)
72	P-63	350	Ductile Iron	1,162.73	28.69	70.44	-9.98	1.03	0.71	-0.56
73	P-100	300	Ductile Iron	1,192.76	1.66	70.41	-9.98	0.52	0.36	-0.06
74	P-91	300	Ductile Iron	1,192.76	1.99	68.57	-9.98	0.52	0.81	-0.2
75	P-249	150	Ductile Iron	1,243.14	61.55	68.31	-9.98	0	0.12	-0.39
76	P-247	150	Ductile Iron	1,243.14	61.48	68.04	-9.98	0.15	0.13	-0.39
77	P-248	150	Ductile Iron	1,243.14	61.12	67.97	-9.98	0	0.15	-0.39
78	P-246	150	Ductile Iron	1,243.14	61.12	67.91	-9.98	0.15	0.16	-0.39
79	P-94	300	Ductile Iron	1,192.76	1.66	67.75	-9.98	0.52	0.08	-0.41
80	P-109	300	ISOPVC	1,192.76	2.02	65.89	-9.98	0.98	0.4	-0.1
81	P-899	300	ISOPE	1,192.76	16.84	65.79	-9.98	1.04	0.72	-0.92
82	P-196	150	ISOPE	1,221.70	61.12	65.75	-9.98	0.29	0.65	-0.21
83	P-197	150	ISOPVC	1,221.70	60.47	64.84	-9.98	0.29	0.65	-0.19
84	P-95	300	ISOPVC	1,192.76	2.25	64.71	-9.98	0.98	0.42	-0.14
85	P-198	150	ISOPVC	1,221.70	60.51	64.63	-9.98	0.29	0.65	-0.19
86	P-199	150	ISOPVC	1,221.70	60.61	64.48	-9.98	0.29	0.65	-0.2
87	P-106	300	ISOPVC	1,192.76	1.76	64.37	-9.98	0.98	1.28	-0.2
88	P-200	150	ISOPVC	1,221.70	60.24	63.87	-9.98	0.29	0.65	-0.2
89	P-898	300	ISOPVC	1,192.76	14.48	63.76	-9.98	1.04	0.74	-0.93
90	P-125	250	ISOPVC	1,195.94	-0.68	63.27	-9.98	0.11	0.53	-0.33
91	P-306	110	ISOPVC	453.46	25.83	63.07	-9.98	0.06	0.53	-0.42
92	P-201	150	ISOPVC	1,221.70	59.65	63.03	-9.98	0.29	0.65	-0.19
93	P-64	350	ISOPVC	1,162.73	26.25	62.55	-9.98	1.03	0.72	-0.57
94	P-896	300	ISOPVC	1,192.76	59.23	62.36	-9.98	0.29	0.77	-0.93
95	P-897	300	ISOPVC	1,192.76	48.02	62.36	-9.98	1.04	0.72	-0.93
96	P-202	150	ISOPVC	1,221.70	10.16	62.36	-9.98	1.04	0.65	-0.2

S.No.	Label	Diameter (mm)	Material	Wave Speed (m/s)	Pressure (Start) (m H2O)	Pressure (Max. Transient) (m H_2O)	Pressure (Min. Transient) (m H_2O)	Velocity (m/s)	Velocity (Max. Transient) (m/s)	Velocity (Min. Transient) (m/s)
97	P-98	300	GS	1,192.76	1.76	61.82	-9.98	0.98	0.18	-1.28
98	P-203	150	ISOPVC	1,221.70	0.87	61.71	-9.98	0.59	0.65	-0.2
99	P-3	400	ISOPVC	1,161.46	58.83	61.71	-9.98	0.29	0.54	-0.05
100	P-204	150	ISOPVC	1,221.70	59.08	61.7	-9.98	0.29	0.65	-0.19
101	P-205	150	JISPVC	1,221.70	58.41	60.78	-9.98	0.29	0.65	-0.19
102	P-708	50	JISPVC	517.57	56.78	60.58	-9.98	0.04	0.5	-0.62
103	P-895	300	JISPVC	1,192.76	8.16	60.24	-9.98	1.04	0.77	-0.92
104	P-4	400	JISPVC	1,161.46	0.87	60.02	-9.98	1.11	0.85	-0.12
105	P-65	350	JISPVC	1,162.73	23.77	59.77	-9.98	1.03	0.72	-0.59
106	P-5	400	JISPVC	1,161.46	-0.7	59.5	-9.98	1.69	1.35	-0.12
107	P-124	250	JISPVC	1,195.94	-0.7	59.48	-9.98	0.11	0.54	-0.39
108	P-206	150	JISPVC	1,221.70	57.16	59.29	-9.98	0.29	0.65	-0.19
109	P-66	350	ISOPVC	1,162.73	21.04	57.97	-9.98	1.03	0.72	-0.71
110	P-207	150	GS	1,221.70	55.89	57.76	-9.98	0.29	0.65	-0.19
111	P-208	150	GS	1,221.70	54.85	56.47	-9.98	0.29	0.65	-0.19
112	P-894	300	ISOPVC	1,192.76	5.96	56.28	-9.98	1.04	0.8	-0.91
113	P-707	50	ISOPVC	517.57	44.52	55.79	-9.98	0.03	0.65	-0.7
114	P-374	100	ISOPVC	473.38	56.82	55.79	-9.98	0.04	0.38	-0.51
115	P-67	350	ISOPVC	1,162.73	18.76	55.71	-9.98	1.03	0.72	-0.78
116	P-209	150	ISOPVC	1,221.70	53.76	55.13	-9.98	0.29	0.65	-0.18
117	P-407	90	ISOPVC	475.81	42.69	54.05	-9.98	0.11	0.97	-0.44
118	P-210	150	ISOPVC	1,221.70	52.61	53.73	-9.98	0.29	0.64	-0.18
119	P-2	400	ISOPVC	1,161.46	-0.09	52.95	-9.98	1.74	1.37	-0.12
120	P-211	150	ISOPVC	1,221.70	51.15	52.02	-9.98	0.29	0.64	-0.18
121	P-222	150	JISPVC	1,221.70	10.72	50.56	-9.98	0.73	0.95	0.51

S.No.	Label	Diameter (mm)	Material	Wave Speed (m/s)	Pressure (Start) (m H2O)	Pressure (Max. Transient) (m H_2O)	Pressure (Min. Transient) (m H_2O)	Velocity (m/s)	Velocity (Max. Transient) (m/s)	Velocity (Min. Transient) (m/s)
122	P-212	150	JISPVC	1,221.70	49.9	50.52	-9.98	0.29	0.64	-0.19
123	P-68	350	JISPVC	1,162.73	17.13	50.51	-9.98	1.03	0.72	-0.86
124	P-69	350	ISOPVC	1,162.73	16.47	49.64	-9.98	1.03	0.72	-0.84
125	P-213	150	ISOPVC	1,221.70	48.5	48.87	-9.98	0.29	0.64	-0.19
126	P-71	350	ISOPE	1,162.73	14.29	48.27	-9.98	1.03	0.73	-0.85
127	P-72	350	ISOPE	1,162.73	12.78	48.27	-9.98	1.03	0.73	-0.87
128	P-70	350	ISOPVC	1,162.73	15.55	48.05	-9.98	1.03	0.73	-0.85
129	P-214	150	ISOPVC	1,221.70	47.11	47.23	-9.98	0.29	0.67	-0.19
130	P-128	200	ISOPVC	1,379.88	-0.27	46.54	-9.98	3.47	2.7	-0.27
131	P-129	200	ISOPVC	1,379.88	-0.09	46.54	-9.98	3.47	0.27	-2.7
132	P-73	350	ISOPVC	1,162.73	11.19	46.12	-9.98	1.03	0.74	-0.88
133	P-893	300	ISOPVC	1,192.76	3.35	45.75	-9.98	1.04	0.86	-0.92
134	P-215	150	ISOPVC	1,221.70	45.9	45.73	-9.98	0.29	0.67	-0.23
135	P-749	50	ISOPVC	517.57	22.62	45.6	-9.98	0.34	0.92	-0.33
136	P-74	350	ISOPE	1,162.73	9.93	44.73	-9.98	1.03	0.74	-0.89
137	P-75	350	ISOPE	1,162.73	8.12	43.69	-9.98	1.03	0.73	-0.91
138	P-138	200	ISOPE	1,200.59	3.35	42.06	-9.98	1.17	1.03	-0.91
139	P-145	200	ISOPE	1,213.64	3.58	42.06	-9.98	1.17	0.89	-1.03
140	P-76	350	ISOPVC	1,162.73	6.24	41.25	-9.98	1.03	0.72	-0.93
141	P-373	100	ISOPVC	473.38	46.93	40.55	-9.98	0.03	0.33	-0.48
142	P-324	100	ISOPVC	473.38	44.23	40.26	-9.98	0.61	1.29	-0.48
143	P-325	100	ISOPVC	473.38	44.09	39.83	-9.98	0.61	1.29	-0.5
144	P-302	110	ISOPVC	453.46	20.08	39.51	-9.98	0.63	1.19	-0.27
145	P-702	50	HDPE	368.93	37.57	39.51	-9.98	0.2	0.95	-0.16
146	P-305	110	ISOPE	453.46	24.97	39.45	-9.98	0.06	0.58	-0.43

S.No.	Label	Diameter (mm)	Material	Wave Speed (m/s)	Pressure (Start) (m H2O)	Pressure (Max. Transient) (m H_2O)	Pressure (Min. Transient) (m H_2O)	Velocity (m/s)	Velocity (Max. Transient) (m/s)	Velocity (Min. Transient) (m/s)
147	P-77	350	ISOPVC	1,162.73	4.52	39.4	-9.98	1.03	0.72	-0.93
148	P-301	110	ISOPVC	453.46	29.89	39.28	-9.98	0.62	1.02	-0.22
149	P-304	110	ISOPE	453.46	24.95	38.96	-9.98	0.06	0.58	-0.46
150	P-655	50	ISOPVC	517.57	42.72	38.85	-9.98	0.19	0.47	-0.19
151	P-173	200	ISOPE	1,200.59	21.57	38.67	-9.98	0.19	0.25	-0.08
152	P-326	100	HDPE	473.38	3.5	38.5	-9.98	0.73	1.3	-0.5
153	P-79	350	HDPE	1,162.73	2.6	38.5	-9.98	0.73	0.84	-0.63
154	P-78	350	HDPE	1,162.73	43.52	38.5	-9.98	0.61	0.81	-0.6
155	P-147	200	ISOPVC	1,200.59	3.5	38.44	-9.98	0.93	-0.18	-1.05
156	P-654	50	ISOPVC	517.57	42.55	38.38	-9.98	0.19	0.49	-0.37
157	P-170	200	ISOPE	1,200.59	3.48	37.98	-9.98	0.93	-0.18	-1.06
158	P-80	350	ISOPE	1,162.73	2.53	37.54	-9.98	0.73	0.85	-0.64
159	P-226	150	JISPVC	1,221.70	3.29	36.77	-9.98	0.58	1.63	0.85
160	P-169	200	JISPVC	1,200.59	2.88	36.47	-9.98	0.6	1.66	0.75
161	P-225	150	ISOPVC	1,221.70	3.29	36.47	-9.98	0.58	1.6	0.85
162	P-341	100	JISPVC	473.38	42.55	35.97	-9.98	0.53	1.24	-0.52
163	P-144	200	JISPVC	1,213.89	4.49	35.21	-9.98	1.17	0.94	-1.04
164	P-139	200	JISPVC	1,200.59	3.01	34.63	-9.98	1.17	1.04	-0.97
165	P-342	100	JISPVC	473.38	41.84	34.57	-9.98	0.53	1.25	-0.54
166	P-343	100	JISPVC	473.38	72.26	33.05	-9.98	0.53	1.26	-0.51
167	P-216	150	JISPVC	1,221.70	2.88	32.06	-9.98	0.53	-0.66	-1.5
168	P-218	150	JISPVC	1,221.70	2.88	32.06	-9.98	0.53	-0.66	-1.5
169	P-344	100	JISPVC	473.38	40.17	31.51	-9.98	0.53	1.26	-0.53
170	P-562	63	JISPVC	330.71	40.34	31.49	-9.98	0.05	0.57	-0.57
171	P-345	100	JISPVC	473.38	39.11	29.83	-9.98	0.53	1.27	-0.56

S.No.	Label	Diameter (mm)	Material	Wave Speed (m/s)	Pressure (Start) (m H2O)	Pressure (Max. Transient) (m H_2O)	Pressure (Min. Transient) (m H_2O)	Velocity (m/s)	Velocity (Max. Transient) (m/s)	Velocity (Min. Transient) (m/s)
172	P-221	150	JISPVC	1,221.70	10.69	28.56	-9.98	0.73	0.87	0.53
173	P-346	100	JISPVC	473.38	38	28.1	-9.98	0.53	1.27	-0.64
174	P-355	100	JISPVC	473.38	41.34	27.73	-9.98	0.42	0.8	0.05
175	P-418	90	JISPVC	475.81	12.02	27.59	-9.98	0.48	1.32	0.52
176	P-349	100	JISPVC	473.38	39.26	27.32	-9.98	0.47	0.94	-0.02
177	P-220	150	JISPVC	1,221.70	10.6	27.3	-9.98	0.73	0.98	0.53
178	P-351	100	JISPVC	473.38	40.36	27.11	-9.98	0.42	0.8	0.02
179	P-352	100	JISPVC	473.38	40.72	27.11	-9.98	0.42	0.8	0.02
180	P-354	100	JISPVC	473.38	40.83	27.1	-9.98	0.42	0.8	0.03
181	P-561	63	JISPVC	330.71	40.36	26.95	-9.98	0.05	0.57	-0.74
182	P-348	100	JISPVC	473.38	37.02	26.87	-9.98	0.47	0.93	-0.04
183	P-701	50	JISPVC	368.93	36.87	26.84	-9.98	0.2	0.96	-0.19
184	P-353	100	JISPVC	473.38	40.64	26.82	-9.98	0.42	0.8	0.03
185	P-347	100	JISPVC	473.38	37.26	26.65	-9.98	0.53	1.28	-0.64
186	P-350	100	JISPVC	473.38	37.02	26.17	-9.98	0.06	1.21	-0.48
187	P-130	200	GS	1,379.88	-0.15	24.7	-9.98	3.47	0.27	-2.72
188	P-127	200	JISPVC	1,379.88	0	24.35	-9.98	3.47	2.72	-0.28
189	P-743	110	GS	517.57	10.6	21.64	-9.98	0.29	1.63	0.3
190	P-417	90	JISPVC	475.81	11.6	21.01	-9.98	0.5	1.34	0.53
191	P-416	90	GS	475.81	11.41	21.33	-9.97	0.5	1.35	0.53
192	P-217	150	JISPVC	1,221.70	2.81	30.21	-9.95	0.53	-0.65	-1.5
193	P-219	150	JISPVC	1,221.70	2.9	30.29	-9.94	0.53	-0.65	-1.5
194	P-744	110	JISPVC	517.57	11.14	20.82	-9.94	0.29	1.66	0.22
195	P-299	110	Ductile Iron	453.46	11.41	20.18	-9.94	0.62	1.07	-0.27
196	P-303	110	ISOPE	453.46	24.88	38.67	-9.75	0.06	0.57	-0.46

S.No.	Label	Diameter (mm)	Material	Wave Speed (m/s)	Pressure (Start) (m H2O)	Pressure (Max. Transient) (m H_2O)	Pressure (Min. Transient) (m H_2O)	Velocity (m/s)	Velocity (Max. Transient) (m/s)	Velocity (Min. Transient) (m/s)
197	P-44	350	Ductile Iron	1,162.73	69.36	98.72	-9.23	1.03	0.71	-0.52
198	P-300	110	ISOPVC	453.46	11.61	38.92	-9.17	0.62	1.14	-0.26
199	P-356	100	JISPVC	473.38	42.18	27.73	-8.81	0.42	0.8	0.03
200	P-174	200	GS	1,200.59	47.87	56.37	-8.68	0.21	0.25	-0.17
201	P-357	100	JISPVC	473.38	42.36	28.26	-7.99	0.42	0.8	0.03
202	P-43	350	Ductile Iron	1,162.73	70.96	100.36	-7.31	1.03	0.71	-0.57
203	P-42	350	Ductile Iron	1,162.73	72.86	101.53	-7.11	1.03	0.7	-0.58
204	P-465	65	JISPVC	479.35	43.52	30.61	-6.73	0.52	0.64	-0.25
205	P-358	100	JISPVC	473.38	43.52	30.35	-6.73	0.15	0.55	0.05
206	P-41	350	Ductile Iron	1,162.73	74.7	114.19	-6.33	1.03	0.71	-0.58
207	P-40	350	Ductile Iron	1,162.73	76.77	118.72	-6.3	1.03	0.71	-0.58
208	P-750	50	ISOPE	517.57	65.21	42.4	-6	0.34	0.9	-0.33
209	P-662	50	ISOPE	517.57	57.89	34.03	-5.5	0.18	0.89	-0.04
210	P-752	50	Ductile Iron	517.57	30.79	73.08	-5.08	0.18	0.29	-0.8
211	P-359	100	JISPVC	473.38	45.78	31.66	-4.77	0.15	0.55	0.04
212	P-39	350	Ductile Iron	1,162.73	79.3	123.98	-4.75	1.03	0.7	-0.59
213	P-110	300	Ductile Iron	1,192.76	119.65	127.86	-4.44	0.98	0.41	-0.05
214	P-751	50	ISOPE	517.57	30.75	43.17	-4.13	0.18	0.29	-0.82
215	P-787	50	ISOPE	517.57	30.75	45.81	-3.84	0.47	0.94	-0.2
216	P-450	75	ISOPE	501.98	35.53	38.8	-3.53	0.02	0.35	-0.15
217	P-360	100	JISPVC	473.38	47.14	33.17	-3.39	0.15	0.55	0.04
218	P-616	63	Steel	330.71	56.71	77.97	-3.3	0.04	0.65	-0.53
219	P-38	350	Ductile Iron	1,162.73	80.91	126.23	-3.26	1.03	0.7	-0.59
220	P-704	50	JISPVC	517.57	46.3	30.28	-3.17	0.79	0.85	-0.43
221	P-705	50	JISPVC	517.57	45.69	33.71	-2.98	0.7	0.67	-0.49

S.No.	Label	Diameter (mm)	Material	Wave Speed (m/s)	Pressure (Start) (m H2O)	Pressure (Max. Transient) (m H_2O)	Pressure (Min. Transient) (m H_2O)	Velocity (m/s)	Velocity (Max. Transient) (m/s)	Velocity (Min. Transient) (m/s)
222	P-86	350	Ductile Iron	1,162.73	3.3	10.72	-2.82	0.22	-0.61	-0.91
223	P-87	350	Ductile Iron	1,162.73	2.5	8.42	-2.82	0.22	-0.61	-0.91
224	P-361	100	JISPVC	473.38	48.7	34.64	-2.58	0.15	0.55	0.04
225	P-37	350	Ductile Iron	1,162.73	82.94	127.3	-2.19	1.03	0.7	-0.59
226	P-703	50	JISPVC	517.57	46.41	30.61	-2.13	0.79	0.85	-0.44
227	P-88	350	Ductile Iron	1,162.73	2.46	7.76	-1.64	0.22	-0.61	-0.92
228	P-85	350	JISPVC	1,162.73	14.91	23.49	-1.18	0.22	-0.61	-0.91
229	P-362	100	JISPVC	473.38	50.22	35.79	-1.02	0.15	0.55	0.03
230	P-36	350	Ductile Iron	1,162.73	84.79	130.74	-0.55	1.03	0.7	-0.58
231	P-771	50	ISOPE	517.57	35.92	46.84	-0.14	0.11	-0.13	-0.97
232	P-660	50	JISPVC	517.57	59.05	31.33	-0.09	0.5	1.6	0.61
233	P-134	200	Ductile Iron	1,379.88	0	6.28	-0.06	0.02	-0.01	-0.02
234	P-133	200	Ductile Iron	1,379.88	-0.02	0	-0.06	0.02	-0.01	-0.02
235	P-172	200	Ductile Iron	1,200.59	-0.02	6.29	-0.04	0	0.03	0.03
236	P-132	200	Ductile Iron	1,379.88	0.1	0.12	-0.04	0.01	0.02	0.02
237	P-137	200	Ductile Iron	1,379.88	-0.04	6.28	0.04	0.03	-0.02	-0.02
238	P-171	200	Ductile Iron	1,379.88	0.11	0.13	0.04	0.03	-0.02	-0.02
239	P-131	200	Ductile Iron	1,379.88	0	6.28	0.08	0.01	0.02	0.02
240	P-6	400	Ductile Iron	1,161.46	0.11	3.67	0.09	0.01	0.01	0.01
241	P-136	200	Ductile Iron	1,379.88	0.14	0.16	0.09	0.01	0.02	0.02
242	P-135	200	Ductile Iron	1,379.88	0.06	6.28	0.12	0.01	0.02	0.02
243	P-420	90	JISPVC	475.81	23.44	34.41	0.47	0.44	1.18	0.47
244	P-363	100	ISOPE	473.38	51.43	36.82	0.49	0.15	0.54	0.03
245	P-419	90	JISPVC	475.81	23.09	26.96	0.73	0.46	1.25	0.5
246	P-513	63	Ductile Iron	479.35	54.2	8.66	1	0.05	-0.03	-0.1

S.No.	Label	Diameter (mm)	Material	Wave Speed (m/s)	Pressure (Start) (m H2O)	Pressure (Max. Transient) (m H_2O)	Pressure (Min. Transient) (m H_2O)	Velocity (m/s)	Velocity (Max. Transient) (m/s)	Velocity (Min. Transient) (m/s)
247	P-514	63	Ductile Iron	479.35	54.21	18.85	1.02	0.05	-0.03	-0.11
248	P-563	63	ISOPE	330.71	56.44	39.71	1.09	0.07	0.46	-0.12
249	P-232	150	ISOPE	1,221.70	14.91	44.23	1.19	0.83	1.16	0.82
250	P-35	350	Ductile Iron	1,162.73	86.66	131.94	1.3	1.03	0.7	-0.56
251	P-753	50	Ductile Iron	517.57	42.13	79.75	1.61	0.18	0.26	-0.88
252	P-364	100	HDPE	473.38	52.51	38.67	1.74	0.15	0.54	0.05
253	P-799	100	Ductile Iron	517.57	39.71	3.28	1.96	0.06	-0.15	-0.15
254	P-564	63	ISOPVC	330.71	57.19	52.5	2.19	0.07	0.46	-0.12
255	P-773	50	JISPVC	517.57	30.25	36.34	2.29	1.25	-1.26	-2.2
256	P-656	50	Ductile Iron	517.57	59.41	77.05	2.33	0.67	2.38	0.94
257	P-661	50	JISPVC	517.57	56.74	29.32	2.38	0.18	0.84	0.01
258	P-663	50	JISPVC	517.57	56.74	29.32	2.63	0.29	1.07	0.36
259	P-34	350	Ductile Iron	1,162.73	88.64	133.26	2.74	1.03	0.7	-0.55
260	P-800	100	Ductile Iron	517.57	40.73	16.35	2.9	0.06	-0.15	-0.15
261	P-307	110	ISOPVC	453.46	43.03	63.07	3.14	0.06	0.46	-0.26
262	P-308	110	Ductile Iron	453.46	43.59	78.53	3.15	0.06	0.46	-0.35
263	P-141	200	Ductile Iron	1,200.59	3.66	5.62	3.22	0.38	0.15	0.09
264	P-140	200	Ductile Iron	1,200.59	4.49	5.1	3.22	0.38	0.15	0.09
265	P-365	100	ISOPE	473.38	54.42	40.61	3.26	0.15	0.54	0.06
266	P-146	200	ISOPVC	1,200.59	3.87	52.14	3.37	0.75	-0.52	-0.63
267	P-89	350	JISPVC	1,162.73	3.87	35.38	3.37	0	0.28	0.25
268	P-142	200	Ductile Iron	1,200.59	3.87	5.62	3.37	0.38	-0.09	-0.15
269	P-611	63	ISOPVC	479.35	48.1	63.61	3.59	0	0.38	-0.41
270	P-7	400	Ductile Iron	1,161.46	3.65	6.68	3.63	0.01	0.01	0.01
271	P-143	200	Ductile Iron	1,200.59	4.09	5.53	3.64	0.38	-0.09	-0.15

S.No.	Label	Diameter (mm)	Material	Wave Speed (m/s)	Pressure (Start) (m H2O)	Pressure (Max. Transient) (m H_2O)	Pressure (Min. Transient) (m H_2O)	Velocity (m/s)	Velocity (Max. Transient) (m/s)	Velocity (Min. Transient) (m/s)
272	P-774	50	ISOPVC	517.57	30.32	38.19	4.01	1.25	-1.25	-2.16
273	P-331	100	Ductile Iron	1,329.46	62.89	19.9	4.26	0	0.01	-0.01
274	P-33	350	Ductile Iron	1,162.73	90.39	135.62	4.45	1.03	0.7	-0.54
275	P-613	63	Ductile Iron	330.71	42.68	68.34	4.55	0.03	0.91	-0.64
276	P-574	63	JISPVC	479.35	43.42	33.25	4.61	0.04	0.06	-0.22
277	P-577	63	JISPVC	479.35	49.39	33.28	4.71	0.01	0.1	-0.09
278	P-409	90	ISOPE	475.81	30.59	38.19	5.03	0.4	-0.39	-0.76
279	P-265	110	JISPVC	453.46	56.48	31.29	5.03	0.05	0.12	-0.34
280	P-484	63	JISPVC	479.35	56.48	22.97	5.03	0.32	1.27	0.05
281	P-84	350	ISOPVC	1,162.73	28.64	36.61	5.18	0.06	-0.43	-0.73
282	P-614	63	Ductile Iron	330.71	44.25	74.25	5.33	0.03	0.58	-0.37
283	P-366	100	ISOPE	473.38	56.41	42.82	5.55	0.15	0.54	0.06
284	P-32	350	Ductile Iron	1,162.73	92.25	137.42	5.77	1.03	0.7	-0.52
285	P-772	50	ISOPVC	517.57	30.48	37.41	5.81	0.11	-0.17	-0.96
286	P-406	90	JISPVC	475.81	99.49	57.81	5.95	0.16	0.31	-0.67
287	P-612	63	JISPVC	330.71	46.99	58.39	5.96	0.03	0.91	-0.7
288	P-114	300	JISPVC	1,192.76	6.27	20.77	6.24	0	0.01	0.01
289	P-609	63	GS	330.71	24.88	56.37	6.25	0.62	3.19	-1.48
290	P-485	63	ISOPVC	479.35	58.05	21.57	6.55	0.32	1.27	0.05
291	P-1	500	JISPVC	1,159.66	6.67	21.35	6.65	0.01	0.01	0.01
292	P-764	50	JISPVC	517.57	32.91	29.8	6.71	0.15	0.11	-0.36
293	P-617	63	JISPVC	479.35	30.25	26.33	6.71	0.8	1.04	0.64
294	P-369	100	ISOPE	473.38	59.25	43.47	6.78	0.15	0.54	0.09
295	P-368	100	ISOPE	473.38	58.97	43.29	6.78	0.15	0.54	0.09
296	P-696	50	Ductile Iron	517.57	71.71	123.2	6.86	0.07	0.62	-0.55

S.No.	Label	Diameter (mm)	Material	Wave Speed (m/s)	Pressure (Start) (m H2O)	Pressure (Max. Transient) (m H_2O)	Pressure (Min. Transient) (m H_2O)	Velocity (m/s)	Velocity (Max. Transient) (m/s)	Velocity (Min. Transient) (m/s)
297	P-164	200	Ductile Iron	1,200.59	65.94	85.55	6.88	0.09	0.55	0.13
298	P-165	200	Ductile Iron	1,200.59	56.65	74.73	6.88	0.09	0.51	0.18
299	P-695	50	Steel	517.57	71.09	93.33	7.02	0.07	0.65	-0.5
300	P-618	63	JISPVC	479.35	30.42	28.25	7.02	0.8	1.03	0.64
301	P-370	100	ISOPE	473.38	59.47	44.39	7.11	0.15	0.53	0.1
302	P-31	350	Ductile Iron	1,162.73	93.81	141.35	7.13	1.03	0.7	-0.52
303	P-367	100	ISOPE	473.38	58.68	43.05	7.15	0.15	0.54	0.08
304	P-449	75	HDPE	501.98	35.92	37.57	7.15	0.02	0.35	-0.18
305	P-698	50	Ductile Iron	517.57	69.86	115.18	7.19	0.08	0.62	-0.43
306	P-697	50	Ductile Iron	517.57	69.3	86.12	7.22	0.08	0.62	-0.43
307	P-768	50	ISOPE	517.57	43.85	41.68	7.41	0.4	-0.17	-0.82
308	P-769	50	ISOPVC	517.57	35.91	41.35	7.48	0.4	-0.25	-0.74
309	P-175	200	Ductile Iron	1,200.59	42.79	85.81	7.49	0.28	0.29	-0.41
310	P-340	100	Steel	473.38	69.3	92.21	7.59	0.03	0.29	-0.28
311	P-770	50	ISOPVC	517.57	35.92	38.45	7.62	0.01	0.25	-0.7
312	P-339	100	Ductile Iron	473.38	69.01	87.34	7.65	0.05	0.43	-0.38
313	P-579	63	JISPVC	479.35	49.44	33.25	7.68	0.03	0.09	-0.03
314	P-266	110	JISPVC	304.82	59.53	22.68	7.74	0	0.21	-0.18
315	P-486	63	JISPVC	479.35	59.53	21.76	7.74	0.27	0.82	0.22
316	P-610	63	ISOPVC	479.35	12.08	62.36	7.87	0	0.43	-0.41
317	P-405	90	Ductile Iron	475.81	56.26	71.16	8.01	0.16	0.24	-0.64
318	P-371	100	ISOPVC	473.38	60.46	45.23	8.05	0.15	0.53	0.11
319	P-657	50	JISPVC	517.57	59.05	31.19	8.22	0.12	0.83	-0.11
320	P-372	100	ISOPE	473.38	61.35	46.85	8.4	0.15	0.53	0.13
321	P-700	50	Ductile Iron	517.57	69.45	106.28	8.43	0.1	0.57	-0.09

S.No.	Label	Diameter (mm)	Material	Wave Speed (m/s)	Pressure (Start) (m H2O)	Pressure (Max. Transient) (m H_2O)	Pressure (Min. Transient) (m H_2O)	Velocity (m/s)	Velocity (Max. Transient) (m/s)	Velocity (Min. Transient) (m/s)
322	P-699	50	Ductile Iron	517.57	69.01	86.06	8.43	0.1	0.57	-0.14
323	P-327	100	JISPVC	1,329.46	64.97	21.9	8.55	0.03	0.08	0.04
324	P-508	63	Ductile Iron	479.35	59.77	17.1	8.55	0.06	0.15	0.07
325	P-224	150	Ductile Iron	1,221.70	57.15	74.1	8.56	0.6	1.74	1.03
326	P-481	63	JISPVC	479.35	59.9	52.7	8.61	0.03	0.34	-0.18
327	P-480	63	JISPVC	479.35	41.02	33.05	8.61	0.03	0.32	-0.19
328	P-338	100	uPVC	473.38	68.77	87.08	8.65	0.09	0.83	-0.53
329	P-267	110	JISPVC	304.82	60.65	28.09	8.66	0	0.2	-0.19
330	P-566	63	ISOPVC	479.35	62.6	46.72	8.72	0.37	1.09	0.35
331	P-227	150	Ductile Iron	1,221.70	59.41	72.66	8.76	0.52	1.57	0.9
332	P-762	50	JISPVC	517.57	36.9	36.37	8.76	0.2	0.17	-0.18
333	P-565	63	ISOPVC	479.35	62.47	46.96	8.77	0.37	1.05	0.34
334	P-509	63	JISPVC	479.35	60.13	26.47	8.79	0.06	0.15	0.07
335	P-30	350	Ductile Iron	1,162.73	95.13	143.58	8.8	1.03	0.7	-0.51
336	P-229	150	Ductile Iron	1,221.70	62.12	77.05	8.87	0.08	0.31	0.08
337	P-166	200	Ductile Iron	1,200.59	57.12	74.71	9.02	0.09	0.51	0.17
338	P-659	50	ISOPVC	517.57	59.57	44.81	9.21	0.06	0.47	-0.06
339	P-658	50	JISPVC	517.57	59.2	30.95	9.22	0.06	0.44	-0.06
340	P-763	50	JISPVC	517.57	33.22	30.62	9.28	0.2	0.12	-0.18
341	P-29	350	Ductile Iron	1,162.73	96.61	145.59	9.34	1.03	0.7	-0.49
342	P-223	150	Ductile Iron	1,221.70	57.28	73.47	9.35	0.6	1.74	1.04
343	P-746	50	Ductile Iron	517.57	57.49	88.47	9.49	0.25	1	-0.63
344	P-745	50	Steel	517.57	56.97	85.53	9.78	0.25	0.96	-0.38
345	P-620	63	ISOPE	479.35	40.07	33.79	9.85	0.71	-0.48	-0.85
346	P-619	63	JISPVC	479.35	42.79	27.02	9.85	0.8	0.99	0.67

S.No.	Label	Diameter (mm)	Material	Wave Speed (m/s)	Pressure (Start) (m H2O)	Pressure (Max. Transient) (m H_2O)	Pressure (Min. Transient) (m H_2O)	Velocity (m/s)	Velocity (Max. Transient) (m/s)	Velocity (Min. Transient) (m/s)
347	P-567	63	ISOPVC	330.71	63.06	47.72	10.01	0.31	0.95	0.19
348	P-330	100	JISPVC	1,329.46	63.81	20.8	10.06	0	0.01	-0.01
349	P-404	90	Ductile Iron	475.81	55.56	83	10.23	0.08	0.43	-0.25
350	P-761	50	JISPVC	517.57	36.64	33.55	10.27	0.2	0.16	-0.17
351	P-760	50	HDPE	517.57	44.09	39.55	10.3	0.38	0.58	0.15
352	P-160	200	Ductile Iron	1,200.59	57.53	73.28	10.32	0.34	1	0.58
353	P-159	200	Ductile Iron	1,200.59	61.71	80.79	10.36	0.24	0.75	0.18
354	P-28	350	Ductile Iron	1,162.73	97.85	155.53	10.44	1.03	0.7	-0.46
355	P-568	63	ISOPVC	479.35	64.15	47.97	10.72	0.31	0.85	0.25
356	P-27	350	Ductile Iron	1,162.73	101.09	158.08	10.76	1.03	0.7	-0.39
357	P-569	63	ISOPVC	479.35	64.42	48.09	10.81	0.31	0.85	0.25
358	P-570	63	ISOPVC	479.35	64.63	49.77	10.87	0.3	0.84	0.23
359	P-665	50	Ductile Iron	517.57	62.68	20.08	10.89	0.65	2.03	0.63
360	P-706	50	JISPVC	517.57	49.43	33.59	10.94	0.62	0.38	-0.64
361	P-329	100	JISPVC	1,329.46	64.35	21.34	11	0.04	0.14	0.03
362	P-495	63	JISPVC	479.35	63.81	21.09	11	0.1	0.32	0.07
363	P-575	63	JISPVC	479.35	49.28	33.41	11.07	0.04	0.05	-0.22
364	P-664	50	JISPVC	517.57	62.72	21.29	11.2	0.65	2.02	0.63
365	P-268	110	JISPVC	304.82	63.4	28.29	11.21	0	0.04	-0.05
366	P-515	63	ISOPE	479.35	64.5	43.56	11.35	0.1	-0.12	-0.23
367	P-496	63	JISPVC	479.35	64.1	24.18	11.39	0.1	0.31	0.07
368	P-328	100	JISPVC	1,329.46	64.76	21.74	11.45	0.04	0.14	0.03
369	P-891	50	JISPVC	517.57	49.58	33.47	11.69	0.01	0.32	-0.64
370	P-576	63	JISPVC	479.35	49.58	33.47	11.69	0.59	0.1	-0.06
371	P-276	110	JISPVC	304.82	65.88	22.8	11.78	0.03	0.15	-0.01

S.No.	Label	Diameter (mm)	Material	Wave Speed (m/s)	Pressure (Start) (m H2O)	Pressure (Max. Transient) (m H_2O)	Pressure (Min. Transient) (m H_2O)	Velocity (m/s)	Velocity (Max. Transient) (m/s)	Velocity (Min. Transient) (m/s)
372	P-493	63	JISPVC	479.35	64.76	22.2	11.78	0.01	0.05	-0.03
373	P-26	350	Ductile Iron	1,162.73	99.49	158.08	12.02	1.03	0.7	-0.41
374	P-478	63	JISPVC	479.35	69.36	35.62	12.12	0.28	-0.48	-0.71
375	P-494	63	ISOPE	479.35	30.14	42.4	12.14	0.01	0.05	-0.03
376	P-123	300	JISPVC	1,192.76	21.18	21.21	12.39	0	-0.01	-0.01
377	P-115	300	Ductile Iron	1,192.76	20.75	20.77	12.39	0	0.01	0.01
378	P-571	63	ISOPVC	479.35	66.74	60.85	12.5	0.27	0.79	0.19
379	P-271	110	JISPVC	304.82	62.64	22.89	12.68	0.08	0.33	0.01
380	P-272	110	Ductile Iron	304.82	62.64	19.82	12.68	0.05	0.16	0.04
381	P-490	63	Ductile Iron	479.35	62.8	20.16	12.71	0.26	0.82	0.2
382	P-487	63	Ductile Iron	479.35	62.64	20.31	12.74	0.26	0.81	0.2
383	P-274	110	Ductile Iron	304.82	62.88	19.92	12.85	0.05	0.15	0.05
384	P-269	110	JISPVC	453.46	62.88	22.83	12.92	0.12	0.3	0.16
385	P-273	110	Ductile Iron	453.46	62.78	19.92	12.93	0.12	0.3	0.16
386	P-578	63	JISPVC	479.35	49.61	33.42	13.04	0.03	0.08	-0.02
387	P-253	110	JISPVC	304.82	62.57	21.41	13.07	0.1	-0.06	-0.35
388	P-252	110	JISPVC	304.82	62.58	21.17	13.07	0.1	-0.05	-0.35
389	P-892	50	JISPVC	517.57	49.61	35.31	13.15	0.52	0.17	-0.71
390	P-251	110	JISPVC	304.82	62.72	21.29	13.17	0.1	-0.04	-0.34
391	P-491	63	JISPVC	330.71	62.81	23.03	13.2	0.01	0.07	-0.01
392	P-275	110	JISPVC	304.82	65.96	22.89	13.2	0.04	0.18	-0.02
393	P-492	63	JISPVC	330.71	66.1	28.81	13.28	0.01	0.06	-0.01
394	P-158	200	Steel	1,192.76	76.93	96.02	13.37	0.24	0.77	0.18
395	P-489	63	ISOPVC	330.71	65.86	39.44	13.38	0.01	0.1	-0.05
396	P-488	63	JISPVC	330.71	65.96	22.89	13.38	0.01	0.1	-0.06

S.No.	Label	Diameter (mm)	Material	Wave Speed (m/s)	Pressure (Start) (m H2O)	Pressure (Max. Transient) (m H_2O)	Pressure (Min. Transient) (m H_2O)	Velocity (m/s)	Velocity (Max. Transient) (m/s)	Velocity (Min. Transient) (m/s)
397	P-254	110	JISPVC	304.82	65.88	23.03	13.41	0.02	0.14	-0.05
398	P-255	110	JISPVC	304.82	62.81	21.43	13.41	0.12	-0.1	-0.39
399	P-256	110	JISPVC	304.82	62.83	23.96	13.42	0.12	-0.09	-0.41
400	P-482	63	JISPVC	330.71	63.75	23.13	13.59	0.02	0.21	-0.15
401	P-483	63	ISOPVC	330.71	47.98	45.51	13.76	0.02	0.22	-0.16
402	P-503	63	JISPVC	479.35	72.15	30.32	13.76	0.05	-0.02	-0.16
403	P-497	63	JISPVC	479.35	66.68	25.73	13.76	0.02	0.07	0.01
404	P-582	63	JISPVC	330.71	48.57	35.44	13.82	0.06	-0.02	-0.18
405	P-581	63	ISOPVC	330.71	48.69	32.78	13.82	0	0.04	-0.05
406	P-580	63	JISPVC	330.71	52.12	36.27	13.9	0	0.03	-0.04
407	P-25	350	Ductile Iron	1,162.73	102.63	160.59	13.93	1.03	0.7	-0.41
408	P-507	63	JISPVC	330.71	64.87	53.17	13.99	0.08	0.3	0.11
409	P-506	63	JISPVC	330.71	64.97	21.9	14	0.08	0.3	0.11
410	P-270	110	JISPVC	453.46	65.76	22.83	14.06	0.06	0.16	0.07
411	P-504	63	JISPVC	479.35	65.76	23.05	14.82	0.16	0.39	0.26
412	P-505	63	JISPVC	479.35	65.92	53.15	14.84	0.16	0.4	0.26

Appendix C: Transient Analysis results without Surge Protection Equipment (Pipes that created a vapor pocket during the analysis or, in other words, pipes exposed to cavitation)

S.No.	Label	Diameter (mm)	Material	Wave Speed (m/s)	Pressure (Start) (m H2O)	Pressure (Maximum, Transient) (m H2O)	Pressure (Minimum, Transient) (m H2O)	Vapor Volume (Maximum, Transient) (L)
1	P-350	100	JISPVC	473.38	36.45	22.47	-9.98	421.6
2	P-347	100	ISOPVC	473.38	36.69	22.8	-9.98	60.7
3	P-702	50	ISOPE	368.93	36.3	22.98	-9.98	59.5
4	P-348	100	JISPVC	473.38	36.45	24.33	-9.98	24.4
5	P-345	100	ISOPVC	473.38	38.54	25.77	-9.98	21.3
6	P-173	200	Ductile Iron	1,200.59	19.16	36.66	-9.98	18.2
7	P-66	350	Ductile Iron	1,162.73	18.7	34.16	-9.98	16.5
8	P-54	350	Ductile Iron	1,162.73	39.46	62.98	-9.98	1.7
9	P-67	350	Ductile Iron	1,162.73	16.61	31.7	-9.98	1.7
10	P-407	90	ISOPVC	475.81	40.2	51.45	-9.98	1.7
11	P-65	350	Ductile Iron	1,162.73	21.25	37.63	-9.98	1.4
12	P-856	350	Ductile Iron	1,162.73	39.46	66.95	-9.98	0.9
13	P-61	350	Ductile Iron	1,162.73	28.98	47.33	-9.98	0.6
14	P-855	100	ISOPVC	473.38	36.69	24.11	-9.98	0.6
15	P-343	100	ISOPVC	473.38	40.43	28.85	-9.98	0.5
16	P-341	100	ISOPVC	473.38	41.95	31.62	-9.98	0.4
17	P-342	100	ISOPVC	473.38	41.25	30.3	-9.98	0.4
18	P-62	350	Ductile Iron	1,162.73	27.18	45.63	-9.98	0.4
19	P-854	150	Ductile Iron	1,221.70	43.62	37.03	-9.98	0.3
20	P-55	350	Ductile Iron	1,162.73	38.6	61.17	-9.98	0.2
21	P-60	350	Ductile Iron	1,162.73	32	51.4	-9.98	0.2

S.No.	Label	Diameter (mm)	Material	Wave Speed (m/s)	Pressure (Start) (m H2O)	Pressure (Maximum, Transient) (m H2O)	Pressure (Minimum, Transient) (m H2O)	Vapor Volume (Maximum, Transient) (L)
22	P-326	100	ISOPVC	473.38	42.92	33.45	-9.98	0.2
23	P-858	110	ISOPVC	453.46	19.16	34.04	-9.98	0.2
24	P-655	50	JISPVC	517.57	41.95	31.78	-9.98	0.1
25	P-68	350	Ductile Iron	1,162.73	15.17	29.7	-9.98	0.1
26	P-325	100	ISOPVC	473.38	43.48	34.82	-9.98	0.1
27	P-344	100	ISOPVC	473.38	39.59	27.39	-9.98	0.1
28	P-324	100	ISOPVC	473.38	43.62	35.08	-9.98	0.1
29	P-63	350	Ductile Iron	1,162.73	25.79	43.86	-9.98	0.1
30	P-64	350	Ductile Iron	1,162.73	23.54	40.68	-9.98	0.1
31	P-712	50	ISOPE	368.93	41.82	25.91	-9.98	0.1
32	P-656	50	JISPVC	517.57	42.13	32.1	-9.98	0.1
33	P-374	100	ISOPVC	473.38	43.91	47.66	-9.98	0.4
34	P-59	350	Ductile Iron	1,162.73	34.36	54.5	-9.98	0.3
35	P-214	150	Ductile Iron	1,221.70	46.49	38.5	-9.98	1.3
36	P-703	50	ISOPE	368.93	37	23.07	-9.98	0.1
37	P-704	50	ISOPE	368.93	37.41	23.97	-9.98	0.1
38	P-708	50	ISOPE	368.93	40.7	25.3	-9.98	0.2
39	P-709	50	ISOPE	368.93	40.49	24.98	-9.98	0.2
40	P-373	100	ISOPVC	473.38	43.62	35.37	-9.98	0.1
41	P-725	50	JISPVC	517.57	56.18	47.61	-9.98	0.1
42	P-710	50	ISOPE	368.93	40.9	25.19	-9.98	0.1
43	P-711	50	ISOPE	368.93	41.38	25.36	-9.98	0.1
44	P-713	50	ISOPE	368.93	42.63	26.73	-9.98	0.1
45	P-714	50	ISOPE	368.93	43.72	27.67	-9.98	0.1

S.No.	Label	Diameter (mm)	Material	Wave Speed (m/s)	Pressure (Start) (m H2O)	Pressure (Maximum, Transient) (m H2O)	Pressure (Minimum, Transient) (m H2O)	Vapor Volume (Maximum, Transient) (L)
46	P-857	50	JISPVC	517.57	20.18	46.77	-9.98	0.1
47	P-562	63	ISOPE	330.71	39.77	25.34	-9.98	0.3
48	P-213	150	Ductile Iron	1,221.70	47.89	40.11	-9.98	1.3
49	P-705	50	ISOPE	368.93	38.57	24.86	-9.98	0.1
50	P-56	350	Ductile Iron	1,162.73	38.89	60.71	-9.98	0.4
51	P-58	350	Ductile Iron	1,162.73	36.9	57.98	-9.98	0.3
52	P-707	50	ISOPE	368.93	40.62	25.49	-9.98	0.1
53	P-212	150	Ductile Iron	1,221.70	49.29	41.71	-9.98	1.3
54	P-715	50	ISOPE	368.93	44.92	28.66	-9.98	0.1
55	P-301	110	ISOPVC	453.46	28.3	36.75	-9.98	0.8
56	P-349	100	JISPVC	473.38	38.69	25.05	-9.98	0.5
57	P-226	150	Ductile Iron	1,221.70	3.23	12.33	-9.98	1
58	P-211	150	Ductile Iron	1,221.70	50.53	43.17	-9.98	1.3
59	P-706	50	ISOPE	368.93	39.73	25.49	-9.98	0.1
60	P-69	350	Ductile Iron	1,162.73	14.69	28.4	-9.98	0.1

Appendix D: Transient Analysis results with Surge Protection Equipment (Pipes exceeded the maximum pressure threshold during the analysis)

S.No.	Label	Diameter (mm)	Material	Wave Speed (m/s)	Pressure (Start) (m H2O)	Pressure (Maximum, Transient) (m H2O)	Pressure (Minimum, Transient) (m H2O)	Velocity (m/s)	Velocity (Maximum, Transient) (m/s)	Velocity (Minimum, Transient) (m/s)	Vapor Volume (Maximum, Transient) (L)
1	P-113	300	Steel	1,192.76	106	113	75	0	0.03	-0.05	0
2	P-98	300	Steel	1,192.76	106	111	75	0	0.05	-0.07	0
3	P-110	300	Steel	1,192.76	106	110	75	1.28	1.28	-0.04	0
4	P-99	300	Steel	1,192.76	105	109	75	1.28	0.07	-1.28	0
6	P-9	350	Ductile Iron	1,162.73	105	107	75	0.94	0.94	-0.09	0
5	P-109	300	Steel	1,192.76	106	106	75	1.28	1.28	0	0
7	P-112	300	Steel	1,192.76	106	106	75	0	0.02	0	0
8	P-844	300	Ductile Iron	1,192.76	104	105	75	0.03	0.66	-1.3	0
10	P-150	200	Ductile Iron	1,200.59	104	105	73	0.93	0.94	-0.18	0
9	P-10	350	Ductile Iron	1,162.73	104	105	73	0.61	0.61	-0.46	0
12	P-13	350	Ductile Iron	1,162.73	102	104	72	0.61	0.61	-0.46	0
11	P-14	350	Ductile Iron	1,162.73	103	104	72	0.61	0.61	-0.46	0
13	P-15	350	Ductile Iron	1,162.73	102	104	72	0.61	0.61	-0.46	0
15	P-11	350	Ductile Iron	1,162.73	102	103	72	0.61	0.61	-0.46	0
14	P-12	350	Ductile Iron	1,162.73	102	103	72	0.61	0.61	-0.46	0
16	P-16	350	Ductile Iron	1,162.73	102	103	72	0.61	0.61	-0.46	0
17	P-17	350	Ductile Iron	1,162.73	101	103	72	0.61	0.61	-0.46	0
18	P-18	350	Ductile Iron	1,162.73	100	102	72	0.61	0.61	-0.46	0
20	P-151	200	Ductile Iron	1,200.59	101	102	62	0.93	0.94	-0.19	0
19	P-19	350	Ductile Iron	1,162.73	99	101	71	0.61	0.61	-0.46	0
22	P-20	350	Ductile Iron	1,162.73	98	100	70	0.61	0.61	-0.46	0

S.No.	Label	Diameter (mm)	Material	Wave Speed (m/s)	Pressure (Start) (m H2O)	Pressure (Maximum, Transient) (m H2O)	Pressure (Minimum, Transient) (m H2O)	Velocity (m/s)	Velocity (Maximum, Transient) (m/s)	Velocity (Minimum, Transient) (m/s)	Vapor Volume (Maximum, Transient) (L)
21	P-21	350	Ductile Iron	1,162.73	97	99	70	0.61	0.61	-0.46	0
23	P-539	63	ISOPVC	479.35	98	98	92	0.94	-0.87	-0.97	0
24	P-540	63	ISOPE	330.71	98	98	92	0.02	0.04	0	0
26	P-542	63	ISOPVC	479.35	93	98	86	0.97	1.01	0.89	0
25	P-541	63	ISOPE	330.71	98	98	77	0.02	0.03	0	0
27	P-407	90	ISOPVC	475.81	93	98	87	0.46	-0.42	-0.47	0
28	P-22	350	Ductile Iron	1,162.73	96	97	69	0.61	0.61	-0.46	0
29	P-23	350	Ductile Iron	1,162.73	95	96	68	0.61	0.61	-0.47	0
30	P-561	63	ISOPE	330.71	89	96	83	0	0.01	-0.01	0
31	P-563	63	ISOPE	330.71	90	96	84	0.01	0.02	0	0
32	P-534	63	ISOPVC	479.35	95	95	88	0.68	0.71	0.63	0
33	P-695	50	GS	1,395.06	95	95	86	0.81	0.85	0.73	0
34	P-24	350	Ductile Iron	1,162.73	93	95	67	0.61	0.61	-0.47	0
35	P-533	63	ISOPVC	479.35	75	95	68	0.68	0.71	0.62	0
36	P-565	63	ISOPVC	479.35	90	95	83	0.02	0.02	0.01	0
37	P-701	50	JISPVC	517.57	79	94	72	0.09	-0.07	-0.09	0
38	P-566	63	ISOPE	330.71	94	94	75	0.13	-0.11	-0.15	0
39	P-559	63	ISOPE	330.71	89	94	83	0.07	0.08	0.06	0
40	P-874	50	JISPVC	517.57	83	94	82	0.26	0.27	0.26	0
41	P-398	100	GS	1,329.46	94	94	82	0.02	0.02	0.02	0
42	P-25	350	Ductile Iron	1,162.73	92	94	66	0.61	0.61	-0.47	0
43	P-406	90	ISOPVC	475.81	87	93	81	0.01	0.02	0	0
44	P-543	63	ISOPE	330.71	93	93	87	0.93	0.97	0.86	0
45	P-544	63	ISOPE	330.71	93	93	84	0.93	0.97	0.86	0

S.No.	Label	Diameter (mm)	Material	Wave Speed (m/s)	Pressure (Start) (m H2O)	Pressure (Maximum, Transient) (m H2O)	Pressure (Minimum, Transient) (m H2O)	Velocity (m/s)	Velocity (Maximum, Transient) (m/s)	Velocity (Minimum, Transient) (m/s)	Vapor Volume (Maximum, Transient) (L)
46	P-468	75	ISOPVC	501.98	73	93	72	0.2	-0.18	-0.2	0
47	P-885	50	JISPVC	517.57	92	93	91	0.52	-0.48	-0.53	0
48	P-886	50	JISPVC	517.57	92	93	83	0.52	-0.48	-0.53	0
49	P-526	63	ISOPVC	479.35	90	93	83	1.1	1.15	1.01	0
50	P-527	63	ISOPE	330.71	93	93	86	0.1	0.11	0.08	0
51	P-528	63	ISOPE	330.71	92	92	83	0.1	0.11	0.08	0
52	P-26	350	Ductile Iron	1,162.73	91	92	65	0.61	0.61	-0.47	0
53	P-403	90	ISOPVC	475.81	92	92	73	0.22	0.23	0.2	0
54	P-557	63	ISOPE	330.71	89	92	83	0.21	0.21	0.2	0
55	P-680	50	JISPVC	517.57	67	92	60	0.15	-0.12	-0.16	0
56	P-681	50	JISPVC	517.57	91	92	84	0.35	-0.32	-0.37	0
57	P-682	50	JISPVC	517.57	91	91	83	0.35	-0.32	-0.37	0
58	P-27	350	Ductile Iron	1,162.73	89	91	64	0.61	0.61	-0.47	0
59	P-564	63	ISOPVC	479.35	90	91	83	0.02	0.02	0.01	0
60	P-683	50	JISPVC	517.57	90	90	78	0.39	-0.34	-0.41	0
61	P-525	63	ISOPVC	479.35	89	90	82	1.1	1.15	1.01	0
62	P-562	63	ISOPE	330.71	89	90	84	0.01	0.02	0	0
63	P-545	63	ISOPE	330.71	89	90	83	0.92	0.94	0.85	0
64	P-560	63	ISOPE	330.71	89	90	83	0	0.01	-0.01	0
65	P-548	63	ISOPE	330.71	88	89	83	0.6	0.61	0.56	0
66	P-28	350	Ductile Iron	1,162.73	88	89	63	0.61	0.61	-0.47	0
67	P-549	63	ISOPE	330.71	89	89	83	0.6	0.61	0.56	0
68	P-546	63	ISOPE	330.71	89	89	83	0.92	0.93	0.86	0
69	P-408	90	ISOPVC	475.81	89	89	83	0.29	0.29	0.27	0

S.No.	Label	Diameter (mm)	Material	Wave Speed (m/s)	Pressure (Start) (m H2O)	Pressure (Maximum, Transient) (m H2O)	Pressure (Minimum, Transient) (m H2O)	Velocity (m/s)	Velocity (Maximum, Transient) (m/s)	Velocity (Minimum, Transient) (m/s)	Vapor Volume (Maximum, Transient) (L)
70	P-299	110	ISOPVC	453.46	81	89	74	0.37	0.4	0.33	0
71	P-104	300	Steel	1,192.76	64	89	0	0	0.07	-0.07	0
72	P-558	63	ISOPE	330.71	88	89	83	0.07	0.08	0.06	0
73	P-550	63	ISOPE	330.71	89	89	83	0.18	0.19	0.17	0
74	P-551	63	ISOPE	330.71	89	89	81	0.18	0.19	0.18	0
75	P-409	90	ISOPVC	475.81	89	89	80	0.19	0.19	0.18	0
76	P-556	63	ISOPE	330.71	88	89	83	0.21	0.21	0.2	0
77	P-547	63	ISOPE	330.71	88	88	83	0.83	0.84	0.78	0
78	P-29	350	Ductile Iron	1,162.73	87	88	62	0.61	0.61	-0.47	0
79	P-95	300	Steel	1,192.76	63	88	1	0	0.07	-0.07	0
80	P-107	300	Steel	1,192.76	63	88	2	0.79	0.79	-0.08	0
81	P-699	50	JISPVC	517.57	79	88	72	0.12	0.12	0.11	0
82	P-405	90	ISOPVC	475.81	79	87	73	0.2	0.21	0.18	0
83	P-535	63	ISOPE	330.71	87	87	81	0.34	0.34	0.32	0
84	P-705	50	JISPVC	517.57	63	87	51	0.13	0.17	0.07	0
85	P-552	63	ISOPE	330.71	87	87	81	0.18	0.18	0.17	0
86	P-703	50	JISPVC	517.57	64	87	53	0.1	0.15	0.03	0
87	P-94	300	Steel	1,192.76	63	87	2	0.79	0.79	-0.08	0
88	P-536	63	ISOPE	330.71	87	87	81	0.34	0.34	0.32	0
89	P-30	350	Ductile Iron	1,162.73	85	87	62	0.61	0.61	-0.47	0
90	P-553	63	ISOPE	330.71	87	87	80	0.18	0.18	0.17	0
91	P-537	63	ISOPE	330.71	87	87	80	0.31	0.31	0.29	0
92	P-697	50	JISPVC	517.57	75	87	68	0.1	0.11	0.08	0
93	P-538	63	ISOPE	330.71	86	86	76	0.31	0.31	0.29	0

S.No.	Label	Diameter (mm)	Material	Wave Speed (m/s)	Pressure (Start) (m H2O)	Pressure (Maximum, Transient) (m H2O)	Pressure (Minimum, Transient) (m H2O)	Velocity (m/s)	Velocity (Maximum, Transient) (m/s)	Velocity (Minimum, Transient) (m/s)	Vapor Volume (Maximum, Transient) (L)
94	P-554	63	ISOPE	330.71	86	86	80	0.36	0.37	0.34	0
95	P-684	50	JISPVC	517.57	86	86	75	0.22	-0.19	-0.24	0
96	P-691	50	JISPVC	517.57	86	86	78	0.19	0.19	0.17	0
97	P-947	300	Ductile Iron	1,192.76	61	86	0	0.79	0.16	-0.79	0
98	P-555	63	ISOPE	330.71	86	86	62	0.36	0.37	0.34	0
99	P-690	50	JISPVC	517.57	81	86	73	0.19	0.2	0.16	0
100	P-31	350	Ductile Iron	1,162.73	84	86	61	0.61	0.61	-0.47	0
101	P-861	50	JISPVC	517.57	85	86	85	0.54	0.55	0.54	0
102	P-862	50	JISPVC	517.57	85	86	74	0.54	0.55	0.54	0
103	P-650	63	ISOPE	330.71	44	86	43	0.2	0.2	0.18	0
104	P-653	63	ISOPE	330.71	85	86	79	0.21	-0.2	-0.23	0
105	P-291	110	ISOPVC	453.46	74	86	67	0.03	0.05	0.01	0
106	P-292	110	ISOPVC	453.46	85	86	75	0.03	0.04	0.02	0
107	P-875	50	JISPVC	517.57	77	85	77	0.1	0.13	0.1	0
108	P-399	100	GS	1,329.46	85	85	77	0	0.01	0	0
109	P-32	350	Ductile Iron	1,162.73	83	85	60	0.61	0.61	-0.47	0
110	P-887	50	JISPVC	517.57	84	84	78	0.84	-0.79	-0.85	0
111	P-897	50	JISPVC	517.57	84	84	83	0.19	0.21	0.17	0
112	P-898	50	JISPVC	517.57	84	84	73	0.19	0.21	0.17	0
113	P-302	110	ISOPVC	453.46	76	84	70	0.26	0.28	0.24	0
114	P-531	63	ISOPVC	479.35	84	84	76	0.8	0.83	0.73	0
115	P-873	50	JISPVC	517.57	80	83	79	0.65	0.66	0.64	0
116	P-33	350	Ductile Iron	1,162.73	81	83	59	0.61	0.61	-0.47	0
117	P-532	63	ISOPVC	479.35	83	83	68	0.8	0.83	0.73	0

S.No.	Label	Diameter (mm)	Material	Wave Speed (m/s)	Pressure (Start) (m H2O)	Pressure (Maximum, Transient) (m H2O)	Pressure (Minimum, Transient) (m H2O)	Velocity (m/s)	Velocity (Maximum, Transient) (m/s)	Velocity (Minimum, Transient) (m/s)	Vapor Volume (Maximum, Transient) (L)
118	P-657	63	ISOPE	330.71	82	83	81	0.04	0.04	0.03	0
119	P-946	300	Ductile Iron	1,192.76	60	83	0	0.79	0.17	-0.79	0
120	P-567	63	ISOPE	330.71	82	83	75	0.13	-0.1	-0.15	0
121	P-340	100	ISOPVC	473.38	83	83	75	0.07	-0.06	-0.08	0
122	P-685	50	JISPVC	517.57	82	83	71	0.1	-0.07	-0.11	0
123	P-694	50	JISPVC	517.57	82	83	75	0.17	0.18	0.15	0
124	P-693	50	JISPVC	517.57	74	82	67	0.17	0.19	0.15	0
125	P-658	63	ISOPE	330.71	82	82	75	0.04	0.04	0.03	0
126	P-688	50	JISPVC	517.57	81	82	74	0.25	-0.22	-0.27	0
127	P-337	100	ISOPVC	473.38	82	82	74	0.13	-0.11	-0.15	0
129	P-338	100	ISOPVC	473.38	82	82	71	0.15	-0.12	-0.16	0
128	P-687	50	JISPVC	517.57	79	81	71	0.25	-0.22	-0.27	0
130	P-652	63	HDPE	330.71	45	81	44	0.02	0.03	0.02	0
131	P-34	350	Ductile Iron	1,162.73	80	81	58	0.61	0.61	-0.47	0
132	P-677	50	JISPVC	517.57	46	81	39	0.04	0.06	0.02	0
133	P-298	110	ISOPVC	453.46	75	81	68	0.37	0.4	0.33	0
134	P-689	50	JISPVC	517.57	81	81	73	0.19	0.2	0.16	0
135	P-295	110	ISOPVC	453.46	74	81	67	0.06	0.07	0.05	0
136	P-941	300	Ductile Iron	1,192.76	60	81	-1	0.79	0.17	-0.79	0
137	P-940	300	Ductile Iron	1,192.76	60	81	-1	0.79	0.16	-0.79	0
138	P-524	63	ISOPVC	479.35	73	81	65	0.06	0.07	0.05	0
139	P-939	300	Ductile Iron	1,192.76	59	81	-1	0.79	0.18	-0.79	0

Appendix E: Transient Analysis results with Surge Protection Equipment (Pipes rated below the minimum pressure threshold during analysis)

S.No.	Label	Diameter (mm)	Material	Wave Speed (m/s)	Pressure (Start) (m H2O)	Pressure (Maximum, Transient) (m H2O)	Pressure (Minimum, Transient) (m H2O)	Velocity (m/s)	Velocity (Maximum, Transient) (m/s)	Velocity (Minimum, Transient) (m/s)	Vapor Volume (Maximum, Transient) (L)
1	P-194	150	Ductile Iron	1,221.70	-1	25	-7	0	0.03	-0.02	0
2	P-108	300	Steel	1,192.76	3	39	-6	1.28	1.28	-0.04	0
3	P-111	300	Steel	1,192.76	3	32	-5	0	0.03	-0.04	0
4	P-105	300	Steel	1,192.76	2	31	-5	0.79	0.79	-0.02	0
5	P-195	150	Ductile Iron	1,221.70	0	25	-5	0	0.06	-0.04	0
6	P-906	300	Ductile Iron	1,192.76	11	32	-5	0.79	0.27	-0.79	0
7	P-126	250	Ductile Iron	1,195.94	0	23	-5	0.21	0.22	-0.27	0
8	P-127	250	Ductile Iron	1,195.94	0	25	-5	0.21	0.21	-0.27	0
9	P-197	150	Ductile Iron	1,221.70	1	26	-5	0	0.06	-0.04	0
10	P-193	150	Ductile Iron	1,221.70	0	27	-5	0.58	0.58	-0.71	0
11	P-2	400	Ductile Iron	1,161.46	0	22	-5	1.24	1.24	-0.13	0
12	P-5	400	Ductile Iron	1,161.46	0	28	-5	1.16	1.16	-0.05	0
13	P-100	300	Steel	1,192.76	3	36	-5	1.28	0.06	-1.28	0
14	P-192	150	Ductile Iron	1,221.70	0	26	-4	0.58	0.58	-0.72	0
15	P-172	200	Ductile Iron	1,200.59	3	9	-2	0.64	0.64	0.14	0
16	P-149	200	Ductile Iron	1,200.59	3	9	-2	0.64	0.64	0.14	0
17	P-850	300	Ductile Iron	1,192.76	5	12	-2	3.45	-3.19	-3.87	0
18	P-229	150	Ductile Iron	1,221.70	3	11	-2	0.83	1.11	0.8	0
19	P-93	300	Steel	1,192.76	3	30	0	0.79	0.79	-0.03	0
20	P-903	300	Ductile Iron	1,192.76	5	22	0	0.79	0.32	-0.79	0
21	P-80	350	Ductile Iron	1,162.73	3	9	0	0.4	0.41	-0.53	0

S.No.	Label	Diameter (mm)	Material	Wave Speed (m/s)	Pressure (Start) (m H2O)	Pressure (Maximum, Transient) (m H2O)	Pressure (Minimum, Transient) (m H2O)	Velocity (m/s)	Velocity (Maximum, Transient) (m/s)	Velocity (Minimum, Transient) (m/s)	Vapor Volume (Maximum, Transient) (L)
22	P-79	350	Ductile Iron	1,162.73	4	10	0	0.61	0.62	-0.49	0
23	P-78	350	Ductile Iron	1,162.73	6	11	0	0.61	0.62	-0.49	0
24	P-228	150	Ductile Iron	1,221.70	3	8	0	0.83	1.11	0.8	0
25	P-171	200	Ductile Iron	1,200.59	3	8	0	0.17	0.48	-0.18	0
26	P-81	350	Ductile Iron	1,162.73	3	7	0	0.4	0.41	-0.53	0
27	P-932	300	Ductile Iron	1,192.76	51	65	0	0.79	0.24	-0.79	0
28	P-940	300	Ductile Iron	1,192.76	60	81	0	0.79	0.16	-0.79	0
29	P-914	300	Ductile Iron	1,192.76	27	50	0	0.79	0.25	-0.79	0
30	P-141	200	Ductile Iron	1,200.59	4	12	0	4.77	4.77	3.62	0
31	P-946	300	Ductile Iron	1,192.76	60	83	0	0.79	0.17	-0.79	0
32	P-929	300	Ductile Iron	1,192.76	47	62	0	0.79	0.24	-0.79	0
33	P-921	300	Ductile Iron	1,192.76	40	65	0	0.79	0.19	-0.79	0
34	P-920	300	Ductile Iron	1,192.76	40	64	0	0.79	0.19	-0.79	0
35	P-219	150	Ductile Iron	1,221.70	3	6	0	0.15	0.17	-0.43	0
36	P-221	150	Ductile Iron	1,221.70	3	6	0	0.15	0.17	-0.43	0
37	P-135	200	Steel	1,379.88	0	0	0	0.01	-0.01	-0.01	0
38	P-136	200	Steel	1,379.88	0	3	0	0.01	-0.01	-0.01	0
39	P-134	200	Steel	1,379.88	0	0	0	0.01	0.01	0.01	0
40	P-174	200	Steel	1,200.59	0	6	0	0.02	0.02	0.02	0
41	P-104	300	Steel	1,192.76	64	89	0	0	0.07	-0.07	0
42	P-931	300	Ductile Iron	1,192.76	50	65	0	0.79	0.24	-0.79	0
43	P-77	350	Ductile Iron	1,162.73	7	13	0	0.61	0.62	-0.49	0
44	P-139	200	Steel	1,379.88	0	3	0	0	0	0	0
45	P-173	200	Steel	1,379.88	0	0	0	0	0	0	0

S.No.	Label	Diameter (mm)	Material	Wave Speed (m/s)	Pressure (Start) (m H2O)	Pressure (Maximum, Transient) (m H2O)	Pressure (Minimum, Transient) (m H2O)	Velocity (m/s)	Velocity (Maximum, Transient) (m/s)	Velocity (Minimum, Transient) (m/s)	Vapor Volume (Maximum, Transient) (L)
46	P-133	200	Steel	1,379.88	0	3	0	0.01	0.01	0.01	0
47	P-138	200	Steel	1,379.88	0	0	0	0	0	0	0
48	P-6	400	Steel	1,161.46	0	4	0	0	0	0	0
49	P-137	200	Steel	1,379.88	0	3	0	0	0	0	0
50	P-947	300	Ductile Iron	1,192.76	61	86	0	0.79	0.16	-0.79	0
51	P-196	150	Ductile Iron	1,221.70	0	26	1	0	0.03	-0.02	0
52	P-129	200	Steel	1,379.88	0	9	1	2.49	2.49	-0.26	0
53	P-912	300	Ductile Iron	1,192.76	23	42	1	0.79	0.27	-0.79	0
54	P-132	200	Steel	1,379.88	0	9	1	2.49	0.26	-2.49	0
55	P-82	350	Ductile Iron	1,162.73	3	5	1	0.4	0.41	-0.54	0
56	P-915	300	Ductile Iron	1,192.76	30	54	1	0.79	0.24	-0.79	0
57	P-930	300	Ductile Iron	1,192.76	48	64	1	0.79	0.24	-0.79	0
58	P-916	300	Ductile Iron	1,192.76	32	58	1	0.79	0.23	-0.79	0
59	P-919	300	Ductile Iron	1,192.76	39	64	1	0.79	0.2	-0.79	0
60	P-95	300	Steel	1,192.76	63	88	1	0	0.07	-0.07	0
61	P-220	150	Ductile Iron	1,221.70	3	5	1	0.15	0.18	-0.43	0
62	P-222	150	Ductile Iron	1,221.70	3	5	1	0.15	0.18	-0.43	0
63	P-918	300	Ductile Iron	1,192.76	36	64	1	0.79	0.22	-0.79	0
64	P-905	300	Ductile Iron	1,192.76	9	27	2	0.79	0.28	-0.79	0
65	P-904	300	Ductile Iron	1,192.76	7	24	2	0.79	0.3	-0.79	0
66	P-917	300	Ductile Iron	1,192.76	34	62	2	0.79	0.23	-0.79	0
67	P-94	300	Steel	1,192.76	63	87	2	0.79	0.79	-0.08	0
68	P-76	350	Ductile Iron	1,162.73	9	15	2	0.61	0.62	-0.49	0
69	P-88	350	Ductile Iron	1,162.73	3	4	2	0.5	-0.5	-0.76	0

S.No.	Label	Diameter (mm)	Material	Wave Speed (m/s)	Pressure (Start) (m H2O)	Pressure (Maximum, Transient) (m H2O)	Pressure (Minimum, Transient) (m H2O)	Velocity (m/s)	Velocity (Maximum, Transient) (m/s)	Velocity (Minimum, Transient) (m/s)	Vapor Volume (Maximum, Transient) (L)
70	P-89	350	Ductile Iron	1,162.73	2	3	2	0.5	-0.5	-0.76	0
71	P-223	150	Ductile Iron	1,221.70	8	10	2	0.73	0.74	0.65	0
72	P-750	110	JISPVC	517.57	8	10	2	0.19	0.86	0.14	0
73	P-230	150	Ductile Iron	1,221.70	8	11	2	0.83	1.11	0.79	0
74	P-356	100	JISPVC	473.38	28	29	2	0.1	0.11	0.06	0
75	P-708	50	ISOPE	368.93	28	30	2	0.35	0.37	0.25	0
76	P-224	150	Ductile Iron	1,221.70	8	10	2	0.73	0.75	0.65	0
77	P-90	350	Ductile Iron	1,162.73	2	4	2	0.5	-0.5	-0.76	0
78	P-225	150	Ductile Iron	1,221.70	8	33	2	0.73	0.75	0.64	0
79	P-354	100	JISPVC	473.38	28	31	2	0.65	0.66	0.25	0
80	P-353	100	ISOPVC	473.38	28	29	2	0.77	0.79	0.32	0
81	P-352	100	ISOPVC	473.38	29	29	2	0.77	0.79	0.32	0
82	P-751	110	JISPVC	517.57	8	10	2	0.19	0.86	0.13	0
83	P-87	350	Ductile Iron	1,162.73	14	14	2	0.5	-0.5	-0.76	0
84	P-351	100	ISOPVC	473.38	30	31	2	0.77	0.79	0.32	0
85	P-106	300	Steel	1,192.76	64	64	2	0.79	0.79	0	0
86	P-107	300	Steel	1,192.76	63	88	2	0.79	0.79	-0.08	0
87	P-146	200	Ductile Iron	1,213.89	4	13	3	4.77	-3.62	-4.77	0
88	P-140	200	Ductile Iron	1,200.59	5	13	3	4.77	4.77	3.63	0
89	P-147	200	Ductile Iron	1,213.64	5	14	3	4.77	-3.63	-4.77	0
90	P-103	300	Steel	1,192.76	64	64	3	0	0.02	0	0
91	P-941	300	Ductile Iron	1,192.76	60	81	3	0.79	0.17	-0.79	0
92	P-304	110	ISOPVC	453.46	8	27	3	0.29	0.41	-0.32	0
93	P-303	110	ISOPVC	453.46	8	10	3	0.29	0.41	-0.32	0

S.No.	Label	Diameter (mm)	Material	Wave Speed (m/s)	Pressure (Start) (m H2O)	Pressure (Maximum, Transient) (m H2O)	Pressure (Minimum, Transient) (m H2O)	Velocity (m/s)	Velocity (Maximum, Transient) (m/s)	Velocity (Minimum, Transient) (m/s)	Vapor Volume (Maximum, Transient) (L)
94	P-423	90	ISOPVC	475.81	8	10	3	0.7	0.73	0.64	0
95	P-709	50	ISOPE	368.93	29	47	3	0.35	0.37	0.25	0
96	P-424	90	ISOPVC	475.81	9	10	3	0.7	0.73	0.64	0
97	P-350	100	ISOPVC	473.38	31	32	3	0.77	0.79	0.32	0
98	P-425	90	ISOPVC	475.81	9	20	3	0.67	0.7	0.62	0
99	P-130	200	Steel	1,379.88	0	19	4	2.49	2.49	-0.26	0
100	P-131	200	Steel	1,379.88	0	19	4	2.49	0.26	-2.49	0
101	P-3	400	Steel	1,161.46	2	30	4	0.44	0.45	-0.03	0
102	P-4	400	Steel	1,161.46	2	32	4	0.72	0.72	-0.06	0
103	P-911	300	Ductile Iron	1,192.76	21	39	4	0.79	0.27	-0.79	0
104	P-910	300	Ductile Iron	1,192.76	19	38	4	0.79	0.26	-0.79	0
105	P-142	200	Ductile Iron	1,200.59	4	5	4	0.13	-0.09	-0.13	0
106	P-143	200	Ductile Iron	1,200.59	4	4	4	0.13	-0.09	-0.13	0
107	P-7	400	Ductile Iron	1,161.46	4	7	4	0	0	0	0
108	P-144	200	Ductile Iron	1,200.59	4	4	4	0.13	0.13	0.09	0
109	P-148	200	Ductile Iron	1,200.59	4	49	4	0.68	-0.63	-0.68	0
110	P-91	350	Ductile Iron	1,162.73	4	34	4	0.13	0.15	0.13	0
111	P-349	100	ISOPVC	473.38	32	33	4	0.77	0.79	0.32	0
112	P-145	200	Ductile Iron	1,200.59	4	5	4	0.13	0.13	0.09	0
113	P-75	350	Ductile Iron	1,162.73	10	15	4	0.61	0.62	-0.49	0
114	P-102	300	Steel	1,192.76	3	30	5	0	0.02	-0.03	0
115	P-96	300	Steel	1,192.76	3	30	5	0	0.05	-0.04	0
116	P-97	300	Steel	1,192.76	3	32	5	0	0.05	-0.06	0
117	P-909	300	Ductile Iron	1,192.76	17	38	5	0.79	0.26	-0.79	0

S.No.	Label	Diameter (mm)	Material	Wave Speed (m/s)	Pressure (Start) (m H2O)	Pressure (Maximum, Transient) (m H2O)	Pressure (Minimum, Transient) (m H2O)	Velocity (m/s)	Velocity (Maximum, Transient) (m/s)	Velocity (Minimum, Transient) (m/s)	Vapor Volume (Maximum, Transient) (L)
118	P-908	300	Ductile Iron	1,192.76	15	37	5	0.79	0.25	-0.79	0
119	P-913	300	Ductile Iron	1,192.76	25	46	5	0.79	0.26	-0.79	0
120	P-943	300	Ductile Iron	1,192.76	59	78	5	0.79	0.19	-0.79	0
121	P-355	100	JISPVC	473.38	30	32	5	0.65	0.67	0.25	0
122	P-348	100	ISOPVC	473.38	33	34	5	0.77	0.79	0.32	0
123	P-74	350	Ductile Iron	1,162.73	11	16	5	0.61	0.62	-0.49	0
124	P-347	100	ISOPVC	473.38	34	35	5	0.77	0.79	0.32	0
125	P-907	300	Ductile Iron	1,192.76	13	35	6	0.79	0.26	-0.79	0
126	P-569	63	ISOPE	330.71	31	32	6	0.1	0.13	0.05	0
127	P-568	63	ISOPE	330.71	31	32	6	0.1	0.12	0.04	0
128	P-357	100	JISPVC	473.38	31	32	6	0.57	0.58	0.22	0
129	P-346	100	ISOPVC	473.38	35	36	6	0.77	0.79	0.32	0
130	P-358	100	JISPVC	473.38	32	32	6	0.57	0.58	0.22	0
131	P-359	100	JISPVC	473.38	31	32	6	0.57	0.58	0.22	0
132	P-756	50	JISPVC	517.57	17	26	6	0.35	0.4	0.15	0
133	P-414	90	ISOPVC	475.81	17	19	6	0.12	0.13	0.05	0
134	P-73	350	Ductile Iron	1,162.73	13	17	6	0.61	0.62	-0.49	0
135	P-413	90	ISOPVC	475.81	37	39	6	0.11	0.14	0.04	0
136	P-116	300	Ductile Iron	1,192.76	6	21	6	0.01	0.01	0.01	0
137	P-360	100	JISPVC	473.38	32	33	6	0.57	0.58	0.22	0
138	P-306	110	ISOPVC	453.46	15	18	6	0.3	0.39	-0.31	0
139	P-933	300	Ductile Iron	1,192.76	52	67	7	0.79	0.24	-0.79	0
140	P-936	300	Ductile Iron	1,192.76	56	76	7	0.79	0.22	-0.79	0
141	P-937	300	Ductile Iron	1,192.76	57	76	7	0.79	0.22	-0.79	0

S.No.	Label	Diameter (mm)	Material	Wave Speed (m/s)	Pressure (Start) (m H2O)	Pressure (Maximum, Transient) (m H2O)	Pressure (Minimum, Transient) (m H2O)	Velocity (m/s)	Velocity (Maximum, Transient) (m/s)	Velocity (Minimum, Transient) (m/s)	Vapor Volume (Maximum, Transient) (L)
142	P-938	300	Ductile Iron	1,192.76	58	79	7	0.79	0.2	-0.79	0
143	P-945	300	Ductile Iron	1,192.76	59	80	7	0.79	0.18	-0.79	0
144	P-944	300	Ductile Iron	1,192.76	59	78	7	0.79	0.19	-0.79	0
145	P-942	300	Ductile Iron	1,192.76	60	80	7	0.79	0.18	-0.79	0
146	P-939	300	Ductile Iron	1,192.76	59	81	7	0.79	0.18	-0.79	0
147	P-175	200	Ductile Iron	1,200.59	16	21	7	0.09	0.12	-0.09	0
148	P-307	110	ISOPVC	453.46	16	18	7	0.3	0.38	-0.3	0
149	P-305	110	ISOPVC	453.46	26	27	7	0.29	0.41	-0.3	0
150	P-661	50	JISPVC	517.57	35	36	7	0.26	0.28	0.12	0
151	P-331	100	ISOPVC	473.38	37	38	7	0.87	0.9	0.37	0
152	P-1	500	Ductile Iron	1,159.66	7	21	7	0	0	0	0
153	P-662	50	JISPVC	517.57	35	37	7	0.26	0.27	0.12	0
154	P-72	350	Ductile Iron	1,162.73	14	18	7	0.61	0.62	-0.49	0
155	P-361	100	JISPVC	473.38	32	33	7	0.57	0.58	0.22	0
156	P-330	100	ISOPVC	473.38	38	38	7	0.87	0.89	0.37	0
157	P-925	300	Ductile Iron	1,192.76	41	57	8	0.79	0.18	-0.79	0
158	P-924	300	Ductile Iron	1,192.76	40	57	8	0.79	0.18	-0.79	0
159	P-923	300	Ductile Iron	1,192.76	40	60	8	0.79	0.18	-0.79	0
160	P-926	300	Ductile Iron	1,192.76	42	58	8	0.79	0.18	-0.79	0
161	P-927	300	Ductile Iron	1,192.76	44	59	8	0.79	0.2	-0.79	0
162	P-329	100	ISOPVC	473.38	38	39	8	0.87	0.89	0.37	0
163	P-379	100	ISOPVC	473.38	38	39	8	0.05	0.07	-0.01	0
164	P-218	150	Ductile Iron	1,221.70	38	39	8	0.42	0.43	0.18	0
165	P-217	150	Ductile Iron	1,221.70	39	41	8	0.42	0.43	0.18	0

S.No.	Label	Diameter (mm)	Material	Wave Speed (m/s)	Pressure (Start) (m H2O)	Pressure (Maximum, Transient) (m H2O)	Pressure (Minimum, Transient) (m H2O)	Velocity (m/s)	Velocity (Maximum, Transient) (m/s)	Velocity (Minimum, Transient) (m/s)	Vapor Volume (Maximum, Transient) (L)
166	P-71	350	Ductile Iron	1,162.73	15	19	8	0.61	0.62	-0.49	0
167	P-362	100	JISPVC	473.38	33	34	8	0.57	0.58	0.22	0
168	P-380	100	ISOPVC	473.38	38	51	8	0.05	0.09	-0.01	0
169	P-69	350	Ductile Iron	1,162.73	16	19	8	0.61	0.62	-0.48	0
170	P-70	350	Ductile Iron	1,162.73	15	19	8	0.61	0.62	-0.48	0
171	P-363	100	JISPVC	473.38	33	35	8	0.57	0.58	0.22	0
172	P-922	300	Ductile Iron	1,192.76	43	65	9	0.79	0.18	-0.79	0
173	P-928	300	Ductile Iron	1,192.76	45	60	9	0.79	0.22	-0.79	0
174	P-67	350	Ductile Iron	1,162.73	19	20	9	0.61	0.62	-0.48	0
175	P-68	350	Ductile Iron	1,162.73	16	19	9	0.61	0.62	-0.48	0
176	P-216	150	Ductile Iron	1,221.70	41	43	9	0.42	0.43	0.18	0
177	P-472	65	JISPVC	479.35	34	37	10	0.51	0.52	-0.07	0
178	P-364	100	JISPVC	473.38	34	37	10	0.24	0.24	0.19	0
179	P-176	200	Ductile Iron	1,200.59	19	39	10	0.12	0.1	-0.12	0
180	P-308	110	ISOPVC	453.46	19	21	10	0.07	0.08	0.01	0
181	P-309	110	ISOPVC	453.46	19	21	10	0.07	0.08	0	0
182	P-310	110	ISOPVC	453.46	19	22	10	0.07	0.08	0	0
183	P-935	300	Ductile Iron	1,192.76	55	74	11	0.79	0.23	-0.79	0
184	P-934	300	Ductile Iron	1,192.76	53	70	11	0.79	0.24	-0.79	0
185	P-215	150	Ductile Iron	1,221.70	42	44	11	0.42	0.43	0.18	0
186	P-66	350	Ductile Iron	1,162.73	21	23	11	0.61	0.62	-0.48	0
187	P-311	110	ISOPVC	453.46	20	39	11	0.07	0.08	0	0
188	P-365	100	JISPVC	473.38	36	38	12	0.24	0.24	0.19	0
189	P-214	150	Ductile Iron	1,221.70	44	46	12	0.42	0.43	0.18	0

S.No.	Label	Diameter (mm)	Material	Wave Speed (m/s)	Pressure (Start) (m H2O)	Pressure (Maximum, Transient) (m H2O)	Pressure (Minimum, Transient) (m H2O)	Velocity (m/s)	Velocity (Maximum, Transient) (m/s)	Velocity (Minimum, Transient) (m/s)	Vapor Volume (Maximum, Transient) (L)
190	P-86	350	Ductile Iron	1,162.73	28	28	12	0.34	-0.33	-0.59	0
191	P-236	150	Ductile Iron	1,221.70	14	33	12	0.9	0.94	0.87	0
192	P-65	350	Ductile Iron	1,162.73	23	26	12	0.61	0.62	-0.48	0
193	P-117	300	Ductile Iron	1,192.76	21	21	12	0.01	0.01	0.01	0
194	P-125	300	Ductile Iron	1,192.76	21	21	12	0	0	0	0
195	P-366	100	JISPVC	473.38	38	40	13	0.24	0.24	0.19	0
196	P-213	150	Ductile Iron	1,221.70	45	47	13	0.42	0.43	0.18	0
197	P-426	90	ISOPVC	475.81	19	20	14	0.64	0.67	0.59	0
198	P-427	90	ISOPVC	475.81	19	26	14	0.6	0.63	0.55	0
199	P-64	350	Ductile Iron	1,162.73	26	28	14	0.61	0.62	-0.48	0
200	P-710	50	JISPVC	517.57	37	37	14	0.71	0.72	-0.21	0
201	P-711	50	JISPVC	517.57	37	37	14	0.71	0.72	-0.21	0
202	P-212	150	Ductile Iron	1,221.70	47	48	14	0.42	0.43	0.18	0